

DOCTORAL THESIS

Rearrangement of Energy Metabolism During Differentiation of Cancer Cells

Ljudmila Klepinina

TALLINN UNIVERSITY OF TECHNOLOGY
DOCTORAL THESIS
24/2021

Rearrangement of Energy Metabolism During Differentiation of Cancer Cells

LJUDMILA KLEPININA



TALLINN UNIVERSITY OF TECHNOLOGY
School of Science
Department of Chemistry and Biotechnology

NATIONAL INSTITUTE OF CHEMICAL PHYSICS AND BIOPHYSICS
Laboratory of Chemical Biology

This dissertation was accepted for the defence of the degree 27/04/2021

Supervisor: Dr. Tuuli Käämbre
Head of the Laboratory of Chemical Biology
National Institute of Chemical Physics and Biophysics
Tallinn, Estonia

Opponents: Prof Michael Lisanti
School of Science, Engineering and Environment
Chair of Translational Medicine
University of Salford
Salford, United Kingdom

Prof Ago Rinke
Institute of Chemistry
Chair of Bioorganic Chemistry
University of Tartu
Tartu, Estonia

Defence of the thesis: 08/06/2021, Tallinn

Declaration:

Hereby I declare that this doctoral thesis, my original investigation and achievement, submitted for the doctoral degree at Tallinn University of Technology has not been submitted for doctoral or equivalent academic degree.

Ljudmila Klepinina

signature



European Union
European Regional
Development Fund



Investing
in your future

Copyright: Ljudmila Klepinina, 2021
ISSN 2585-6898 (publication)
ISBN 978-9949-83-697-0 (publication)
ISSN 2585-6901 (PDF)
ISBN 978-9949-83-698-7 (PDF)
Printed by Koopia Niini & Rauam

TALLINNA TEHNIKAÜLIKOOL
DOKTORITÖÖ
24/2021

Energiametabolismi ümberkorraldamine kasvajakkude diferentseerimisel

LJUDMILA KLEPININA



Contents

List of Publications	7
Author's Contribution to the Publications	8
Introduction	9
Abbreviations	10
1 Literature Review	11
1.1 Heterogeneity of cancer	11
1.2 Cancer metabolism	13
1.2.1 Metabolic reprogramming of cancer cells	13
1.2.2 When glycolysis takes over	14
1.2.3 Essential role of oxidative phosphorylation in cancer	15
1.2.4 Alternative metabolic fuels for cancer cells	15
1.3 Phosphotransfer networks.....	16
1.3.1 Glycolytic phosphotransfer system.....	16
1.3.2 Creatine kinase phosphotransfer system.....	17
1.3.3 Adenylate kinase phosphotransfer system.....	18
1.3.4 Phosphotransfer enzymes and cancer	19
2 Aims of the study	22
3 Materials and Methods	23
4 Results	25
4.1 Bioenergetic profile of embryonal carcinoma cells distinguishes them from normal stem cells (Paper I).....	25
4.1.1 The respiration is compromised in 2102Ep cells compared to hESCs.....	25
4.1.2 2102Ep cells demonstrated stronger coupling between HK and OXPHOS than hESCs.....	28
4.2 The differentiation of colon cancer cells leads to the rearrangement of mitochondrial network and enhanced oxidative metabolism (Paper II)	29
4.2.1 Treatment with sodium butyrate (NaBT) induced time and dose-dependent inhibition of cell growth	29
4.2.2 The differentiation with NaBT enhanced an oxidative metabolism of Caco-2 cells .	31
4.3 Flexibility of phosphotransfer networks in cancer cells (Papers I, II and III).....	33
4.3.1 Organization of phosphotransfer network depends on the differentiation state of the cell (Papers I, II and III).....	33
4.3.2 Cellular distribution and localization of AKI and AKII (Papers I and III).....	34
4.3.3 The organization of phosphotransfer network depends on the availability of key metabolic substrates (Paper II)	36
5 Discussion.....	39
5.1 Bioenergetic profiles of normal and malignant stem cells.....	39
5.2 Effect of cellular differentiation on the bioenergetics of colon cancer cells	40
5.3 Flexibility of phosphotransfer networks in cancer cells with distinct differentiation states.....	41
5.4 Limitations of the study	42
5.5 Concluding remarks and future directions.....	43
6 Conclusions	44

List of Figures	45
List of Tables	46
References	47
Acknowledgements.....	55
Abstract.....	56
Lühikokkuvõte.....	57
Appendix 1	59
Publication I	59
Appendix 2	71
Publication II	71
Appendix 3	97
Publication III	97
Curriculum vitae.....	117
Elulookirjeldus.....	120

List of Publications

This thesis is based on the following publications:

- I **Ounpuu, L.**, Klepinin, A., Pook, M., Teino, I., Peet, N., Paju, K., Tepp, K., Chekulayev, V., Shevchuk, I., Koks, S., Maimets, T., Kaambre, T. (2017). 2102Ep embryonal carcinoma cells have compromised respiration and shifted bioenergetic profile distinct from H9 human embryonic stem cells. *Biochim Biophys Acta Gen Subj.* *1861*, *8*, 2146–2154. DOI: 10.1016/j.bbagen.2017.05.020
- II **Klepinina, L.**, Klepinin, A., Truu, L., Chekulayev, V., Kuus, K., Teino, I., Pook, M., Maimets, T., Kaambre, T. (2021). Colon cancer cell differentiation by sodium butyrate modulates metabolic plasticity of Caco-2 cells via alteration of phosphotransfer network. *PLOS ONE* *16*(1): e0245348. DOI: 10.1371/journal.pone.0245348
- III Klepinin, A., **Ounpuu, L.**, Guzun, R., Chekulayev, V., Timohhina, N., Tepp, K., Shevchuk, I., Schlattner, U., Kaambre, T. (2016). Simple oxygraphic analysis for the presence of adenylate kinase 1 and 2 in normal and tumor cells. *J Bioenerg Biomembr.* *48*, *5*, 531–548. DOI: 10.1007/s10863-016-9687-3

Author's Contribution to the Publications

- I The author contributed to the design of the study, cultured 2102Ep cells, planned and conducted the experiments (high-resolution respirometry, enzyme activity assays), performed the data analysis (except for the metabolic control analysis) and wrote the manuscript.
- II The author conceived and designed the study, cultured cells, conducted all experiments (except for PCR and UPLC) and analyzed the results. Data interpretation, writing and editing of the manuscript were also performed by the author.
- III The author conducted the immunoblot analysis, assisted in the oxygraphic analysis and enzyme activity assays, participated in the data interpretation and manuscript writing.

Introduction

Cancers contain phenotypically heterogeneous populations of cells in various states of proliferation and differentiation. The presence of tumor initiating or cancer stem cells within the tumor mass has been associated with disease recurrence, metastasis and drug resistance. There is mounting evidence that targeting of poorly differentiated cancer cells will result in successful eradication of the tumor. Therefore, studies of specific features distinguishing these cells from non-stem cancer cells and normal cells will enhance our understanding of the cancer progression and provide new opportunities for more effective therapy.

Cancer stem cells have currently been found to display the unique metabolic and bioenergetic phenotype which allows them to survive and disseminate in stressful conditions of oxygen and nutrient starvation. However, being a relatively new and largely unexplored research field, the bioenergetics of cancer stem cells possess numerous questions and controversial results. For example, it remains unclear whether cancer stem cells use glycolysis, oxidative metabolism or alternative pathways for energy production. Moreover, mechanisms behind the metabolic flexibility of cancer need to be determined.

The current study aimed to investigate the relationship between differentiation state and the bioenergetic phenotype of cancer cell. The involvement of glycolytic pathway and oxidative phosphorylation in the energy production was analyzed. In addition, the energy transfer pathways were characterized and their role in the regulation of metabolic plasticity of cancer cell was evaluated.

Abbreviations

α -KG	α -ketoglutarate
ADP	Adenosine diphosphate
AK	Adenylate kinase
ALP	Alkaline phosphatase
AMPK	AMP-activated protein kinase
ANC	Adenine nucleotide carrier
ATP	Adenosine triphosphate
CK	Creatine kinase
CSC	Cancer stem cell
Cyt c	Cytochrome c
DAPI	4',6-diamidino-2-phenylindole
DOG	2-deoxyglucose
FADD	Fas-associated with death domain protein
FCCP	Carbonyl cyanide-4-(trifluoromethoxy)phenylhydrazone
G6P	Glucose-6-phosphate
GAPDH	Glutaraldehyde 3-phosphate dehydrogenase
GLUT	Glucose transporter
GTP	Guanosine triphosphate
HDAC	Histone deacetylase
hESC	Human embryonic stem cell
HIF	Hypoxia-inducible transcription factor
HK	Hexokinase
IMS	Intermembrane space
ITP	Inosine triphosphate
LDH	Lactate dehydrogenase
MIM	Mitochondrial inner membrane
MOM	Mitochondrial outer membrane
MTT	3-(4,5-dimethylthiazol-2-yl)-2,5-diphenyltetrazolium bromide
NaBT	Sodium butyrate
NAD	Nicotinamide adenine dinucleotide
Oct-4	Octamer-binding transcription factor 4
OXPPOS	Oxidative phosphorylation
PEP	Phosphoenolpyruvate
PFK	Phosphofructokinase
PGK	Phosphoglycerate kinase
PIC	Inorganic phosphate carrier
PK	Pyruvate kinase
PKM2	M2 isoform of PK
RCI	Respiration control index
ROX	Residual oxygen consumption
SEM	Standard error of means
TCA	Tricarboxylic acid
TMPD	N,N,N',N'-tetramethyl-p-phenylenediamine
UPLC	Ultra-performance liquid chromatography
VDAC	Voltage-dependent anion channel

1 Literature Review

1.1 Heterogeneity of cancer

Despite considerable advances in cancer treatment and drug development over the past decades, a significant proportion of patients continue to struggle from cancer recurrence and development of distant metastasis. The heterogeneity and the molecular complexity of many cancers provide tumor cells with beneficial environment for the development of drug resistance contributing to the treatment failure and disease progression (Dagogo-Jack and Shaw, 2017). The diversity of cancers appears at multiple different levels (Figure 1). Cancers from the same site of origin can display distinct morphological and molecular features, from different growth rate and regions of necrosis to genomic and epigenomic differences between single cells (Grzywa et al., 2017). In addition, the tumor microenvironment can further increase the heterogeneity of cancer cells. The availability of oxygen and essential nutrients in tumor microenvironment can impose different selective pressures on cancer cells, resulting in existence of various dominant subclones in different spatial regions of the same tumor (Anderson et al., 2006).

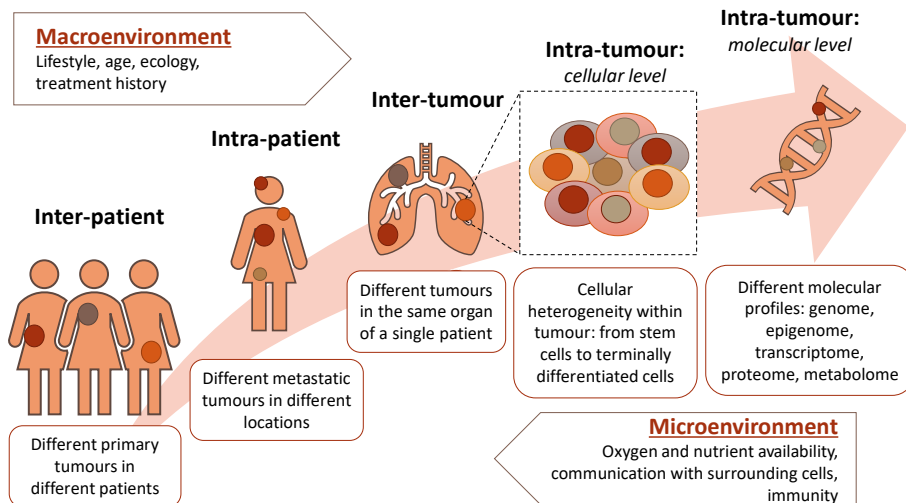
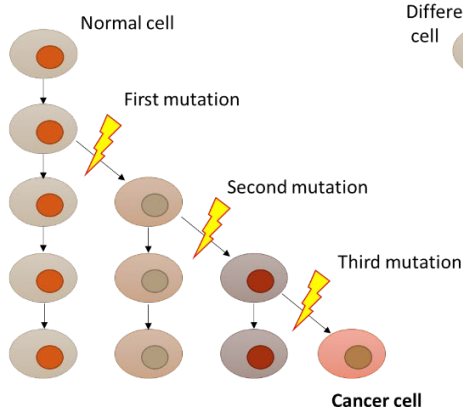


Figure 1. Cancer heterogeneity appears at many different levels. The differences among the same tumor in different patients constitute the interpatient heterogeneity. Metastatic lesions can evolve at different secondary sites and display distinct clinical behavior resulting in intrapatient heterogeneity. Intratumor heterogeneity refers to the existence of cell populations with specific morphological, genetic, epigenetic and phenotypic features.

Different models have been proposed to explain the phenotypic diversity of cancer cells (Figure 2). The clonal evolution theory suggests that most tumors arise through sequential accumulation of mutations in the original clone from a single cell of origin (Nowell, 1976). The parallel evolutionary pressure exerted by tumor microenvironment leads to stepwise selection of more aggressive subclones accounting for cancer progression. According to this model, each cancer cell is capable to form a tumor.

The Clonal Evolution Theory



The Cancer Stem Cell model

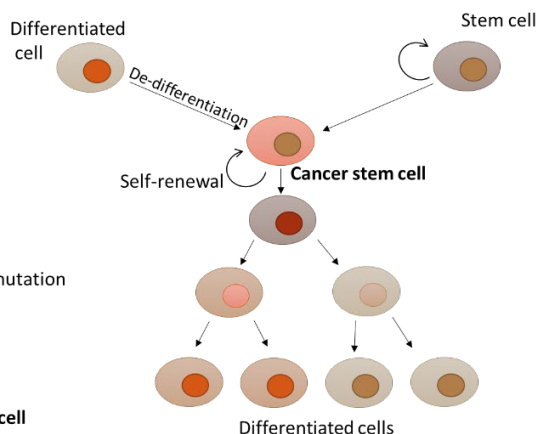


Figure 2. Models explaining phenotypic heterogeneity of cancer cells. According to the clonal evolution theory, the normal cell gradually undergoes series of mutations to form cancer cell that clonally expands generating tumor mass. Thus, every cancer cell clone is equally able to regenerate the tumor. On the contrary, the cancer stem cell model proposes that cancer originates from cancer stem cells (CSCs) that can self-renew or differentiate. CSCs are highly tumorigenic with ability to establish new tumor and induce metastasis.

In contrast, a second model, the cancer stem cell (CSC) theory, implies that the cancer is sustained and propagated by a small group of stem-like cells (Shackleton et al., 2009). Tumors are viewed as a hierarchically organized tissue, where CSCs are located at the apex of a pyramid and are able to generate the full repertoire of cells forming the bulk of the tumor. Just as normal stem cells may proliferate to produce more of the same type of stem cells and differentiate into diverse other cell types, CSCs exhibit self-renewal property and multilineage differentiation capacity. CSCs have been detected in various tumors, including leukemia (Lapidot et al., 1994), breast (Al-Hajj et al., 2003), colon (Ricci-Vitiani et al., 2007), lung (Eramo et al., 2008), brain (Singh et al., 2004), head and neck cancers (Prince et al., 2007). The origin of CSCs has stirred much controversy among researchers. Whether CSCs derive from normal adult stem cells, progenitor, differentiated cells or non-stem cancer cells remain elusive. As the cells that appear to drive tumor growth and progression, seeding of metastasis, tumor relapse and development of treatment resistance, CSCs represent an important target for new drugs (Visvader, 2011).

It is noteworthy that two above-mentioned models are not mutually exclusive and a more dominant population of CSCs may arise through the clonal evolution (Peiris-Pagès et al., 2016). In addition, it is now becoming evident that the stemness of cancer cells is partly defined by environmental cues and is a much more dynamic property than previously thought. For example, signals from the tumor microenvironment, such as growth factors, can restore CSC phenotype in more differentiated cancer cells (Vermeulen et al., 2010). The heterogeneity and a remarkable plasticity of cancer cells are also supported by the dynamic changes occurring in the energy metabolism during the adaptation to severe tumor environment.

1.2 Cancer metabolism

1.2.1 Metabolic reprogramming of cancer cells

The metabolic activity of normal non-transformed cell depends on its differentiation state. While quiescence of cells is associated with lower metabolic activity and induction of pathways that maintain structural integrity and normal function of cell, proliferating cells require building blocks in the form of nucleotides, amino and fatty acids to generate new cells. Cellular metabolism is tightly regulated by multiple signaling pathways that ensure physiological function of cell. Not surprisingly, mutations in oncogenes and tumor-suppressor genes alter these signaling networks facilitating cancer progression.

The ability of cancer cells to rewire their metabolism has been recognized as one of the most important hallmarks of cancer (Hanahan and Weinberg, 2011). Changes in the energy production networks allow cancer cells to survive in harsh environmental conditions enable rapid proliferation, invasion, metastasis and development of resistance to treatments. The most striking changes in cancer metabolism include increased glycolysis and glutaminolysis, induced pentose phosphate pathway, enhanced mitochondrial biogenesis and elevated synthesis of amino acids and lipids (Martinez-Outschoorn et al., 2017) (Figure 3).

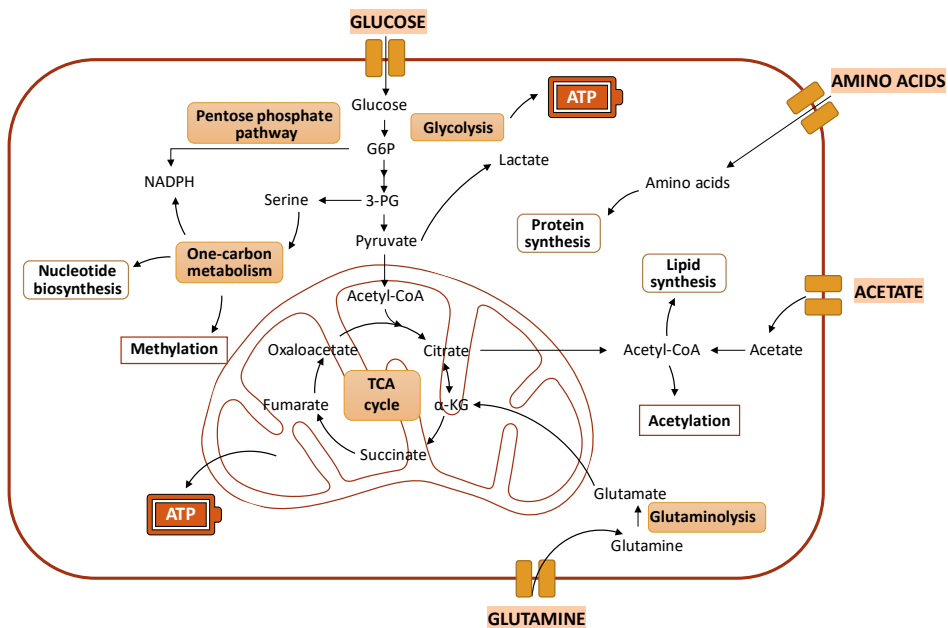


Figure 3. Metabolic pathways that undergo remodeling in cancer. Cancer cells show enhanced glycolysis and pentose phosphate pathway. The one-carbon metabolism sustains nucleotide synthesis and provide substrates for methylation reactions. Increased uptake of amino acids promotes protein synthesis. Glutamine fuels tricarboxylic acid (TCA) cycle. Lipid synthesis is supported by increased acetate consumption. Acetate is also used as a precursor for acetylation of proteins including histones supporting thereby epigenetic and post-translational modifications. Figure was created on the basis of data from (Martinez-Outschoorn et al., 2017) and (DeBerardinis and Chandel, 2016). G6P, glucose-6-phosphate; 3-PG, 3-phosphoglycerate; α -KG, α -ketoglutarate.

1.2.2 When glycolysis takes over

One of the most described metabolic features of cancer cells is an increased glucose uptake and lactate secretion. This phenomenon can be observed even under aerobic conditions in the presence of fully functioning mitochondria and is known as aerobic glycolysis or the Warburg effect. An increased glycolytic rate has been demonstrated in various types of tumors and has been exploited in clinic for the cancer diagnostics (Hsu and Sabatini, 2008).

Many glycolytic enzymes are overexpressed in cancer cells and tissues. The upregulation of glucose transporters (GLUTs) causes increased glucose uptake in cancer. GLUT1 and GLUT3 have been shown to be upregulated in many different cancer types. The first step of glycolysis or conversion of glucose to glucose-6-phosphate by hexokinase (HK) enzyme is also frequently affected. There are four isoforms of hexokinase in mammals. Although HK2 is absent from most adult tissues except skeletal and adipose tissues, it is overexpressed in many cancers and has been correlated with poor clinical outcome in various solid tumors (Liu et al., 2016). In addition, the preferential mitochondrial localization of HK1 and HK2 not only provides direct access to ATP produced by oxidative phosphorylation (OXPHOS) but also has been implicated in prevention of cancer cell death (Mathupala et al., 2006).

Another essential component of glycolytic pathway is pyruvate kinase (PK), which catalyzes the conversion of phosphoenolpyruvate (PEP) to pyruvate. The M2 isoform of PK (PKM2) is upregulated in proliferating and cancer cells supporting the anabolic metabolic pathways (Israelsen and Vander Heiden, 2015).

The further fate of pyruvate depends on the cellular state and microenvironmental conditions. In quiescent differentiated cells, pyruvate enters mitochondria, where it is completely oxidized. In cancer cells, pyruvate is converted to lactic acid. This reaction is catalyzed by lactate dehydrogenase (LDH). The increased expression of LDH is observed in many cancer types and has been correlated with tumor growth, development and metastasis. This enzyme is often considered as a potential predictive biomarker for various cancers and as an important therapeutic target for new anticancer treatments (Gallo et al., 2015).

Although the aerobic glycolysis has been extensively studied for decades, the reasons why cancer cells use less efficient energy production pathway remain unclear. One possible explanation for this paradox is that increased glycolysis is the consequence of oncogene activation and the loss of tumor suppressors. For example, the mutations in oncogene Ras promote glycolysis while loss of tumor suppressor protein p53 impairs the function of mitochondria. In addition to the genetic changes, the tumor microenvironment also contributes to the metabolic remodeling in cancer cells. As the tumor expands, the local blood supply became insufficient leading to hypoxia and stabilization of hypoxia-inducible transcription factor (HIF). HIF promotes the expression of multiple glycolytic enzymes, glucose transporters, inhibitors of mitochondrial metabolism and angiogenesis promoting factors, which altogether allow cancer cells to survive during oxygen deprivation. Moreover, altered glucose metabolism provides cancer cells with essential substrates for biosynthetic pathways. In addition to involvement in cell proliferation, increased glycolytic flow promote other cancer-essential functions such as inhibition of apoptosis and supporting the cancer specific signaling (Hsu and Sabatini, 2008).

1.2.3 Essential role of oxidative phosphorylation in cancer

Although an enhanced glycolysis has long been considered as the main feature of cancer cell, a rapidly growing body of evidence indicates an important role of OXPHOS for cancer growth and development. Indeed, an active mitochondrial metabolism has been demonstrated in various tumors. Moreover, an increased rate of mitochondrial-driven ATP synthesis has been associated with the ability of tumor to metastasize and develop chemoresistance. Mitochondrial biogenesis is crucial for survival and propagation of CSCs. For instance, CSCs isolated from ovarian cancer patients overexpress genes associated with OXPHOS and fatty acid oxidation (Pastò et al., 2014). In addition, ovarian and brain CSCs were more resistant to glucose deprivation compared to their non-stem counterpart (Flavahan et al., 2013). CSCs isolated from small lung cancer cells have shown a higher dependence on OXPHOS and mitochondrial function (Lamb et al., 2015). The upregulation of OXPHOS have been indicated in classical Hodgkin lymphoma, colon and breast cancers (Birkenmeier et al., 2016; Whitaker-Menezes et al., 2011). Moreover, maintenance of mitochondrial membrane potential by the electron transport system is essential for cancer cells to support their proliferation (Martínez-Reyes et al., 2016). Cancer cell can also exploit a truncated TCA cycle. For example, citrate can be exported to the cytosol for production of acetyl-CoA to fuel lipid and protein synthesis (Scalise et al., 2017).

1.2.4 Alternative metabolic fuels for cancer cells

The metabolism of cancer cells is altered by various cell intrinsic and extrinsic factors such as oncogene mutations, nutrients and oxygen availability. In order to cope with harsh environmental conditions and support rapid proliferation, cancer cells adopt different metabolic strategies and utilize alternative nutrients.

One of the most important demands of proliferating cancer cells is the material for biosynthetic reactions. As mentioned above, lipid synthesis is often maintained by the extraction of citrate from TCA cycle. Non-essential amino acid, glutamine, can be used by cancer cells to replenish the TCA cycle. In fact, many cancer cells use glutamine as a carbon source (DeBerardinis and Chandel, 2016; Keenan and Chi, 2015). Firstly, glutamine is metabolized to glutamate by glutaminase and then to the TCA cycle intermediate α -ketoglutarate (α -KG) by dehydrogenase or transaminase enzymes (DeNicola and Cantley, 2015). In case of mitochondrial dysfunction or under hypoxia, glutamine can support lipid generation by being converted to pyruvate and subsequently to acetyl-CoA (Keenan and Chi, 2015). In addition, glutamine and glutamate serve as important nitrogen donors for the nucleotide and amino acids biosynthesis (DeNicola and Cantley, 2015; Keenan and Chi, 2015). In addition to glutamine, cancer cells were shown to be addicted to various other amino acids including asparagine (Clavell et al., 1986), leucine (Sheen et al., 2011), arginine (Scott et al., 2000), methionine (Kreis et al., 1980), valine (Ohtawa et al., 1998), cysteine (Chung et al., 2005), glycine and serine (Locasale, 2013).

Additionally, proliferating cells require fatty acids for the building of new cellular membranes. Fatty acids can be synthesized *de novo* or incorporated from the microenvironment. The oxidation of fatty acids serves as important source of ATP for cancer cells (DeNicola and Cantley, 2015). Acetate is another alternative fuel for cancer cells. It is used to generate acetyl-CoA, which drives TCA cycle, fatty acid synthesis and various acetylation reactions in cancer cells (Keenan and Chi, 2015). Furthermore, cancer cells enhance pentose phosphate pathway, which is required for the synthesis of

nucleotides and NADPH. NADPH is used in various biosynthetic reactions as well as for scavenging of reactive oxygen species (Cho et al., 2018). The ability of cancer cells to various alternative energy sources explains an exceptional metabolic plasticity of tumors. The insight into the key metabolic features of cancer cells will enable more effective therapeutic strategies that would eliminate cancer cells while minimizing damage to normal cells.

1.3 Phosphotransfer networks

ATP is often called the “energy currency” of the cell because this molecule plays a key role in energy transfer within cells. The energy released by ATP hydrolysis is used to power many important processes, including cellular division, motility, synthesis and breakdown of macromolecules, exocytosis and endocytosis, cellular respiration etc. To support normal cell functioning, an effective coordination of energy production and energy consumption processes is required (Dzeja and Terzic, 2003). The direct diffusion of ATP to the site of its utilization would be kinetically and thermodynamically inefficient because of necessity to sustain a significant concentration gradient, inhibition of ATPases by end products (ADP, Pi, H⁺), inability to maintain the high free energy of ATP hydrolysis and possible energy dissipation. Restricted ATP diffusion could be overcome by direct channeling of ATP or conducting of energy rich phosphoryls through the chain of enzymatic reactions from mitochondria to the energy consumption site (Dzeja and Terzic, 2003).

The most common cellular phosphotransfer circuits are facilitated by creatine kinase (CK), adenylate kinase (AK) and glycolytic enzymes. These enzyme networks catalyze a series of rapidly equilibrating reactions that provide the driving force for high-energy phosphoryl flux. In addition, the phosphotransfer network enzymes maintain high ATP/ADP turnover rate at the energy generation/consumption sites by removing the end products of ATP synthesis/hydrolysis (Dzeja and Terzic, 2003).

1.3.1 Glycolytic phosphotransfer system

Glycolytic enzymes have been recognized as the important components of intracellular high-energy phosphoryl transfer. ATP produced via OXPHOS can be used to phosphorylate glucose and fructose-6-phosphate at the first stages of glycolytic pathway. Meanwhile, the pyruvate kinase catalyzes the phosphorylation of ADP at energy consumption sites. In addition, energy-rich phosphoryls can be transferred by glutaraldehyde 3-phosphate dehydrogenase and phosphoglycerate kinase (GAPDH/PGK) networks in exchange for NADH and ADP (Figure 4) (Dzeja and Terzic, 2003). Energy generated by glycolysis is used to sustain various cellular functions, such as muscle contraction, cell motility or nuclear processes (Masters et al., 1987; Ottaway and Mowbray, 1977).

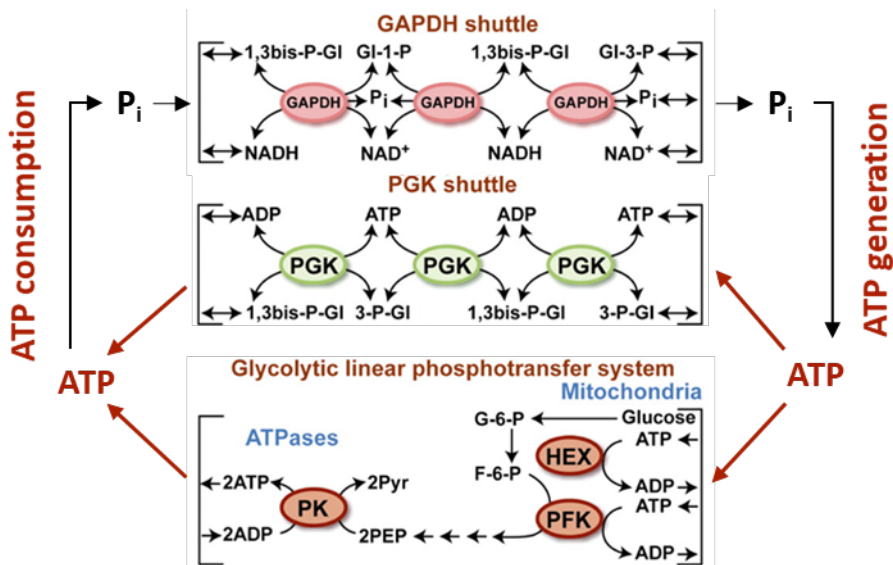


Figure 4. Integrated communication between cellular sites of ATP-consumption and ATP-generation facilitated by glycolytic phosphotransfer system. To maintain an efficient energy turnover, cells use enzymatic shuttles that promote ATP delivery and removal of ATPase byproducts (ADP, Pi and H⁺). The glycolytic phosphotransfer system consists of hexokinase (Hex), pyruvate kinase (PK), phosphofructokinase (PFK) and near-equilibrium glyceraldehyde-3-phosphate dehydrogenase/3-phosphoglycerate kinase (GAPDH/PGK) enzymes. Modified with permission from (Dzeja and Terzic, 2003). Gl, glucose; PEP, phospho-enol pyruvate; Pyr, pyruvate.

1.3.2 Creatine kinase phosphotransfer system

CK is present in various tissues and cell types, where it helps to regulate the concentration of ATP. The expression of CK is enhanced in tissues with high energy demand, such as skeletal muscles, heart and nerve cells (Wallimann and Hemmer; Wallimann et al., 1992). The enzyme catalyzes the phosphorylation of creatine to form phosphocreatine, which is used as an energy storage system in cells (Wallimann et al., 1992). This reaction is reversible, and when ATP is needed, it can easily be regenerated by the CK from the phosphocreatine pool:



There are five major CK isoforms, which are encoded by four independent genes and have been named for the tissue from which they were isolated. The cytosolic CK isoenzymes, exist as dimers, consisting of either B (brain type) or M (muscle type) subunits. Thus, there are three common forms of cytosolic CK: CK-BB, CK-MM and CK-MB. CK-BB isoenzyme is widely distributed in brain, smooth muscle, nervous system and other tissues, whereas CK-MM is predominantly expressed in highly differentiated skeletal muscles and the heart. CK-MB is mostly found in the heart and to a lesser extent in skeletal muscles. In addition to cytosolic isoforms, there are two mitochondrial CK isoenzymes, the ubiquitous (uMtCK) and the sarcomeric (sMtCK) isoenzymes. While uMtCK is widely distributed in different tissues, the sMtCK is exclusively expressed in heart and skeletal muscles. The mitochondrial isoforms generally exist as octamers consisting of four dimers each. However, the octamers can be readily dissociated to dimers to regulate CK activity (McLeish and Kenyon, 2005).

The cellular energy homeostasis is maintained by the interplay between cytosolic and mitochondrial CK isoforms (Schlattner et al., 2006). Both isoenzymes supply a phosphocreatine pool, which serves as a temporal energy buffer and prevent cells from a rapid decline in total ATP concentrations. Moreover, the direct or indirect association of CK isoenzymes with mitochondrial membrane proteins and cytosolic ATPases facilitates a direct exchange of ADP and ATP between the association partners connecting sites of energy generation with sites of energy consumption (Figure 5) (Dzeja and Terzic, 2003).

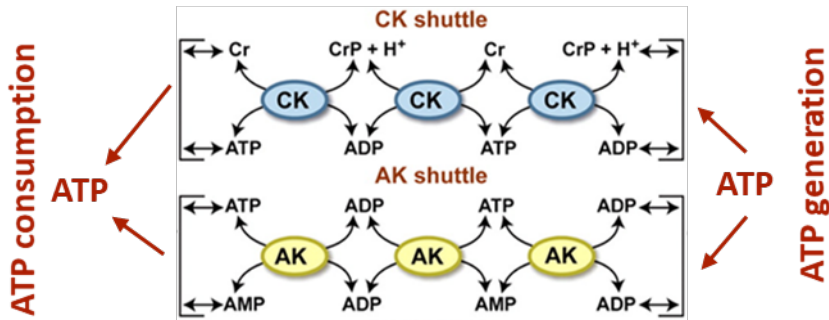


Figure 5. Creatine kinase and adenylate kinase phosphotransfer networks. Mitochondrial isoforms of creatine kinase (CK) and adenylate kinase (AK) support oxidative phosphorylation machinery with ADP and facilitate ATP export. Cytosolic isoforms of CK and AK catalyze sequential chains of reactions transferring ATP to ATPases. Modified with permission from (Dzeja and Terzic, 2003). Cr, creatine.

The CK deficiency leads to compromised energy delivery and, as a result, defective cell functioning. However, glycolytic enzymes and AK may replace to some extent the phosphotransfer functions of CK, rescuing the cellular bioenergetics (Dzeja et al., 2004).

1.3.3 Adenylate kinase phosphotransfer system

The main function of AK is to regulate the adenine nucleotide ratios in different intracellular compartments. AK catalyzes the reversible phosphotransfer between AMP, ADP and ATP:



There are nine different AK isoforms (AK1-AK9) that have been isolated and characterized in human tissues so far. They all vary in molecular weight, tissue distribution, intracellular localization, kinetic properties, substrate and phosphate donor specificity (Panayiotou et al., 2014). Thus, AK1 and AK2 specifically bind AMP and prefer binding to ATP over other nucleotide triphosphates, while AK3, which is also specific for the phosphorylation of AMP, can only use GTP or ITP as the phosphoryl donor. AK isoenzymes can exist as monomers, dimers and higher molecular structures (Dzeja and Terzic, 2009).

Due to the unique ability of AK to monitor and alter the levels of ATP and other nucleotides, this enzyme has been recognized as a sensitive reporter of the cellular energy state. Under different metabolic stresses, when the balance between ATP and ADP changes, AK is able to increase significantly the intracellular concentration of AMP, that stimulates various signaling pathways. Thus, AMP can activate various

AMP-dependent receptors and metabolic enzymes such as those involved in glycolytic and glycogenolytic pathways, AMP-activated protein kinase (AMPK), K-ATP channels and adenosine metabolic signaling cascades. The communication between energetic and metabolic signaling pathways ensures cellular energy homeostasis and supports a broad range of functional activities including cell motility, nuclear transport, DNA synthesis and repair, hormone secretion, cellular differentiation and apoptosis (Dzeja and Terzic, 2009).

1.3.4 Phosphotransfer enzymes and cancer

As discussed previously, phosphotransfer enzymes are involved in the regulation of various cellular processes. Not surprisingly, malignant transformation has been associated with multiple alterations in the phosphotransfer systems (Table 1).

Altered glycolytic pathway is a well-described feature of cancer cells. The majority of glycolytic enzymes are overexpressed in cancer (Phan et al., 2014). Numerous oncogenes such as Ras, Myc and HIF-1 α are reported to be master inducers of glycolysis (DeBerardinis et al., 2008; Jones and Thompson, 2009). An elevated transcriptional activity of c-Myc and HIF-1 α promotes the expression of key glycolytic enzymes such as glucose transporter GLUT1, HK2, phosphofructokinase (PFKM) and LDHA (Phan et al., 2014).

The aberrant CK activity and protein concentration in the blood serum has been observed in various cancers during the last 40 years (Yan, 2016). However, it remains unknown whether the release of CK into the serum is a consequence of cell injury or a part of pathological processes. It has been recently proposed that the extracellular CKB promotes the metastatic progression of colorectal cancer (Loo et al., 2015). Disseminated metastatic colon cells released this enzyme into the liver extracellular space, where it generated phosphocreatine. The phosphocreatine was then transported back and used to produce intracellular ATP that sustained the survival and division of metastatic cells in hypoxic conditions of liver microenvironment (Loo et al., 2015). Moreover, the inhibition of CKB suppressed the metastatic growth of colon cancer cells. On the contrary, another study revealed decreased serum CK levels in cases of breast cancer (Pan et al., 2013). It was suggested that low CK levels may attribute to the host immune response, as CKB was previously shown to regulate the development and activation of T lymphocytes (Zhang et al., 2009). These findings indicate that both up- and down-regulation of serum CK level can be observed in cancer depending on the type and origin of particular tumor, different stage and metastatic ability.

Table 1. Phosphotransfer enzymes in cancer

ENZYME	TYPE OF CANCER	STATUS	EXPERIMENTAL MODEL	REF.
Glycolytic enzyme network				
LDH	Lung cancer	↑	Blood plasma	(Liu et al., 2017)
HK	Hepatocellular carcinoma, gastric cancer and colorectal cancer	↑	Meta-analysis of 21 studies	(Liu et al., 2016)
HK	Digestive system cancers	↑	Meta-analysis of 15 studies	(Wu et al., 2017)
PKM2	Colon cancer	↑	Tissue samples	(Zhou et al.)
PKM2	Gastric cancer	↑	Tissue samples	(Shiroki et al., 2017)
Adenylate kinase network				
AK1	Transformed embryonic fibroblasts	↓	ras ^{v12} /E1A-transformed primary mouse embryonic fibroblasts	(Vasseur et al., 2005)
AK2	Breast cancer	↑	Estrogen receptor negative breast cancer	(Speers et al., 2009)
AK2	Breast cancer	↓	Breast cancer cell lines	(Kim et al., 2014)
AK4	Lung cancer	↑	Tissue samples Various cell lines	(Jan et al., 2012)
AK6	Breast cancer Colon cancer	↑	Colon adenocarcinoma and breast cancer tissues	(Bai et al., 2016)
AK6	Colon cancer	↑	CSCs from CRC tissues	(Ji et al., 2017)
Creatine kinase network				
CK	Breast cancer	↓	Blood serum	(Pan et al., 2013)
CK	Colon cancer	↓	Tissue samples	(Friedman et al., 2004)
CK	Lung cancer	↓	Blood plasma	(Liu et al., 2017)
CK	Sarcoma	↓		(Patra et al., 2008)
CK	Prostate cancer	↓	Tissue samples	(Amamoto et al., 2016)
CK	Oral cancer	↓	Oral squamous carcinoma cell line	(Onda et al., 2006)

AK – adenylate kinase, CK – creatine kinase, HK – hexokinase, LDH – lactate dehydrogenase, PKM2 – M2 isoform of pyruvate kinase.

Altered expression of intracellular CK was also associated with cancer progression. High levels of CKB were found in lung and breast cancer (Liu et al., 2017; Zarghami et al., 1996). Alternatively, mitochondrial CK was shown to be down regulated in several cancer types including prostate cancer (Amamoto et al., 2016), oral squamous cell carcinoma (Onda et al., 2006) and sarcoma (Patra et al., 2008). Data from our research group indicated decreased CK activity and expression level in colorectal cancer (Kaldma et al., 2014), breast cancer (Kaambre et al., 2012) and neuroblastoma (Klepinin et al., 2014). Since CK expression is increased in most normal tissues with high energy demands, the downregulation of this enzyme may be necessary for the transformation of normal cells into cancer cells (Yan, 2016).

Interestingly, a loss of mitochondrial creatine kinase was associated with the upregulation of AK in different experimental models (Kaambre et al., 2012; Kaldma et al., 2014; Klepinin et al., 2016; Lam et al., 2010) suggesting the flexibility of phosphotransfer system. Altered expression and activity of AK isoenzymes were also demonstrated in various cancers.

The expression of AK1 was shown to be decreased during malignant transformation of mouse embryonic fibroblasts (Vasseur et al., 2005). In fact, the formation of alternative product of AK1 gene, AK1 β , is regulated by p53 (Collavin et al., 1999). Thus, the downregulation of AK1 in cancer may reflect the reduction in AK1 β level and may be associated with the suppression of p53. In addition to AK1, AK2 was also proposed as a negative regulator of tumor growth. The expression of this isoenzyme was downregulated in various breast cancer cell lines (Kim et al., 2014). Moreover, a significant amount of AK2, which is usually located in the mitochondria, was detected in the nucleus, where interacting with other enzymes it can affect tumor cell growth (Kim et al., 2014). In addition, AK has been found to modulate nuclear energetics through association with mitotic spindle (Dzeja et al., 2011). The study of Speers and colleagues identified increased expression of AK2 in estrogen receptor-negative breast cancer. Our group also demonstrated the upregulation of both AK1 and AK2 in neuroblastoma, colon and breast cancer. Increased AK4 expression was found in glioma and lung cancer. The overexpression of AK4 was shown to protect cells against oxidative stress. In addition, hypoxia was shown to enhance AK4 expression in HeLa and HEK293 cells (Fujisawa et al., 2016; Kong et al., 2013). It was proposed that AK4 may form multienzyme complex consisting of mitochondrial membrane proteins, ATP transporter and HK2. This complex provides HK2 with the direct access to the newly synthesized mitochondrial ATP supporting high glycolytic activity of cancer cells (Fujisawa et al., 2016). By contrast, hypoxia decreased AK4 expression in HepG2 cell line suggesting the existence of alternative scenarios for AK4-mediated response to cellular stress conditions (Kong et al., 2013). The overexpression of another AK isoform, AK6, was detected in colorectal adenocarcinoma and breast cancer tissues and cell lines (Bai et al., 2016). AK6 was shown to participate in the ribosome biogenesis and promote cancer cell growth through upregulation of cancer-associated genes' translation (Bai et al., 2016). Moreover, highly expressed AK6 was found to promote migration and invasion of colorectal cancer cells. This study revealed the ability of AK6 to enhance the resistance of colorectal cancer cells to metabolic stress through upregulation of glycolytic pathway (Ji et al., 2017).

2 Aims of the study

The overall aim of the study was to investigate the relationship between the differentiation state and the energy metabolism of cancer cells.

Following research objectives were stated to facilitate the achievement of this aim:

1. To characterize the bioenergetic profiles of normal and cancer cell lines with distinct differentiation potentials including normal pluripotent stem cells (H9), relatively nullipotent carcinoma stem cells (2102Ep), non-differentiated and differentiated colon cancer cells (Caco-2) and neuroblastoma (Neuro-2A cells)
2. To determine the differences in the oxygen consumption of cell lines with distinct stemness properties
3. To evaluate the involvement of OXPHOS and glycolysis in the ATP production by studied cell lines
4. To analyze the performance of phosphotransfer networks in cells with distinct differentiation states

3 Materials and Methods

To characterize the bioenergetic profiles of cancer cells with distinct differentiation potentials, we estimated three parameters related to cellular energy metabolism: rates of oxygen consumption, glycolytic capacity and activities of phosphotransfer enzymes. The overall summary of the applied approaches and techniques is depicted in Figure 6.

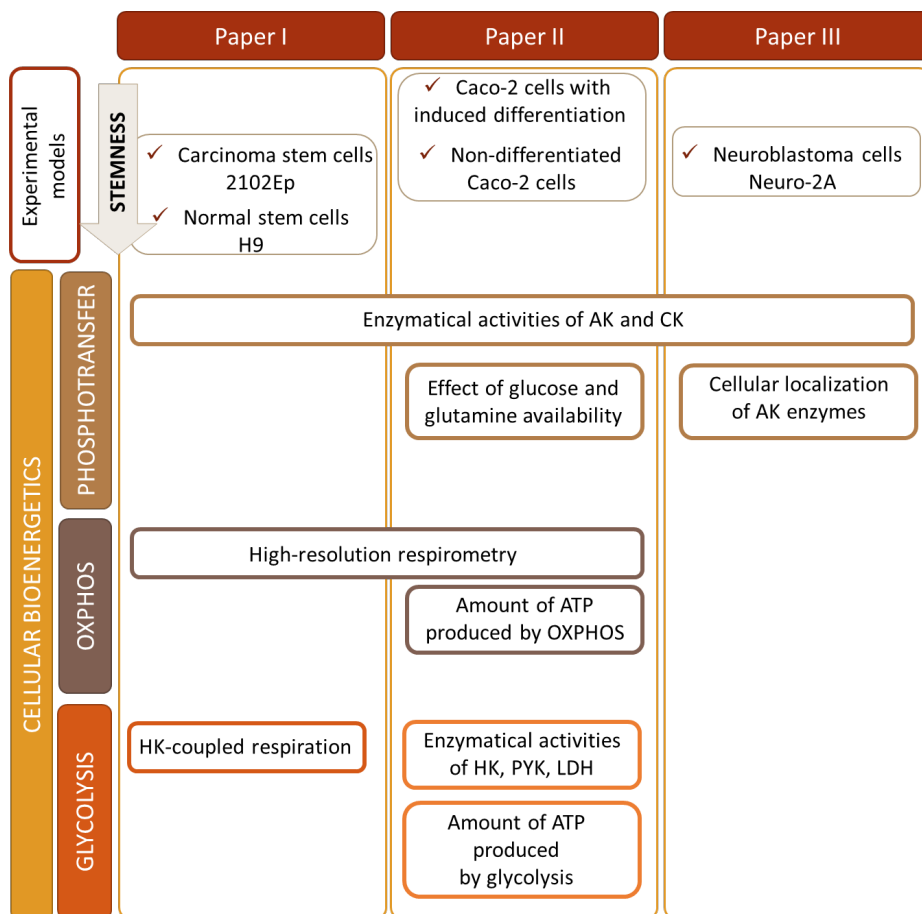


Figure 6. Design of the study

The following methods, described in more detail in the respective publications, were used in the study:

- Growing of cell lines (H9, 2102Ep, Caco-2, Neuro-2A) – Publications I, II, III
- Trypan Blue dye exclusion test – Publications I, II, III
- MTT Assay for cell viability assessment – Publication II
- LDH release Assay for cytotoxicity measurements – Publication II
- High-resolution respirometry – Publications I, II, III
- Immunofluorescence analysis – Publications I, II

- Enzymatic activity assays – Publications I, II, III
- Measurement of ATP level and ATP:ADP ratio by ultra-performance liquid chromatography (UPLC) – Publication II
- Immunoblot analysis – Publication III

4 Results

4.1 Bioenergetic profile of embryonal carcinoma cells distinguishes them from normal stem cells (Paper I)

4.1.1 The respiration is compromised in 2102Ep cells compared to hESCs

To compare the energy metabolism of normal stem cells with their malignant counterparts, we used the H9 cell line as a model of human embryonic stem cells (hESCs) and the embryonal carcinoma 2102Ep cell line as a model of CSCs. Both cell lines expressed the pluripotency marker Oct-4 and contained some spontaneously differentiated cells (Figure 7). Despite this similarity, hESCs grow as colonies unlike 2102Ep which grow as a monolayer. In addition, hESCs displayed higher nucleus to cytoplasm ratio compared to 2102Ep cells, which contained considerably larger volumes of cytoplasm. Although mitochondria in both cell lines appeared small, round and punctate, these organelles were localized around the nuclei in hESCs whereas in the 2102Ep cells they were randomly distributed in the cytoplasm.

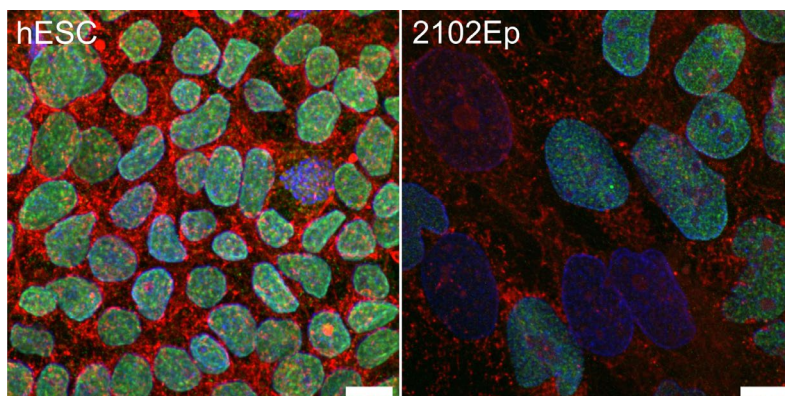


Figure 7. Mitochondrial localization in hESC and 2102Ep cells. Laser scanning confocal microscopy images showing immunocytochemical analysis of Oct-4 (green) and MitoTracker Red (red). Nuclei are stained with DAPI (blue). Scale bars, 10 μ m.

To investigate mitochondrial performance, we measured oxygen consumption rates in studied cell lines using high-resolution respirometry. As a first step, the rate of oxygen consumption was monitored in the presence of complex I and II substrates (10 mM glutamate, 2 mM malate, 10 mM succinate) to reveal State 2 respiration. Here, State 2 is the respiration stimulated by endogenously produced ADP. Subsequently, 2 mM ADP was added to induce State 3 respiration or ADP stimulated respiration. Then the respiratory control indexes (RCI) were calculated as ratios between State 3 and State 2 rates. Although both cell lines had similar rates of State 2 respiration, 2102Ep cells showed a significantly lower State 3 respiration compared with hESCs (Figure 8A). The reduction in respiration was also confirmed by the RCI, which was two times lower in the 2102Ep cells compared to hESCs (Figure 8B).

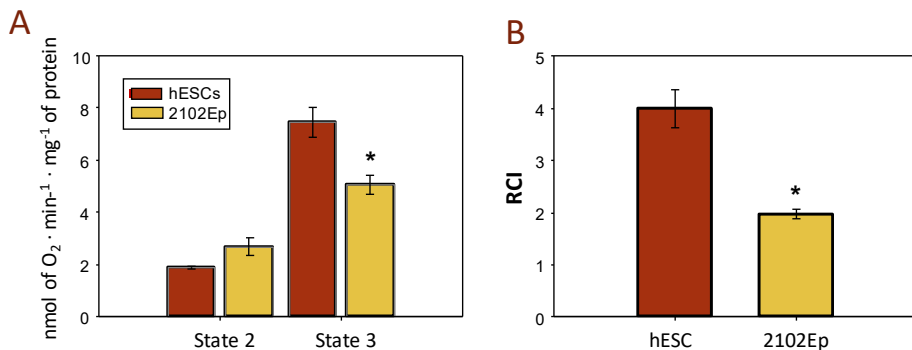


Figure 8. Respiratory properties of hESC and 2102Ep cells. Oxygen consumption rates were determined using the Oroboros® Oxygraph-2K (Oroboros Instruments). Approximately 2×10^6 of cells per chamber were used. Cell membranes were permeabilized with saponin (40 μg per ml) to enable an access of substrates to mitochondria. State 2 respiration rate was recorded in the presence of 10 mM glutamate, 2 mM malate, 10 mM succinate. State 3 respiration was induced by 2 mM ADP. The rates of oxygen consumption were normalized to the total protein amount in the cells (nmol of O₂ \times min⁻¹ \times mg⁻¹ of protein). (A) State 2 and state 3 respiration rates. (B) Respiratory control indexes (RCIs). RCIs were calculated as the ratios between state 2 and state 3 rates. All data are mean \pm SEM of 5–6 independent experiments. * $p < 0.05$.

To identify the mechanisms behind the lower oxygen consumption rates in 2102Ep cells, we examined the overall mitochondrial performance as well as functional activities of individual respiratory chain complexes in both cell lines (Figure 9). The key parameters of mitochondrial functioning were assessed using “stress test” protocol described in Papers I and II. In this approach, well-characterized inhibitors (oligomycin, antimycin A and rotenone) and uncoupler of respiration (carbonyl cyanide-4-(trifluoromethoxy)phenylhydrazone (FCCP)) were used to dissect processes that are contributing to mitochondrial oxygen consumption. Firstly, the basal State 2 respiration was monitored. Then 2 μM of oligomycin was added to inhibit ATP synthase and reveal ATP-linked respiration. To uncouple respiration from ATP synthesis, the stepwise titration by FCCP was used (0.5 μM per step until maximal respiration was reached). The FCCP stimulated respiration was used to calculate mitochondrial reserve capacity, defined as the difference between maximal and basal respiration. Finally, 0.5 μM of rotenone (complex I inhibitor) and 2.5 μM antimycin A (complex III inhibitor) were added to fully inhibit mitochondrial respiration and enable the calculation of nonmitochondrial respiration driven by processes outside the mitochondria. Although 2102Ep cells demonstrated lower rates of respiration than hESCs (Figure 9A), the calculation of specific functional parameters did not reveal any impairments in the mitochondrial performance (Figure 9B). The proton leak and ATP-dependent respiration appeared to be very similar in both cell lines. The maximal respiration and mitochondrial reserve capacity were even higher in carcinoma cells compared with hESCs.

In addition, we analyzed the functional activity of individual respiratory chain complexes by measuring respiration rates during substrate-inhibitor titration. Firstly, the respiration was activated by 2 mM ADP. Then complex I was inhibited by rotenone (20 μM). Subsequent addition of 10 mM succinate restored respiration by stimulating complex II activity. The addition of 10 μM antimycin A inhibited complex III. Finally,

the functional activity of complex IV was confirmed by the addition of electron donors ascorbic acid (5 mM) and N,N,N',N'-tetramethyl-p-phenylenediamine (TMPD, 1 mM) that enhanced oxygen consumption in both cell types. Our results showed that all complexes within the mitochondrial respiratory chain of hESCs and 2102Ep cells were functionally active and their activities were equivalent in both cell lines (Figure 9C).

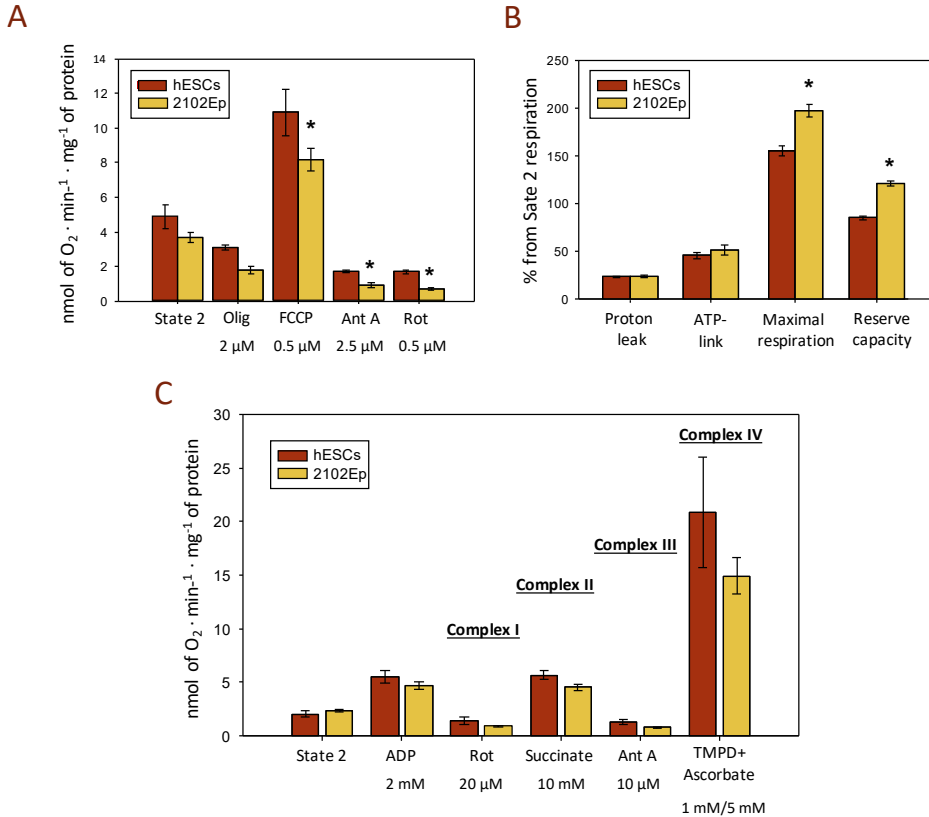


Figure 9. Assessment of mitochondrial function in hESCs and 2102Ep cells. Oxygen consumption rates were determined using the Oxygraph-2K (Oroboros Instruments). Approximately 2×10^6 of cells were added to oxygraph chamber. (A) Quantitative analysis of mitochondrial stress test protocol. Measurements were performed in intact non-permeabilized cells. (B) Functional properties of mitochondrial respiration. Proton leak = $V_{Olig} - V_{Rot}$, ATP-link = $V_{State\ 2} - V_{Olig}$, Maximal respiration = $V_{Olig} - V_{Rot}$, Reserve capacity = $V_{max} - V_{State\ 2}$. (C) Functional activity of respiratory chain complexes. To subtract chemical background caused by an autooxidation of TMPD+Ascorbate, 1 mM of NaCN was added in the end of experiment. The Complex IV-dependent respiration was calculated as $V_{TMPD/Asc} - V_{TMPD/Asc+NaCN}$, where $V_{TMPD/Asc}$ and $V_{TMPD+NaCN}$ are TMPD-stimulated respiration rates before and after addition of NaCN. Results represent means \pm SEM, $n=5$. Ant A – antimycin A, Olig – oligomycin, Rot – rotenone, TMPD – N,N,N',N'-tetramethyl-p-phenylenediamine. * $p < 0.05$.

4.1.2 2102Ep cells demonstrated stronger coupling between HK and OXPHOS than hESCs

To evaluate the coupling between HK and OXPHOS (Figure 10A), we investigated the effect of glucose on the cellular respiration. As shown on figure 10B, the addition of 0.1 mM ATP increased the rates of respiration in hESCs indicating the generation of a larger flux of ADP from ATPases in these cells. The effect of glucose on the oxygen consumption was characterized by glucose index (I_{glu}), which represents the degree of glucose-stimulated respiration compared to ADP stimulated respiration. The I_{glu} calculated for 2102Ep cells was considerably higher compared to hESCs, suggesting that coupling between HK reactions and OXPHOS and thus the aerobic glycolysis is more pronounced in 2102Ep cells.

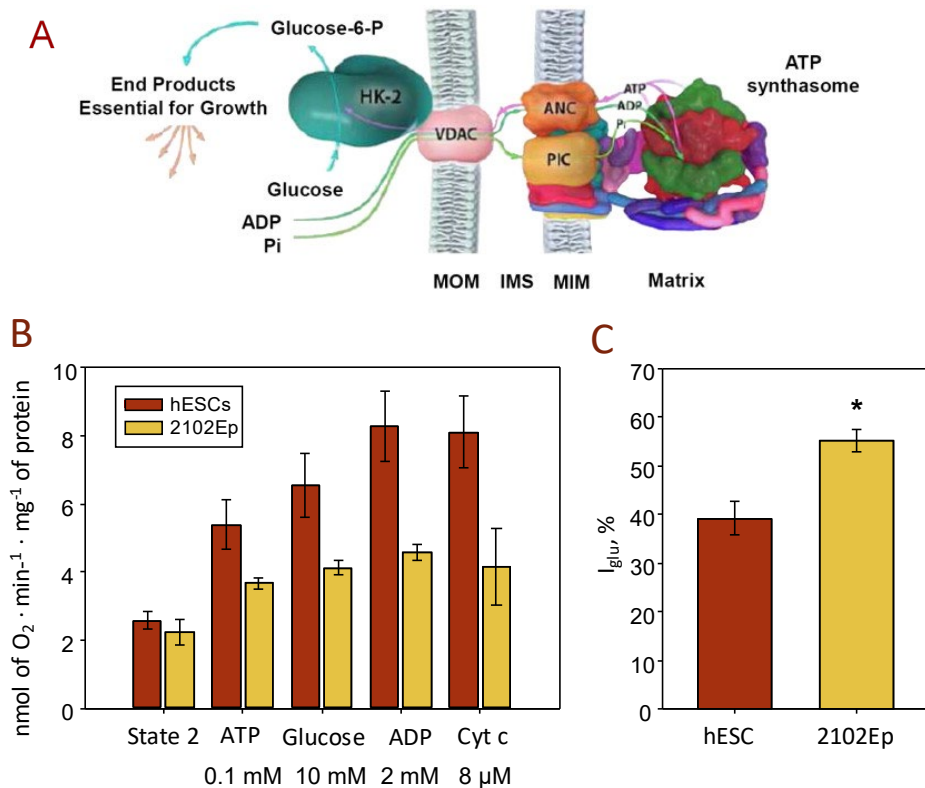


Figure 10. Effect of exogenously added glucose on the rate of oxygen consumption. (A) Hexokinase (HK-2) binding to the mitochondrial outer membrane through the voltage anion channel (VDAC) facilitates the preferential access to the mitochondrial generated ATP to maintain the high glycolytic flux. From (Pedersen, 2007) with permission. (B, C) The effect of glucose was estimated as a degree of glucose-mediated respiration compared to State 3 respiration and expressed as the glucose index (I_{glu}): $I_{glu} (\%) = (V_{glu} - V_{ATP}) / (V_{ADP} - V_{ATP})$. Results represent means \pm SEM, $n=5$. * $p < 0.05$. ANC – adenine nucleotide carrier, IMS – intermembrane space, MIM – mitochondrial inner membrane, MOM – mitochondrial outer membrane, Pi – inorganic phosphate, PIC – inorganic phosphate carrier, Cyt c – cytochrome c.

4.2 The differentiation of colon cancer cells leads to the rearrangement of mitochondrial network and enhanced oxidative metabolism (Paper II)

4.2.1 Treatment with sodium butyrate (NaBT) induced time and dose-dependent inhibition of cell growth

To evaluate a possible relationship between cellular differentiation and energy metabolism in cancer cells, we treated colon adenocarcinoma cells (Caco-2) with NaBT and examined the alterations in the energy metabolism caused by induced cellular differentiation. Initially, we validated the best experimental conditions (concentration of NaBT and incubation time) to avoid any possible interferences, which might be caused by cytotoxic effect of NaBT.

Gradual inhibition of cell growth was observed after 48 hours of incubation with NaBT (Figure 11A). The viability of metabolically active cells decreased from 100% (untreated control) to $90\pm 2\%$ with 1 mM NaBT, $73\pm 7\%$ with 2 mM, $56\pm 10\%$ with 5 mM and $37\pm 3\%$ with 10 mM. An extension of incubation time to 72 hours caused even more prominent reduction in the number of viable cells. The decreased cellular viability (measured by MTT assay) might indicate either the toxicity of NaBT or the inhibition of cellular proliferation. To evaluate the cytotoxic effect of NaBT, cell culture mediums were checked on the presence of LDH, which is released into the surrounding matrix by damaged or dying cells. The cytotoxicity of NaBT appeared after 48 h of treatment at concentrations above 2 mM (Figure 11B). After 72 hours, the cytotoxic effect was also observed at 2 mM concentration. In contrast, 1 mM NaBT was non-toxic for Caco-2 cells at all studied time points. Thus, lower doses of NaBT (1-2 mM) inhibited the proliferation of Caco-2 cells, while higher concentrations (5-10 mM) were cytotoxic.

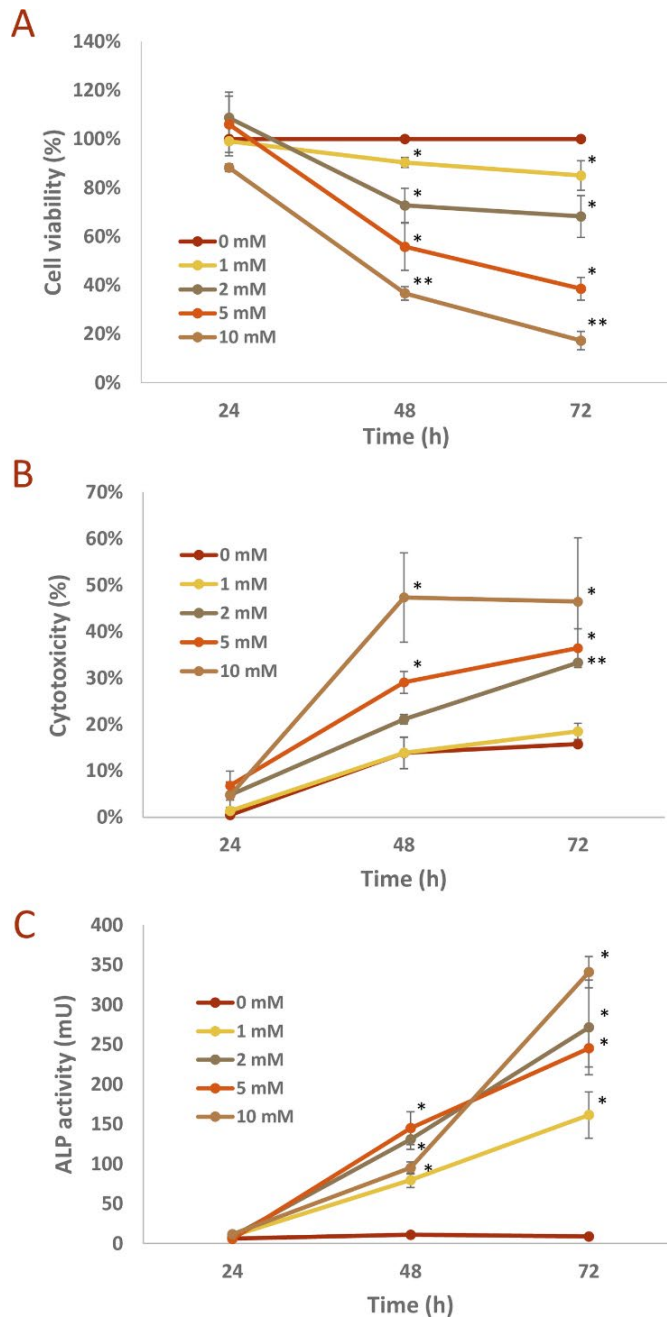


Figure 11. Effect of NaBT on the Caco-2 cell growth. Cells were incubated in the presence of various concentrations of NaBT for 24, 48 or 72 hours. (A): The viability of cells was analyzed by MTT assay. (B): Cytotoxicity was estimated by measurement of lactate dehydrogenase release after treatment with NaBT. (C): Alkaline phosphatase (ALP) activity assay was used to estimate differentiation status of the cells. Data are presented as mean \pm SEM ($n=3-5$ independent experiment); * $p < 0.01$; ** $p < 0.001$).

The reduction in cellular viability was also accompanied by increased ALP activity, which is a well-established marker of colon cell differentiation (Shin et al., 2014). After 48 h of incubation with 1 mM NaBT, the ALP activity increased almost 10 times compared with untreated control (Figure 11C). Furthermore, treated cells resembled epithelial-like cells with a polygonal shape and had more regular dimensions compared to cells cultured in the absence of NaBT (Figure 12). Thus, the incubation of cells with 1 mM NaBT for 48 h was sufficient to induce cell differentiation without any notable toxic effect.

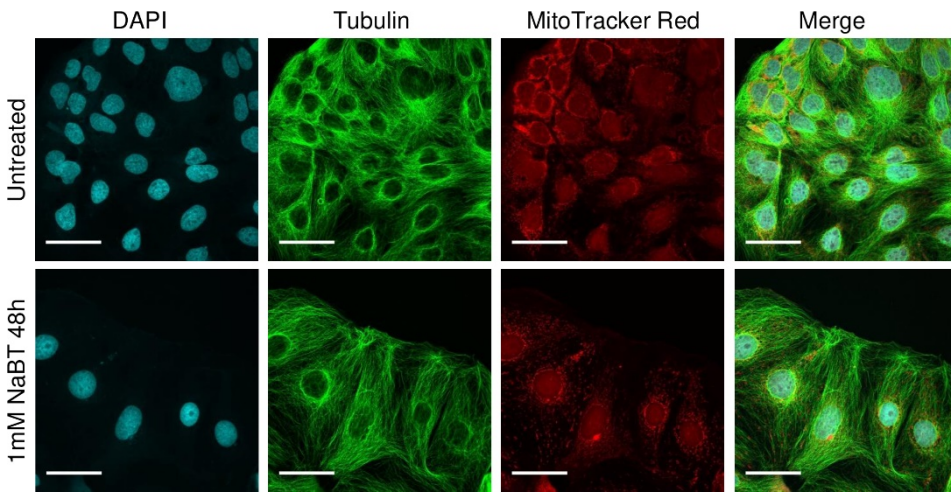


Figure 12. Confocal microscopy of untreated and sodium butyrate (NaBT)-treated Caco-2 cells. Morphological changes occur after treatment of cells for 48h with 1mM NaBT. Cells were stained with MitoTracker (red), anti-whole tubulin (green) and DAPI (blue). For all the above, representative images are shown. Scale bars: 50 μ m.

4.2.2 The differentiation with NaBT enhanced an oxidative metabolism of Caco-2 cells

To evaluate functional properties of mitochondria in treated and untreated Caco-2 cells, we applied high-resolution respirometry. The rates of oxygen consumption were measured in the absence and in the presence of NaBT in the respiratory medium (Figure 13A, B). In addition, the impact of Complex I and II on the overall respiratory performance of cells was assessed by the addition of glutamate/malate and succinate to the respiratory medium. In the absence of butyrate, treated and untreated cells displayed similar rates of oxygen consumption (Figure 13A). However, the supplementation of respiratory medium with NaBT increased respiration rates in treated cells with each substrate tested suggesting that butyrate is used as a substrate for an oxidative metabolism in more differentiated colon cancer cells (Figure 13B). To further analyze the impact of NaBT on the key parameters of mitochondrial respiration, we measured oxygen consumption rates in non-permeabilized Caco-2 cells using mitochondrial stress test protocol (Figure 13C). Although the routine respiration, proton leak and ATP-coupled respiration were similar in both experimental groups, the maximal respiration rate and spare respiratory capacity were significantly higher in NaBT-treated cells compared with untreated control cells, indicating that treated cells are more adaptable to cellular stress.

Furthermore, the increased non-mitochondrial residual oxygen consumption (ROX) after treatment of cells with NaBT may indicate that NaBT can activate alternative oxidases or promote other oxygen consuming processes in cell cytosol.

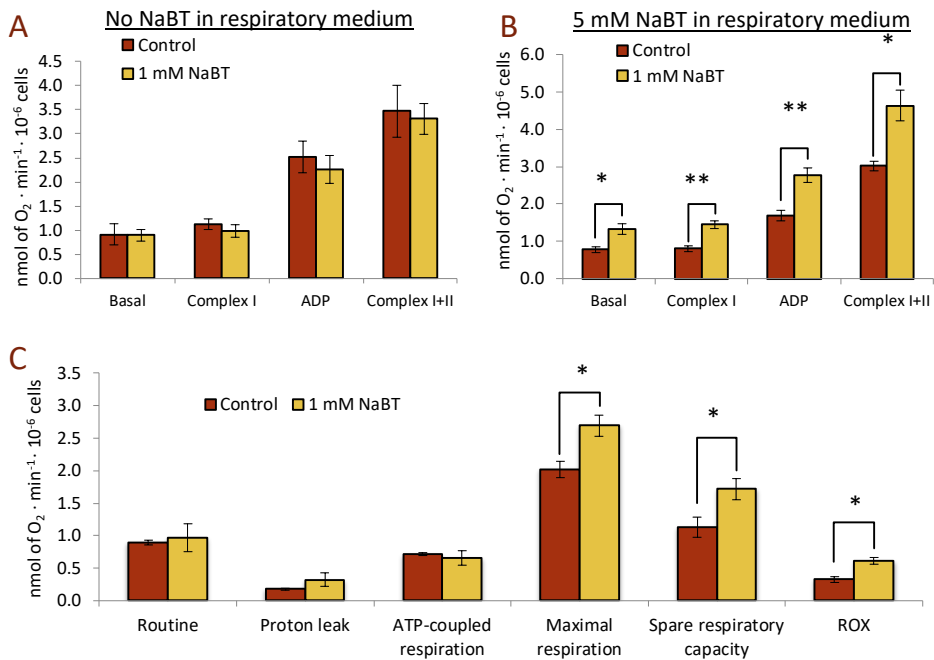


Figure 13. Treatment with sodium butyrate induces an increase in oxidative metabolism of Caco-2 cells. Caco-2 cells were treated with 1 mM NaBT or control (sterile mQ water) which was added to the cell growth medium 48 h before cells were harvested and used for high-resolution respirometry. 2×10^6 of cells per oxygraph chamber were used. The rates of oxygen consumption were normalized to the cell number ($\text{nmol of O}_2 \times \text{min}^{-1} \times 10^{-6}$ cells). (A): Oxygen consumption rates in the absence of sodium butyrate in the respiratory medium. After cell membranes were permeabilized with $40 \mu\text{g} \times \text{ml}^{-1}$ of saponin, the basal respiration was monitored. Then 10 mM glutamate and 2 mM malate were added to measure Complex I respiration. 2 mM ADP was added to stimulate OXPHOS. Finally, 10 mM succinate was added to reveal Complex I+II respiration rate. (B): Oxygen consumption rates in the presence of sodium butyrate. 5 mM NaBT was added directly to the oxygraph chamber prior to measurements. Then, the respirometry study was conducted as mentioned above. (C): Parameters of mitochondrial respiration obtained using mitochondrial stress test protocol. All data are presented as mean \pm SEM ($n = 3-5$; $p < 0.05$). ROX – residual oxygen consumption.

To estimate the contribution of glycolysis and OXPHOS to ATP production, we incubated treated and untreated cells with inhibitors of OXPHOS ($0.5 \mu\text{M}$ rotenone, $2.5 \mu\text{M}$ antimycin A and $2 \mu\text{M}$ oligomycin) or glycolysis (6 mM 2-deoxyglucose (DOG)) and subsequently measured amounts of ATP and the ratio of ATP/ADP (Figure 14). The total ATP level as well as the ratio of ATP/ADP were similar in NaBT-treated and untreated cells. However, the level of ATP produced by OXPHOS was increased and the amount of ATP generated by glycolysis was slightly decreased after incubation of cells with NaBT (Figure 14B). In percent equivalent, untreated cells produced $33 \pm 1\%$ and $67 \pm 1\%$ of total ATP by OXPHOS and glycolysis, respectively. The treatment with NaBT shifted this ratio to $44 \pm 3\%$ and $56 \pm 2\%$ of ATP from OXPHOS and glycolysis, respectively.

These results together with data from high-resolution respirometry suggest that differentiation of Caco-2 cells with NaBT causes rearrangement of cellular metabolism leading to enhanced OXPHOS and utilization of NaBT as a preferred energy source.

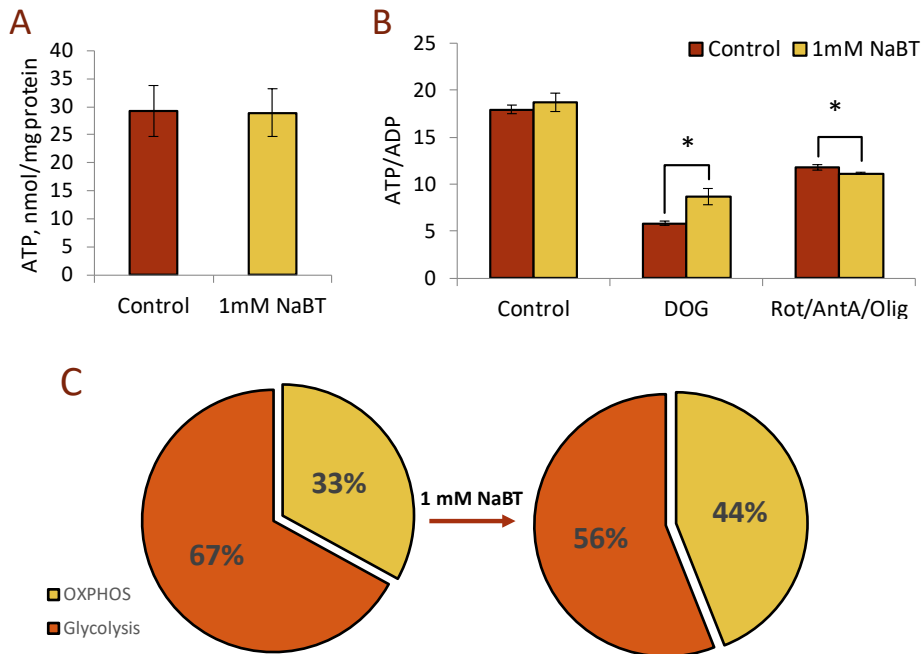


Figure 14. The contribution of glycolysis and oxidative phosphorylation to ATP production. Caco-2 cells were treated with 1 mM NaBT or control (sterile mQ water) which was added to the cell growth medium 48 h before experimental procedures. (A): ATP concentration in treated and control cells was measured by UPLC. (B): Effect of glycolysis and OXPHOS inhibition on the ATP/ADP ratio. Treated and control cells were divided into 3 groups. The first one (control group) was incubated with ethanol, both glycolysis and OXPHOS remained functional. In the second group the glycolysis was inhibited by 6 mM of 2-deoxyglucose (DOG). The third group was incubated with the mixture of OXPHOS inhibitors (0.5 μ M rotenone, 2.5 μ M antimycin A and 2 μ M oligomycin). Exposure time to inhibitors was 30 min. (C): Contribution of OXPHOS and glycolysis to ATP production in control and NaBT-treated Caco-2 cells. All data are presented as mean \pm SEM ($n = 3-5$; * $p < 0.05$).

4.3 Flexibility of phosphotransfer networks in cancer cells (Papers I, II and III)

4.3.1 Organization of phosphotransfer network depends on the differentiation state of the cell (Papers I, II and III)

The current study revealed an altered regulation of phosphotransfer system in cancerous stem cells as well as restructuring of CK and AK enzyme networks during differentiation of cancer cells. Our previous work demonstrated that the total CK activity is decreased in colon cancer tissues. Here, we show that carcinoma stem cells as well as undifferentiated cancer cells also exhibit decreased CK activities (Table 2). However, the differentiation of cancer cells caused the increase in CK activity from 167 to 203 Units in Caco-2 cells and from 8 ± 1 to 12 ± 1 Units in Neuro-2a cells. Concomitant to increase in CK activity, the differentiation of cancer cells was accompanied by decreased AK

activity, from 77 to 57 Units in Caco-2 cell and from 245 ± 12 to 172 ± 15 Units in Neuro-2a cells. In addition, normal hESCs displayed lower AK activities compared to embryonal carcinoma stem cells (2102Ep). Furthermore, AK activity was significantly increased (almost two times) in colon cancer tissues compared to healthy colon.

Table 2. AK and CK enzymatical activities

Cells/Tissues	AK Activity mU/mg protein	P values	CK Activity mU/mg protein	P values
hESCs (H9)	64 ± 3	<0.001	160 ± 4	<0.0001
2102Ep	180 ± 6		13 ± 2	
Non-dif. Caco-2	77 ± 4	<0.05	167 ± 8	<0.05
Dif. Caco-2	57 ± 6		203 ± 7	
Non-dif. Neuro-2A ^a	245 ± 12	<0.05	8 ± 1	<0.001
Dif. Neuro-2A ^a	172 ± 15		12 ± 1	
Colon cancer tissue ^b	411 ± 43	<0.05	204 ± 84	<0.05
Normal colon tissue ^b	257 ± 35		497 ± 142	

^a Data from (Klepinin et al., 2014); ^b Data from (Chekulayev et al., 2015)

4.3.2 Cellular distribution and localization of AKI and AKII (Papers I and III)

The specific activities of AK1 and AK2 were measured spectrophotometrically in hESCs, 2102Ep, Neuro-2a cells and breast cancer tissues. A recently developed oxygraphic analysis for the semi-quantifying the ratio between AK1 and AK2 was also applied for Neuro-2A cells.

The increased total AK activity in embryonal carcinoma stem cells was most probably due to an increase in AK2 specific activity in these cells (Table 3). The expression level of AK2 was also increased in 2102Ep cells compared to hESCs (Paper I, Figure 1). In contrast, both AK1 and AK2 were increased 5 to 7 times in breast cancer tissues with AK1 remaining the predominant isoform.

Table 3. AK1 and AK2 distribution in normal and cancer cells/tissues. The adenylate kinase index (I_{AK}) that reflects the strength of AK coupling with the OXPHOS was used to quantify AK1 and AK2 in studied material. For additional information see Publications I, II and III.

Cells/Tissues	AK1 mU/mg protein	AK2 mU/mg protein	I_{AK1} , %	I_{AK2} , %
hESCs (H9)	29 ± 2 (46% ^a)	33 ± 1 (54%)	–	–
2102Ep	37 ± 4 (21%)	142 ± 3 (79%)	–	–
Breast cancer tissue	208 ± 64 (69%)	82 ± 15 (31%)	–	–
Normal tissue	42 ± 4 (80%)	11 ± 2 (20%)	–	–
Non-dif. Neuro-2A	136 ± 9 (56%)	109 ± 8 (44%)	53	47
Dif. Neuro-2A	81 ± 10 (47%)	91 ± 8 (53%)	39	61
Rat cardiomyocytes	2394 ± 102 (96%)	99 ± 18 (4%)	80	20

^a % from the total AK activity

In Neuro-2a cells, differentiation was accompanied by the decrease in both AK1 and AK2 activities (Table 3). However, the ratio between AK1 and AK2 remained unaltered. Western blot analysis and additional spectrophotometric analysis confirmed similar expression levels of AK1 and AK2 and cytosolic localization of AK1 in undifferentiated Neuro-2A cells (Figure 15). Rat cardiomyocytes, where cytosolic AK1 is the predominant AK isoform, were used as a control to confirm the specificity of elaborated oxygraphic method.

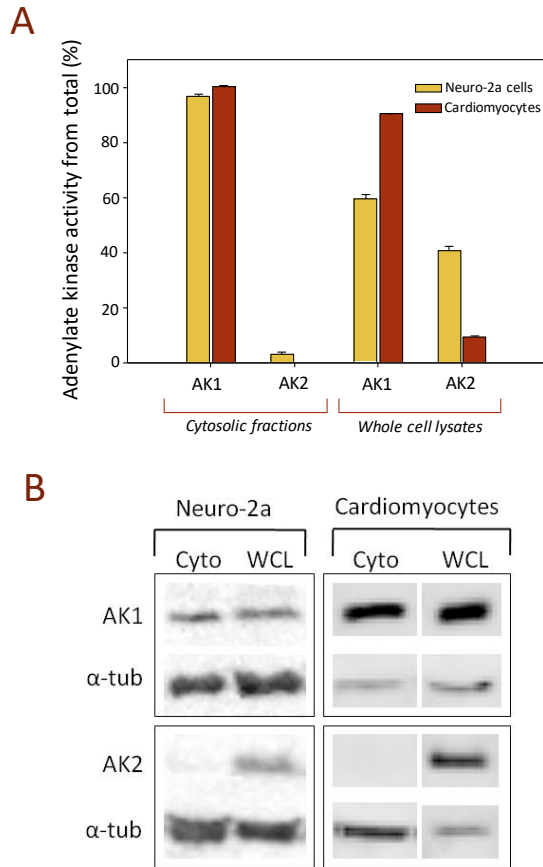


Figure 15. Intracellular location of adenylylase kinase 1 (AK1) and adenylylase kinase 2 (AK2) in Neuro-2a cells and cardiomyocytes. To isolate cytosolic fractions, cell membranes were lysed with 35 μg of digitonin per 4×10^6 of Neuro-2a cells or with 25 $\mu\text{g}/\text{ml}$ of digitonin for rat cardiomyocytes. Then, cell suspensions were centrifuged at 1000 g for 10 min. Supernatants containing cytosolic fraction were further centrifuged at 10000 g for 15 min to pellet any remaining cellular debris. (A) Enzymatical activities of AK1 and AK2 were measured in cytosolic fractions and whole cell lysates. Firstly, the total AK activity was measured. Then, samples were incubated with specific AK1 inhibitor N-ethylmaleimide for 1 h at 25°C and the AK activity attributed to AK2 was measured. Results are presented as mean \pm SEM ($n = 3$). (B) Western blot analysis on the presence of AK1 and AK2 in the cytoplasm (Cyto) and whole cell lysates (WCL) of Neuro-2a cells and cardiomyocytes. α -tubulin (α -tub) was used as a loading control.

4.3.3 The organization of phosphotransfer network depends on the availability of key metabolic substrates (Paper II)

Since glucose and glutamine are important carbon sources for cancer cells (Figure 16A), we investigated whether their availability may alter the phosphotransfer networks of cancer cells. Activities of main enzymes of glycolytic, AK and CK phosphotransfer networks were analyzed in the presence and in the absence of glutamine as well as under the physiological levels of glucose (5 mM) and at high glucose concentration (25 mM), which is usually used in most common cell growth mediums, such as Dulbecco's Modified Eagle's medium.

The glycolytic pathway was analyzed by HK, PK and LDH activities. The HK activity remained unchanged in all experimental groups (Figure 16B). PK and LDH activities were significantly decreased after treatment of cells with NaBT in the presence of glutamine in the growth media (Figure 16C-D). Thus, the differentiation of Caco-2 cells with 1 mM NaBT affected later stages of glycolytic pathway, rather than earlier stages. Although in glutamine-free media, PK and LDH activities decreased after NaBT-treatment, an enrichment of growth media with additional glucose resulted in similar activities of those enzymes in treated and untreated cells.

The activity of CK was independent on either the availability of glutamine in the growth medium or fluctuations in glucose concentration (Figure 16E). The pattern of CK activity after differentiation of cells with NaBT also remained unchanged in different growth conditions. In contrast, the pattern of AK activity changed in glutamine-free medium (Figure 16F). Firstly, the suppressive effect of NaBT on AK activity, which was observed in the presence of glutamine, disappeared completely after removing of glutamine from the growth medium. Secondly, the supplementation of glutamine-free media with additional glucose resulted in the decreased AK activity. However, the suppression of AK activity upon NaBT-treatment was not restored.

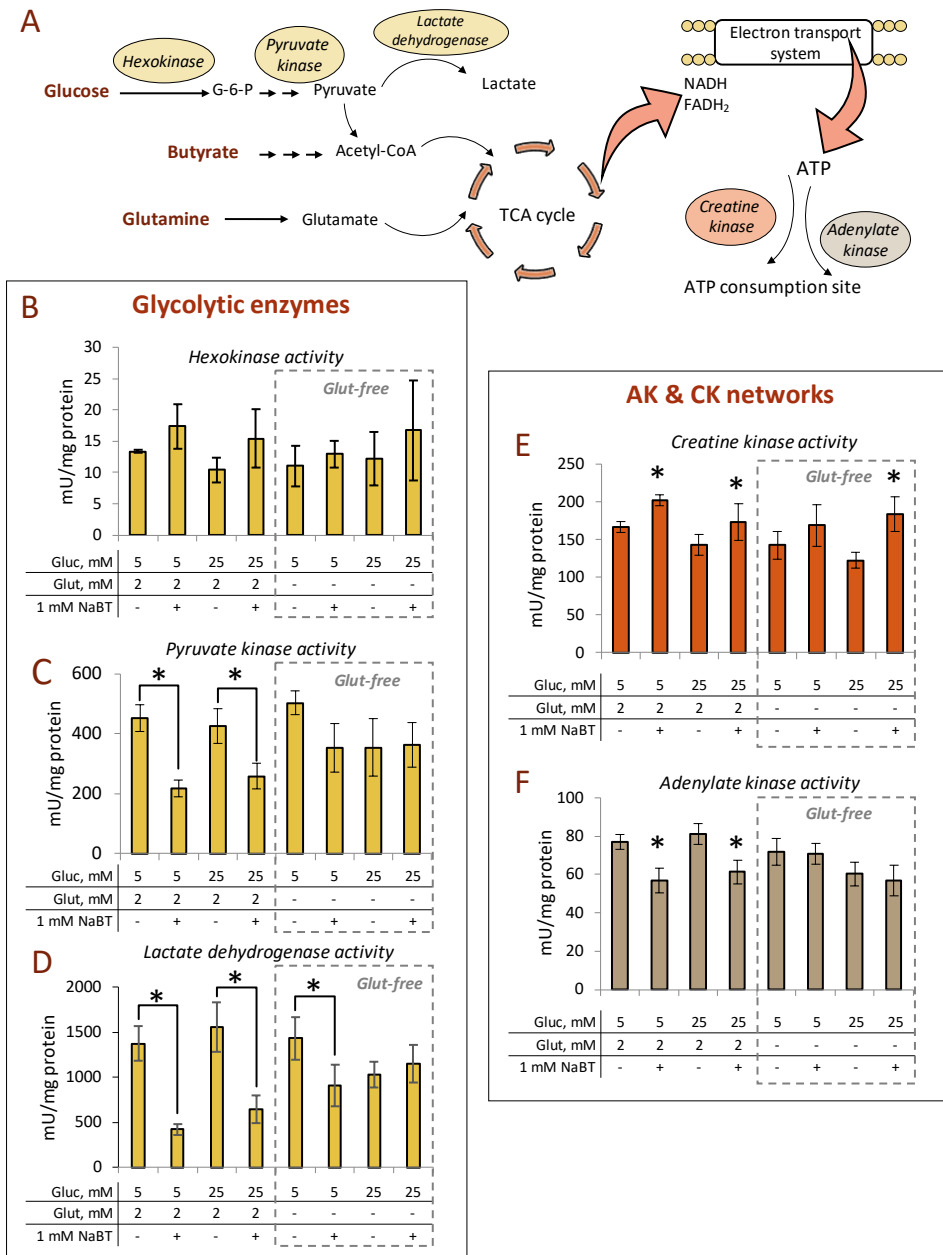


Figure 16. Rearrangement of phosphotransfer system after treatment of Caco-2 cells with sodium butyrate. (A): Schematic representation of main pathways analyzed. (B): Hexokinase activity. (C): Pyruvate kinase activity. (D): Lactate dehydrogenase activity. (E): Creatine kinase activity. (F): Adenylate kinase activity. For this study, Caco-2 cells were grown under different conditions. Lower panels on each graph indicate glucose (Gluc) and glutamine (Glut) concentration in cell growth medium as well as whether cells were treated with 1 mM NaBT or not. All data are presented as mean \pm SEM ($n = 3-5$; $*p < 0.05$). AK – adenylate kinase, CK – creatine kinase, G-6-P – glucose-6-phosphate, NaBT – sodium butyrate, TCA – tricarboxylic acid.

5 Discussion

5.1 Bioenergetic profiles of normal and malignant stem cells

The unique metabolic flexibility of less differentiated cancer cells allows them to survive and expand in harsh microenvironmental conditions. The ability to switch between glycolysis and OXPHOS as well as activate alternative energy pathways makes from eradication of these cells an extremely complicated mission. There is an increasing interest to identify specific metabolic signature of CSCs that can be used to distinguish them from other cells and specifically eliminate. The current study uncovers several aspects of the relationship between the differentiation state and the energy metabolism of cancer cells.

In Paper I, it was established that the bioenergetic profiles of normal and embryonal carcinoma stem cells show distinct features. It was demonstrated that carcinoma stem cells exhibit lower rates of cellular respiration and higher rates of aerobic glycolysis compared to their non-malignant counterparts. The reduction in oxygen consumption rate might indicate the impairment of mitochondrial respiratory chain or inability to generate an effective proton gradient. However, our results confirmed the intactness of mitochondrial membranes and functional activity of individual respiratory chain complexes. Moreover, the rate of proton leak was similar in both cell lines. The maximal respiration and mitochondrial reserve capacity were even higher in carcinoma stem cells indicating the higher resistance of this cell line to cellular stress factors (such as low oxygen and nutrient levels) (Desler et al., 2012). Recent studies have indicated that the maintenance of high mitochondrial reserve capacity (also called bioenergetic reserve capacity) is critical for survival of cells experiencing acute and chronic stress. When the tissue needs a sudden burst of additional cellular energy to resist under a variety of stress conditions or increased workload, the reserve capacity can be used (Desler et al., 2012). The loss of the reserve capacity has been associated with cellular death of neurons, cardiomyocytes, endothelial cells as well as heart failure in vivo (Choi et al., 2009; Dranka et al., 2010; Gong et al., 2003). One of the major factors that regulate the magnitude of mitochondrial reserve capacity is the substrate availability (Sansbury et al., 2011). Interestingly, another study comparing the metabolic signatures of normal and carcinoma stem cells revealed an enriched amount of TCA cycle intermediates in carcinoma stem cells (Abu Dawud et al., 2012). It is possible that the increased TCA cycle activity supports mitochondrial reserve capacity by supplying additional NADH in carcinoma stem cells. Moreover, the intermediates of TCA cycle might be used as alternative energy sources in case of nutrient deficiency or as a raw material for nucleotide, lipid or protein synthesis (Jose et al., 2011). Nevertheless, the increased mitochondrial reserve capacity in addition to increased autophagy and antioxidant system serves as an essential component of defence system that helps cancer cells to survive in harsh environmental conditions and develop resistance to chemotherapeutic agents.

5.2 Effect of cellular differentiation on the bioenergetics of colon cancer cells

Since human carcinoma stem cells, 2102Ep, are relatively nullipotent and, thus, have a reduced capacity to differentiate, we took another cell line to investigate the effect of cellular differentiation on the bioenergetics of cancer cells. Caco-2 cell line was originally derived from a large intestine adenocarcinoma (Fogh, 1975) and has been demonstrated to contain a subpopulation of CSCs with tumor initiating capacity characterized by the expression of CD133 and CD44 surface markers (Haraguchi et al., 2008). When Caco-2 cells are cultured under specific conditions, they become differentiated and display morphological and biochemical characteristics of the absorptive enterocytes (Sambuy et al., 2005).

In the present work, we used sodium salt of butyrate, NaBT, to induce differentiation in Caco-2 cells. Butyrate is a short-chain fatty acid, which is usually produced in the colon during bacterial fermentation of the dietary fiber. It serves as the primary energy source for colonocytes, promotes growth and proliferation of normal colonic epithelial cells, improves colonic defense barrier and has anti-inflammatory and anticancerogenic properties (Gonçalves and Martel, 2013). Interestingly, tumors more frequently develop in distal parts of the colon, where the level of butyrate is commonly lower. Moreover, the inverse relationship was found between the levels of butyrate in the human colon and the incidence of colon cancer (Bingham et al., 2003; Clausen et al., 1991). The anticarcinogenic effect of butyrate has been attributed to its ability to function as a histone deacetylase (HDAC) inhibitor. The inhibition of HDACs leads to altered expression of genes that regulate cell proliferation, differentiation and apoptosis (Gonçalves and Martel, 2013). The suppressive effect of NaBT on the growth of cancer cells is time and dose dependent (Amoêdo et al., 2011). The results of the current study show that the inhibition of cellular proliferation is caused by the induced differentiation of Caco-2 cells at lower doses of NaBT (1-2 mM), while higher doses of NaBT (5-10 mM) activated cellular death programs. Previous research work, where the normal colonic epithelial stem cells were studied, have indicated that the antiproliferative effect of butyrate is reversible at lower doses but becomes permanent at higher concentrations of NaBT through induction of apoptotic pathway (Kaiko et al., 2016). This dual action of NaBT could be potentially utilized to increase the effectiveness of anticancer treatments. On the one hand, butyrate is able to induce the death of cancerous colonocytes, on the other hand it could induce the differentiation of CSCs, thereby, making them more susceptible for conventional therapies. However, the rapid uptake and metabolism of butyrate by normal cells significantly reduce the efficacy of butyrate utilization as a chemotherapeutic drug (Miller et al., 1987). Therefore, the discovery of more stable butyrate derivatives is required. The maintenance of butyrate-producing microbiota through fiber-rich diet might serve as a more successful tool in the prevention of colon cancer and can be potentially used as a complementary strategy for cancer treatment (Donohoe et al., 2012).

Depending on the availability of oxygen and nutrients in the tumoral microenvironment, cancer cells may use glycolysis or OXPHOS for energy production (DeBerardinis and Chandel, 2016). In rapidly proliferating and expanding tumor tissue, oxygen diffusion is hampered, and cells often reside in hypoxic conditions. Therefore, cancer cells enhance glycolytic flux to produce sufficient level of energy and macromolecules for biosynthetic needs (Muz et al., 2015). Our results show that Caco-2 cells produce about 70 % of their

total ATP by glycolysis while only 30 % was derived from the OXPHOS. Treatment of cells with NaBT shifted energy metabolism towards more oxidative pathway, where butyrate is used as a preferred substrate. Similar results were previously obtained using other cancer cell lines including lung, breast and colon cancer cells (Alcarraz-Vizán et al., 2010; Amoêdo et al., 2011; Blouin et al., 2011; Li et al., 2018; Rodrigues et al., 2015). Reduced glycolytic flux in Caco-2 cells was accompanied by decreased PK and LDH activities suggesting that NaBT affected the later stages of glycolytic pathway, rather than the earlier steps. However, it is noteworthy to mention that different cancer cell lines might respond in an individual manner to NaBT depending on the metabolic phenotype of utilized cell type. Thus, treatment of H460 lung cancer cells with NaBT increased HK activity, while PK and LDH activities remained unaltered (Amoêdo et al., 2011). In the study investigating the effect of NaBT on various breast cancer cells, treatment with NaBT enhanced PK activity in highly metastatic MDA-MB-231 cells only, while LDH activity was enhanced specifically in T-47D cells (Rodrigues et al., 2015). Nevertheless, despite diverse effect of NaBT on the activity of specific glycolytic enzymes, it in general affected the energy metabolism of all studied cancer cell lines enhancing OXPHOS and decreasing glycolysis.

5.3 Flexibility of phosphotransfer networks in cancer cells with distinct differentiation states

Although much is known about the rearrangements in energy producing pathways that occur during malignant transformation, the way how the energy is being transported within the cancer cell remains underestimated and largely undiscovered. Meanwhile, well organized energy transfer system is vital for intracellular communication between ATP-producing and ATP-consuming cellular processes (Dzeja and Terzic, 2003). Any disturbances in the highly organized phosphotransfer network may lead to the fatal consequences for the normal functioning, growth and development of the cell (Bai et al., 2016; Pucar et al., 2002). The increased levels of various AK isoenzymes were detected in lung, breast and colon cancers (Bai et al., 2016; Jan et al., 2012; Ji et al., 2017; Speers et al., 2009). Moreover, AK6 was found to promote migration and invasion of colorectal CSCs (Ji et al., 2017). Comparing breast and colon cancer tissues with adjacent normal tissues, we showed previously that the phosphotransfer network undergo substantial rearrangements during malignant transformation (Chekulayev et al., 2015). More specifically, cancer tissues exhibited a decreased CK activity, which was compensated by upregulation of AK network. The same pattern of alterations in AK and CK activities was detected in embryonal carcinoma stem cells (Paper I). Moreover, an elevated AK2 expression was found to be responsible for the dominance of AK network over CK network in malignant stem cells. There are several evidence indicating that AK2 could be involved in the regulation of cellular proliferation and differentiation. For example, AK2 was found to regulate viability and cell growth during insect development (Chen et al., 2012). Furthermore, AK2 can mediate mitochondrial apoptosis by binding to Fas-associated with death domain protein (FADD) and caspase-10 (Kim et al., 2014; Lee et al., 2007). The AK2 deficiency was shown to impair the proliferation, survival and differentiation of hematopoietic stem cells (Six et al., 2015). Thus, an elevated AK2 expression might be necessary for increased proliferation of tumor initiating cells.

In Papers II and III we estimated the ability of cellular differentiation to reverse cancer-induced changes in the phosphotransfer system. Indeed, the differentiation of

Caco-2 cells with NaBT as well as differentiation of neuroblastoma cells with retinoic acid resulted in decreased AK activities and increased CK activities. Interestingly, both differentiation agents, NaBT and retinoic acid, have been reported to modulate directly or indirectly the AMPK activity (Ishijima et al., 2015; Peng et al., 2009). The AMPK has been proposed to act as a tumor suppressor by regulating energy levels, enforcing metabolic checkpoints and inhibiting cell proliferation (Li et al., 2015). The AMPK can be activated by changes in the intracellular ATP/ADP ratio (Dzeja and Terzic, 2009). Since AK mediates nucleotide exchange and AMP signaling, we assume that poorly differentiated cancer cell can prevent AMPK activation by upregulation of AK. However, whether altered AK network in differentiated cancer cells is a consequence or a cause of AMPK activation needs to be determined.

The availability of different energy sources within cell microenvironment determines the metabolic preferences and energetic status of the cell and can potentially affect phosphotransfer network. The effect of butyrate and glutamine availability on the AK, CK and glycolytic enzyme activities was analyzed in Paper II. The differentiation of Caco-2 cells with NaBT resulted in increased CK activity independently on the absence or presence of glutamine in the growth medium. On contrary, AK activity was sensitive to glutamine and glucose presence in the growth medium. Thus, AK activity remained unchanged after treatment with NaBT in conditions of glutamine deprivation. However, the activity dropped in both treated and untreated cells after addition of supplemental glucose. There is no earlier work done in this area and hence it is important subject for future research.

The supplementation of glutamine-free medium with additional glucose also abolished suppressive effect of butyrate on PK and LDH activities. Most probably, the removal of glutamine forced cells to adjust their metabolic pathways to cope with novel conditions. The maintenance of high glycolytic flux might serve as a compensatory mechanism to manage the emerging imbalance in NADH and NAD⁺ ratio caused by glutamine starvation (Fan et al., 2013). Altogether, these results indicate the link between rearrangements in phosphotransfer network with metabolic alterations induced by differentiation of colon cancer cells with NaBT.

5.4 Limitations of the study

There are several limitations in this study that could be addressed in the future research. First, the experiments were conducted under normoxic conditions (21 % of O₂ in the air), while the oxygen level in hypoxic tumor tissues is significantly lower ranging between 1 % – 2 % and below (Muz et al., 2015). The oxygen consumption rates will most probably decline in hypoxic conditions. However, the effect of low oxygen concentrations on the overall mitochondrial performance involving proton leak, ATP-linked respiration, maximal respiration and mitochondrial reserve capacity is not so obvious. For example, it was reported that neural stem/progenitor cells grown at low oxygen tension have a significantly higher mitochondrial reserve capacity compared to that under normoxia (Chen et al., 2015). Moreover, it was shown that hypoxia enhances the expression of stemness markers and increases the number of stem cells (Chen et al., 2015). In the light of these observations, it would be plausible to estimate the impact of hypoxia on stemness/ability to differentiate and the bioenergetic profile of CSCs.

The second limitation concerns the phenotypic diversity of cancer initiating cells or CSCs. Here, we compared undifferentiated with differentiated cancer cells. However, it should be taken into consideration that undifferentiated cell culture may contain

several genetic subclones in distinct differentiation states including spontaneously differentiated cells. Furthermore, distinct subpopulations of CSCs may represent different metabolic and bioenergetic properties (Fiorillo et al., 2019). Studying the features of cancer cells in the context of independent subclones is essential as all subclones and the corresponding CSCs need to be eradicated for successful treatment. In addition, cancer cell lines may not represent the whole repertoire of subclones present in the primary tumor. Therefore, future investigations using CSCs derived from patients' tumors are necessary to validate the kinds of conclusions that can be drawn from this study.

5.5 Concluding remarks and future directions

This research aimed to investigate the relationship between cellular differentiation and the energy metabolism of cancer cells. By comparing the bioenergetic profiles of cancer cells in distinct differentiation states, it can be concluded that cellular differentiation is accompanied by profound alterations in the energy producing and transferring pathways. Human embryonal carcinoma stem cells as well as undifferentiated neuroblastoma and colon adenocarcinoma cells were found to share a common bioenergetic signature characterized by reduced oxidative metabolism compensated by increased glycolysis and shifted phosphotransfer towards adenylate kinase network. Treatment of cells with differentiation agents was able to reverse these cancer-induced alterations. Moreover, adenylate kinase network was identified as an important player in the regulation of metabolic plasticity of cancer cells. However, the effect of cellular differentiation or certain differentiation agents on the phosphotransfer system should be further examined in depth at the molecular level. Nevertheless, a deeper focus on the mechanisms that support metabolic plasticity of cancer cells and allow them to survive in harsh microenvironmental conditions would provide novel more effective targets for anti-cancer therapy.

6 Conclusions

- The bioenergetic profile of embryonal carcinoma stem cells clearly distinguished them from normal embryonal stem cells (*Paper I*):
 - Embryonal carcinoma cells had reduced respiration and stronger coupling between HK and OXPHOS compared to normal embryonal stem cells
 - The phosphotransfer system of embryonal carcinoma stem cells was shifted towards AK network
- An organization of phosphotransfer systems depended on the differentiation state of the cell (*Papers II and III*):
 - Undifferentiated colon cancer cells and neuroblastoma cells displayed reduced CK activity compensated by increased AK activity
 - Induction of cellular differentiation reversed cancer-induced alterations in the phosphotransfer system increasing CK activity and reducing AK activity
- The response of phosphotransfer system to the butyrate treatment was modulated by the availability of glutamine in the growth medium (*Paper II*)

List of Figures

Figure 1. Cancer heterogeneity appears at many different levels.	11
Figure 2. Models explaining phenotypic heterogeneity of cancer cells.	12
Figure 3. Metabolic pathways that undergo remodeling in cancer.	13
Figure 4. Integrated communication between cellular sites of ATP-consumption and ATP-generation facilitated by glycolytic phosphotransfer system.	17
Figure 5. Creatine kinase and adenylate kinase phosphotransfer networks.	18
Figure 6. Design of the study	23
Figure 7. Mitochondrial localization in hESC and 2102Ep cells.	25
Figure 8. Respiratory properties of hESC and 2102Ep cells.	26
Figure 9. Assessment of mitochondrial function in hESCs and 2102Ep cells.	27
Figure 10. Effect of exogenously added glucose on the rate of oxygen consumption. ...	28
Figure 11. Effect of NaBT on the Caco-2 cell growth.	30
Figure 12. Confocal microscopy of untreated and sodium butyrate (NaBT)-treated Caco-2 cells.	31
Figure 13. Treatment with sodium butyrate induces an increase in oxidative metabolism of Caco-2 cells	32
Figure 14. The contribution of glycolysis and oxidative phosphorylation to ATP production.....	33
Figure 15. Intracellular location of adenylate kinase 1 (AK1) and adenylate kinase 2 (AK2) in Neuro-2a cells and cardiomyocytes.	36
Figure 16. Rearrangement of phosphotransfer system after treatment of Caco-2 cells with sodium butyrate.....	38

List of Tables

Table 1. Phosphotransfer enzymes in cancer	20
Table 2. AK and CK enzymatical activities	34
Table 3. AK1 and AK2 distribution in normal and cancer cells/tissues.	35

References

- Abu Dawud, R., Schreiber, K., Schomburg, D., and Adjaye, J. (2012). Human embryonic stem cells and embryonal carcinoma cells have overlapping and distinct metabolic signatures. *PLoS One* 7, e39896.
- Al-Hajj, M., Wicha, M.S., Benito-Hernandez, A., Morrison, S.J., and Clarke, M.F. (2003). Prospective identification of tumorigenic breast cancer cells. *Proc. Natl. Acad. Sci.* 100, 3983–3988.
- Alcarraz-Vizán, G., Boren, J., Lee, W.-N.P., and Cascante, M. (2010). Histone deacetylase inhibition results in a common metabolic profile associated with HT29 differentiation. *Metabolomics* 6, 229–237.
- Amamoto, R., Uchiumi, T., Yagi, M., Monji, K., Song, Y., Oda, Y., Shiota, M., Yokomizo, A., Naito, S., and Kang, D. (2016). The Expression of Ubiquitous Mitochondrial Creatine Kinase Is Downregulated as Prostate Cancer Progression. *J. Cancer* 7, 50–59.
- Amoêdo, N.D., Rodrigues, M.F., Pezzuto, P., Galina, A., da Costa, R.M., de Almeida, F.C.L., El-Bacha, T., and Rumjanek, F.D. (2011). Energy Metabolism in H460 Lung Cancer Cells: Effects of Histone Deacetylase Inhibitors. *PLoS One* 6, e22264.
- Anderson, A.R.A., Weaver, A.M., Cummings, P.T., and Quaranta, V. (2006). Tumor Morphology and Phenotypic Evolution Driven by Selective Pressure from the Microenvironment. *Cell* 127, 905–915.
- Bai, D., Zhang, J., Li, T., Hang, R., Liu, Y., Tian, Y., Huang, D., Qu, L., Cao, X., Ji, J., et al. (2016). The ATPase hCINAP regulates 18S rRNA processing and is essential for embryogenesis and tumor growth. *Nat. Commun.* 7, 12310.
- Bingham, S.A., Day, N.E., Luben, R., Ferrari, P., Slimani, N., Norat, T., Clavel-Chapelon, F., Kesse, E., Nieters, A., Boeing, H., et al. (2003). Dietary fibre in food and protection against colorectal cancer in the European Prospective Investigation into Cancer and Nutrition (EPIC): an observational study. *Lancet (London, England)* 361, 1496–1501.
- Birkenmeier, K., Dröse, S., Wittig, I., Winkelmann, R., Käfer, V., Döring, C., Hartmann, S., Wenz, T., Reichert, A.S., Brandt, U., et al. (2016). Hodgkin and Reed-Sternberg cells of classical Hodgkin lymphoma are highly dependent on oxidative phosphorylation. *Int. J. Cancer* 138, 2231–2246.
- Blouin, J.-M., Penot, G., Collinet, M., Nacfer, M., Forest, C., Laurent-Puig, P., Coumoul, X., Barouki, R., Benelli, C., and Bortoli, S. (2011). Butyrate elicits a metabolic switch in human colon cancer cells by targeting the pyruvate dehydrogenase complex. *Int. J. Cancer* 128, 2591–2601.
- Chekulayev, V., Mado, K., Shevchuk, I., Koit, A., Kaldma, A., Klepinin, A., Timohhina, N., Tepp, K., Kandashvili, M., Ounpuu, L., et al. (2015). Metabolic remodeling in human colorectal cancer and surrounding tissues: alterations in regulation of mitochondrial respiration and metabolic fluxes. *Biochem. Biophys. Reports* 4, 111–125.
- Chen, H.-C., Lee, J.-T., Shih, C.-P., Chao, T.-T., Sytwu, H.-K., Li, S.-L., Fang, M.-C., Chen, H.-K., Lin, Y.-C., Kuo, C.-Y., et al. (2015). Hypoxia Induces a Metabolic Shift and Enhances the Stemness and Expansion of Cochlear Spiral Ganglion Stem/Progenitor Cells. *Biomed Res. Int.* 2015, 359537.

- Chen, R.-P., Liu, C.-Y., Shao, H.-L., Zheng, W.-W., Wang, J.-X., and Zhao, X.-F. (2012). Adenylate kinase 2 (AK2) promotes cell proliferation in insect development. *BMC Mol. Biol.* *13*, 31.
- Cho, E.S., Cha, Y.H., Kim, H.S., Kim, N.H., and Yook, J.I. (2018). The Pentose Phosphate Pathway as a Potential Target for Cancer Therapy. *Biomol. Ther. (Seoul)*. *26*, 29–38.
- Choi, S.W., Gerencser, A.A., and Nicholls, D.G. (2009). Bioenergetic analysis of isolated cerebrocortical nerve terminals on a microgram scale: spare respiratory capacity and stochastic mitochondrial failure. *J. Neurochem.* *109*, 1179–1191.
- Chung, W.J., Lyons, S.A., Nelson, G.M., Hamza, H., Gladson, C.L., Gillespie, G.Y., and Sontheimer, H. (2005). Inhibition of Cystine Uptake Disrupts the Growth of Primary Brain Tumors. *J. Neurosci.* *25*, 7101–7110.
- Clausen, M.R., Bonnén, H., and Mortensen, P.B. (1991). Colonic fermentation of dietary fibre to short chain fatty acids in patients with adenomatous polyps and colonic cancer. *Gut* *32*, 923–928.
- Clavell, L.A., Gelber, R.D., Cohen, H.J., Hitchcock-Bryan, S., Cassady, J.R., Tarbell, N.J., Blattner, S.R., Tantravahi, R., Leavitt, P., and Sallan, S.E. (1986). Four-Agent Induction and Intensive Asparaginase Therapy for Treatment of Childhood Acute Lymphoblastic Leukemia. *N. Engl. J. Med.* *315*, 657–663.
- Collavin, L., Lazarevic, D., Utrera, R., Marzinotto, S., Monte, M., and Schneider, C. (1999). wt p53 dependent expression of a membrane-associated isoform of adenylate kinase. *Oncogene* *18*, 5879–5888.
- Dagogo-Jack, I., and Shaw, A.T. (2017). Tumor heterogeneity and resistance to cancer therapies. *Nat. Rev. Clin. Oncol.* *15*, 81–94.
- DeBerardinis, R.J., and Chandel, N.S. (2016). Fundamentals of cancer metabolism. *Sci. Adv.* *2*, e1600200.
- DeBerardinis, R.J., Lum, J.J., Hatzivassiliou, G., and Thompson, C.B. (2008). The Biology of Cancer: Metabolic Reprogramming Fuels Cell Growth and Proliferation. *Cell Metab.* *7*, 11–20.
- DeNicola, G.M., and Cantley, L.C. (2015). Cancer’s Fuel Choice: New Flavors for a Picky Eater. *Mol. Cell* *60*, 514–523.
- Desler, C., Hansen, T.L., Frederiksen, J.B., Marcker, M.L., Singh, K.K., and Juel Rasmussen, L. (2012). Is There a Link between Mitochondrial Reserve Respiratory Capacity and Aging? *J. Aging Res.* *2012*, 192503.
- Donohoe, D.R., Collins, L.B., Wali, A., Bigler, R., Sun, W., and Bultman, S.J. (2012). The Warburg effect dictates the mechanism of butyrate-mediated histone acetylation and cell proliferation. *Mol. Cell* *48*, 612–626.
- Dranka, B.P., Hill, B.G., and Darley-Usmar, V.M. (2010). Mitochondrial reserve capacity in endothelial cells: The impact of nitric oxide and reactive oxygen species. *Free Radic. Biol. Med.* *48*, 905–914.
- Dzeja, P., and Terzic, A. (2009). Adenylate Kinase and AMP Signaling Networks: Metabolic Monitoring, Signal Communication and Body Energy Sensing. *Int. J. Mol. Sci.* *10*, 1729–1772.
- Dzeja, P.P., and Terzic, A. (2003). Phosphotransfer networks and cellular energetics. *J. Exp. Biol.* *206*, 2039–2047.
- Dzeja, P.P., Terzic, A., and Wieringa, B. (2004) Phosphotransfer dynamics in skeletal muscle from creatine kinase gene-deleted mice. *Mol. Cell. Biochem.* *256–257*, 13–27.

- Dzeja, P.P., Chung, S., Faustino, R.S., Behfar, A., and Terzic, A. (2011). Developmental enhancement of adenylate kinase-AMPK metabolic signaling axis supports stem cell cardiac differentiation. *PLoS One* *6*, e19300.
- Eramo, A., Lotti, F., Sette, G., Pilozzi, E., Biffoni, M., Di Virgilio, A., Conticello, C., Ruco, L., Peschle, C., and De Maria, R. (2008). Identification and expansion of the tumorigenic lung cancer stem cell population. *Cell Death Differ.* *15*, 504–514.
- Fan, J., Kamphorst, J.J., Mathew, R., Chung, M.K., White, E., Shlomi, T., and Rabinowitz, J.D. (2013). Glutamine-driven oxidative phosphorylation is a major ATP source in transformed mammalian cells in both normoxia and hypoxia. *Mol. Syst. Biol.* *9*, 712.
- Fiorillo, M., Sotgia, F., and Lisanti, M.P. (2019). “Energetic” Cancer Stem Cells (e-CSCs): A New Hyper-Metabolic and Proliferative Tumor Cell Phenotype, Driven by Mitochondrial Energy. *Front. Oncol.* *8*, 677.
- Flavahan, W.A., Wu, Q., Hitomi, M., Rahim, N., Kim, Y., Sloan, A.E., Weil, R.J., Nakano, I., Sarkaria, J.N., Stringer, B.W., et al. (2013). Brain tumor initiating cells adapt to restricted nutrition through preferential glucose uptake. *Nat. Neurosci.* *16*, 1373–1382.
- Fogh, J. (1975). *Human tumor cells in vitro* (Springer Science+Business Media).
- Friedman, D.B., Hill, S., Keller, J.W., Merchant, N.B., Levy, S.E., Coffey, R.J., and Caprioli, R.M. (2004). Proteome analysis of human colon cancer by two-dimensional difference gel electrophoresis and mass spectrometry. *Proteomics* *4*, 793–811.
- Fujisawa, K., Terai, S., Takami, T., Yamamoto, N., Yamasaki, T., Matsumoto, T., Yamaguchi, K., Owada, Y., Nishina, H., Noma, T., et al. (2016). Modulation of anti-cancer drug sensitivity through the regulation of mitochondrial activity by adenylate kinase 4. *J. Exp. Clin. Cancer Res.* *35*, 48.
- Gallo, M., Sapio, L., Spina, A., Naviglio, D., Calogero, A., and Naviglio, S. (2015). Lactic dehydrogenase and cancer: an overview. *Front. Biosci. (Landmark Ed.)* *20*, 1234–1249.
- Gonçalves, P., and Martel, F. (2013). Butyrate and Colorectal Cancer: The Role of Butyrate Transport. *Curr. Drug Metab.* *14*, 994–1008.
- Gong, G., Liu, J., Liang, P., Guo, T., Hu, Q., Ochiai, K., Hou, M., Ye, Y., Wu, X., Mansoor, A., et al. (2003). Oxidative capacity in failing hearts. *Am. J. Physiol. Circ. Physiol.* *285*, H541–H548.
- Grzywa, T.M., Paskal, W., and Włodarski, P.K. (2017). Intratumor and Intertumor Heterogeneity in Melanoma. *Transl. Oncol.* *10*, 956–975.
- Hanahan, D., and Weinberg, R.A. (2011). Hallmarks of Cancer: The Next Generation. *Cell* *144*, 646–674.
- Haraguchi, N., Ohkuma, M., Sakashita, H., Matsuzaki, S., Tanaka, F., Mimori, K., Kamohara, Y., Inoue, H., and Mori, M. (2008). CD133+CD44+ Population Efficiently Enriches Colon Cancer Initiating Cells. *Ann. Surg. Oncol.* *15*, 2927–2933.
- Vander Heiden, M.G., Cantley, L.C., and Thompson, C.B. (2009). Understanding the Warburg Effect: The Metabolic Requirements of Cell Proliferation. *Science* (80-.). *324*, 1029–1033.
- Hsu, P.P., and Sabatini, D.M. (2008). Cancer Cell Metabolism: Warburg and Beyond. *Cell* *134*, 703–707.
- Ishijima, N., Kanki, K., Shimizu, H., and Shiota, G. (2015). Activation of AMP-activated protein kinase by retinoic acid sensitizes hepatocellular carcinoma cells to apoptosis induced by sorafenib. *Cancer Sci.* *106*, 567–575.

- Israelsen, W.J., and Vander Heiden, M.G. (2015). Pyruvate kinase: Function, regulation and role in cancer. *Semin. Cell Dev. Biol.* *43*, 43–51.
- Jan, Y.-H., Tsai, H.-Y., Yang, C.-J., Huang, M.-S., Yang, Y.-F., Lai, T.-C., Lee, C.-H., Jeng, Y.-M., Huang, C.-Y., Su, J.-L., et al. (2012). Adenylate Kinase-4 Is a Marker of Poor Clinical Outcomes That Promotes Metastasis of Lung Cancer by Downregulating the Transcription Factor ATF3. *Cancer Res.* *72*, 5119–5129.
- Ji, Y., Yang, C., Tang, Z., Yang, Y., Tian, Y., Yao, H., Zhu, X., Zhang, Z., Ji, J., and Zheng, X. (2017). Adenylate kinase hCINAP determines self-renewal of colorectal cancer stem cells by facilitating LDHA phosphorylation. *Nat. Commun.* *8*, 15308.
- Jones, R.G., and Thompson, C.B. (2009). Tumor suppressors and cell metabolism: a recipe for cancer growth. *Genes Dev.* *23*, 537–548.
- Jose, C., Bellance, N., and Rossignol, R. (2011). Choosing between glycolysis and oxidative phosphorylation: A tumor's dilemma? *Biochim. Biophys. Acta - Bioenerg.* *1807*, 552–561.
- Kaambre, T., Chekulayev, V., Shevchuk, I., Karu-Varikmaa, M., Timohhina, N., Tepp, K., Bogovskaja, J., Kütner, R., Valvere, V., and Saks, V. (2012). Metabolic control analysis of cellular respiration in situ in intraoperational samples of human breast cancer. *J. Bioenerg. Biomembr.* *44*, 539–558.
- Kaiko, G.E., Ryu, S.H., Koues, O.I., Pearce, E.L., Oltz, E.M., and Stappenbeck Correspondence, T.S. (2016). The Colonic Crypt Protects Stem Cells from Microbiota-Derived Metabolites. *Cell* *165*.
- Kaldma, A., Klepinin, A., Chekulayev, V., Mado, K., Shevchuk, I., Timohhina, N., Tepp, K., Kandashvili, M., Varikmaa, M., Koit, A., et al. (2014). An in situ study of bioenergetic properties of human colorectal cancer: The regulation of mitochondrial respiration and distribution of flux control among the components of ATP synthasome. *Int. J. Biochem. Cell Biol.* *55*, 171–186.
- Keenan, M.M., and Chi, J.-T. (2015). Alternative fuels for cancer cells. *Cancer J.* *21*, 49–55.
- Kim, H., Lee, H.-J., Oh, Y., Choi, S.-G., Hong, S.-H., Kim, H.-J., Lee, S.-Y., Choi, J.-W., Su Hwang, D., Kim, K.-S., et al. (2014). The DUSP26 phosphatase activator adenylate kinase 2 regulates FADD phosphorylation and cell growth. *Nat. Commun.* *5*, 3351.
- Klepinin, A., Chekulayev, V., Timohhina, N., Shevchuk, I., Tepp, K., Kaldma, A., Koit, A., Saks, V., and Kaambre, T. (2014). Comparative analysis of some aspects of mitochondrial metabolism in differentiated and undifferentiated neuroblastoma cells. *J. Bioenerg. Biomembr.* *46*, 17–31.
- Klepinin, A., Ounpuu, L., Guzun, R., Chekulayev, V., Timohhina, N., Tepp, K., Shevchuk, I., Schlattner, U., and Kaambre, T. (2016). Simple oxygraphic analysis for the presence of adenylate kinase 1 and 2 in normal and tumor cells. *J. Bioenerg. Biomembr.* *48*, 531–548.
- Kong, F., Binas, B., Moon, J.H., Kang, S.S., and Kim, H.J. (2013). Differential expression of adenylate kinase 4 in the context of disparate stress response strategies of HEK293 and HepG2 cells. *Arch. Biochem. Biophys.* *533*, 11–17.
- Kreis, W., Baker, A., Ryan, V., and Bertasso, A. (1980). Effect of nutritional and enzymatic methionine deprivation upon human normal and malignant cells in tissue culture. *Cancer Res.* *40*, 634–641.

- Lam, Y.W., Yuan, Y., Isaac, J., Babu, C.V.S., Meller, J., and Ho, S.-M. (2010). Comprehensive identification and modified-site mapping of S-nitrosylated targets in prostate epithelial cells. *PLoS One* *5*, e9075.
- Lamb, R., Bonuccelli, G., Ozsvári, B., Peiris-Pagès, M., Fiorillo, M., Smith, D.L., Bevilacqua, G., Mazzanti, C.M., McDonnell, L.A., Naccarato, A.G., et al. (2015). Mitochondrial mass, a new metabolic biomarker for stem-like cancer cells: Understanding WNT/FGF-driven anabolic signaling. *Oncotarget* *6*, 30453–30471.
- Lapidot, T., Sirard, C., Vormoor, J., Murdoch, B., Hoang, T., Caceres-Cortes, J., Minden, M., Paterson, B., Caligiuri, M.A., and Dick, J.E. (1994). A cell initiating human acute myeloid leukaemia after transplantation into SCID mice. *Nature* *367*, 645–648.
- Lee, H.-J., Pyo, J.-O., Oh, Y., Kim, H.-J., Hong, S., Jeon, Y.-J., Kim, H., Cho, D.-H., Woo, H.-N., Song, S., et al. (2007). AK2 activates a novel apoptotic pathway through formation of a complex with FADD and caspase-10. *Nat. Cell Biol.* *9*, 1303–1310.
- Li, Q., Cao, L., Tian, Y., Zhang, P., Ding, C., Lu, W., Jia, C., Shao, C., Liu, W., Wang, D., et al. (2018). Butyrate Suppresses the Proliferation of Colorectal Cancer Cells via Targeting Pyruvate Kinase M2 and Metabolic Reprogramming. *Mol. Cell. Proteomics* *17*, 1531–1545.
- Li, W., Saud, S.M., Young, M.R., Chen, G., and Hua, B. (2015). Targeting AMPK for cancer prevention and treatment. *Oncotarget* *6*, 7365–7378.
- Liu, L., He, Y., Ge, G., Li, L., Zhou, P., Zhu, Y., Tang, H., Huang, Y., Li, W., and Zhang, L. (2017). Lactate dehydrogenase and creatine kinase as poor prognostic factors in lung cancer: A retrospective observational study. *PLoS One* *12*, e0182168.
- Liu, Y., Wu, K., Shi, L., Xiang, F., Tao, K., and Wang, G. (2016). Prognostic Significance of the Metabolic Marker Hexokinase-2 in Various Solid Tumors: A Meta-Analysis. *PLoS One* *11*, e0166230.
- Locasale, J.W. (2013). Serine, glycine and one-carbon units: cancer metabolism in full circle. *Nat. Rev. Cancer* *13*, 572–583.
- Loo, J.M., Scherl, A., Nguyen, A., Man, F.Y., Weinberg, E., Zeng, Z., Saltz, L., Paty, P.B., and Tavazoie, S.F. (2015). Extracellular Metabolic Energetics Can Promote Cancer Progression. *Cell* *160*, 393–406.
- Martinez-Outschoorn, U.E., Peiris-Pagés, M., Pestell, R.G., Sotgia, F., and Lisanti, M.P. (2017). Cancer metabolism: a therapeutic perspective. *Nat. Rev. Clin. Oncol.* *14*, 11–31.
- Martínez-Reyes, I., Diebold, L.P., Kong, H., Schieber, M., Huang, H., Hensley, C.T., Mehta, M.M., Wang, T., Santos, J.H., Woychik, R., et al. (2016). TCA Cycle and Mitochondrial Membrane Potential Are Necessary for Diverse Biological Functions. *Mol. Cell* *61*, 199–209.
- Masters, C.J., Reid, S., and Don, M. (1987). Glycolysis--new concepts in an old pathway. *Mol. Cell. Biochem.* *76*, 3–14.
- Mathupala, S.P., Ko, Y.H., and Pedersen, P.L. (2006). Hexokinase II: cancer's double-edged sword acting as both facilitator and gatekeeper of malignancy when bound to mitochondria. *Oncogene* *25*, 4777–4786.
- McLeish, M.J., and Kenyon, G.L. (2005). Relating structure to mechanism in creatine kinase. *Crit. Rev. Biochem. Mol. Biol.* *40*, 1–20.
- Miller, A.A., Kurschel, E., Osieka, R., and Schmidt, C.G. (1987). Clinical pharmacology of sodium butyrate in patients with acute leukemia. *Eur. J. Cancer Clin. Oncol.* *23*, 1283–1287.

- Muz, B., de la Puente, P., Azab, F., and Azab, A.K. (2015). The role of hypoxia in cancer progression, angiogenesis, metastasis, and resistance to therapy. *Hypoxia (Auckland, N.Z.)* 3, 83–92.
- Nowell, P.C. (1976). The clonal evolution of tumor cell populations. *Science* 194, 23–28.
- Ohtawa, K., Ueno, T., Mitsui, K., Kodera, Y., Hiroto, M., Matsushima, A., Nishimura, H., and Inada, Y. (1998). Apoptosis of leukemia cells induced by valine-deficient medium. *Leukemia* 12, 1651–1652.
- Onda, T., Uzawa, K., Endo, Y., Bukawa, H., Yokoe, H., Shibahara, T., and Tanzawa, H. (2006). Ubiquitous mitochondrial creatine kinase downregulated in oral squamous cell carcinoma. *Br. J. Cancer* 94, 698–709.
- Ottaway, J.H., and Mowbray, J. (1977). The role of compartmentation in the control of glycolysis. *Curr. Top. Cell. Regul.* 12, 107–208.
- Pan, H., Xia, K., Zhou, W., Xue, J., Liang, X., Cheng, L., Wu, N., Liang, M., Wu, D., Ling, L., et al. (2013). Low serum creatine kinase levels in breast cancer patients: a case-control study. *PLoS One* 8, e62112.
- Panayiotou, C., Solaroli, N., and Karlsson, A. (2014). The many isoforms of human adenylate kinases. *Int. J. Biochem. Cell Biol.* 49, 75–83.
- Pastò, A., Bellio, C., Pilotto, G., Ciminale, V., Silic-Benussi, M., Guzzo, G., Rasola, A., Frasson, C., Nardo, G., Zulato, E., et al. (2014). Cancer stem cells from epithelial ovarian cancer patients privilege oxidative phosphorylation, and resist glucose deprivation. *Oncotarget* 5.
- Patra, S., Bera, S., SinhaRoy, S., Ghoshal, S., Ray, S., Basu, A., Schlattner, U., Wallimann, T., and Ray, M. (2008). Progressive decrease of phosphocreatine, creatine and creatine kinase in skeletal muscle upon transformation to sarcoma. *FEBS J.* 275, 3236–3247.
- Pedersen, P.L. (2007). Warburg, me and Hexokinase 2: Multiple discoveries of key molecular events underlying one of cancers' most common phenotypes, the "Warburg Effect", i.e., elevated glycolysis in the presence of oxygen. *J. Bioenerg. Biomembr.* 39, 211–222.
- Peiris-Pagès, M., Martinez-Outschoorn, U.E., Pestell, R.G., Sotgia, F., and Lisanti, M.P. (2016). Cancer stem cell metabolism. *Breast Cancer Res.* 18, 55.
- Peng, L., Li, Z.-R., Green, R.S., Holzman, I.R., and Lin, J. (2009). Butyrate Enhances the Intestinal Barrier by Facilitating Tight Junction Assembly via Activation of AMP-Activated Protein Kinase in Caco-2 Cell Monolayers. *J. Nutr.* 139, 1619–1625.
- Phan, L.M., Yeung, S.-C.J., and Lee, M.-H. (2014). Cancer metabolic reprogramming: importance, main features, and potentials for precise targeted anti-cancer therapies. *Cancer Biol. Med.* 11, 1–19.
- Prince, M.E., Sivanandan, R., Kaczorowski, A., Wolf, G.T., Kaplan, M.J., Dalerba, P., Weissman, I.L., Clarke, M.F., and Ailles, L.E. (2007). Identification of a subpopulation of cells with cancer stem cell properties in head and neck squamous cell carcinoma. *Proc. Natl. Acad. Sci.* 104, 973–978.
- Pucar, D., Bast, P., Gumina, R.J., Lim, L., Drahl, C., Juranic, N., Macura, S., Janssen, E., Wieringa, B., Terzic, A., et al. (2002). Adenylate kinase AK1 knockout heart: energetics and functional performance under ischemia-reperfusion. *Am. J. Physiol. Circ. Physiol.* 283, H776–H782.
- Ricci-Vitiani, L., Lombardi, D.G., Pilozzi, E., Biffoni, M., Todaro, M., Peschle, C., and De Maria, R. (2007). Identification and expansion of human colon-cancer-initiating cells. *Nature* 445, 111–115.

- Rodrigues, M.F., Carvalho, É., Pezzuto, P., Rumjanek, F.D., and Amoêdo, N.D. (2015). Reciprocal Modulation of Histone Deacetylase Inhibitors Sodium Butyrate and Trichostatin A on the Energy Metabolism of Breast Cancer Cells. *J. Cell. Biochem.* *116*, 797–808.
- Sambu, Y., De Angelis, I., Ranaldi, G., Scarino, M.L., Stammati, A., and Zucco, F. (2005). The Caco-2 cell line as a model of the intestinal barrier: influence of cell and culture-related factors on Caco-2 cell functional characteristics. *Cell Biol. Toxicol.* *21*, 1–26.
- Sansbury, B.E., Jones, S.P., Riggs, D.W., Darley-Usmar, V.M., and Hill, B.G. (2011). Bioenergetic function in cardiovascular cells: the importance of the reserve capacity and its biological regulation. *Chem. Biol. Interact.* *191*, 288–295.
- Scalise, M., Pochini, L., Galluccio, M., Console, L., and Indiveri, C. (2017). Glutamine Transport and Mitochondrial Metabolism in Cancer Cell Growth. *Frontiers in oncology* *7*, 306.
- Schlattner, U., Tokarska-Schlattner, M., and Wallimann, T. (2006). Mitochondrial creatine kinase in human health and disease. *Biochim. Biophys. Acta - Mol. Basis Dis.* *1762*, 164–180.
- Scott, L., Lamb, J., Smith, S., and Wheatley, D.N. (2000). Single amino acid (arginine) deprivation: rapid and selective death of cultured transformed and malignant cells. *Br. J. Cancer* *83*, 800–810.
- Shackleton, M., Quintana, E., Fearon, E.R., and Morrison, S.J. (2009). Heterogeneity in Cancer: Cancer Stem Cells versus Clonal Evolution. *Cell* *138*, 822–829.
- Sheen, J.-H., Zoncu, R., Kim, D., and Sabatini, D.M. (2011). Defective Regulation of Autophagy upon Leucine Deprivation Reveals a Targetable Liability of Human Melanoma Cells In Vitro and In Vivo. *Cancer Cell* *19*, 613–628.
- Shin, J., Carr, A., Corner, G.A., Tögel, L., Dávaos-Salas, M., Tran, H., Chueh, A.C., Al-Obaidi, S., Chionh, F., Ahmed, N., et al. (2014). The Intestinal Epithelial Cell Differentiation Marker Intestinal Alkaline Phosphatase (ALPi) Is Selectively Induced by Histone Deacetylase Inhibitors (HDACi) in Colon Cancer Cells in a Kruppel-like Factor 5 (KLF5)-dependent Manner. *J. Biol. Chem.* *289*, 25306.
- Shiroki, T., Yokoyama, M., Tanuma, N., Maejima, R., Tamai, K., Yamaguchi, K., Oikawa, T., Noguchi, T., Miura, K., Fujiya, T., et al. (2017). Enhanced expression of the M2 isoform of pyruvate kinase is involved in gastric cancer development by regulating cancer-specific metabolism. *Cancer Sci.* *108*, 931–940.
- Singh, S.K., Hawkins, C., Clarke, I.D., Squire, J.A., Bayani, J., Hide, T., Henkelman, R.M., Cusimano, M.D., and Dirks, P.B. (2004). Identification of human brain tumor initiating cells. *Nature* *432*, 396–401.
- Six, E., Lagresle-Peyrou, C., Susini, S., De Chappedelaine, C., Sigrist, N., Sadek, H., Chouteau, M., Cagnard, N., Fontenay, M., Hermine, O., et al. (2015). AK2 deficiency compromises the mitochondrial energy metabolism required for differentiation of human neutrophil and lymphoid lineages. *Cell Death Dis.* *6*, e1856.
- Speers, C., Tsimelzon, A., Sexton, K., Herrick, A.M., Gutierrez, C., Culhane, A., Quackenbush, J., Hilsenbeck, S., Chang, J., and Brown, P. (2009). Identification of Novel Kinase Targets for the Treatment of Estrogen Receptor-Negative Breast Cancer. *Clin. Cancer Res.* *15*, 6327–6340.

- Vasseur, S., Malicet, C., Calvo, E.L., Dagorn, J., and Iovanna, J.L. (2005). Gene expression profiling of tumors derived from rasV12/E1A-transformed mouse embryonic fibroblasts to identify genes required for tumor development. *Mol. Cancer* 4, 4.
- Vermeulen, L., De Sousa E Melo, F., van der Heijden, M., Cameron, K., de Jong, J.H., Borovski, T., Tuynman, J.B., Todaro, M., Merz, C., Rodermond, H., et al. (2010). Wnt activity defines colon cancer stem cells and is regulated by the microenvironment. *Nat. Cell Biol.* 12, 468–476.
- Visvader, J.E. (2011). Cells of origin in cancer. *Nature* 469, 314–322.
- Wallimann, T., and Hemmer, W. Creatine kinase in non-muscle tissues and cells. *Mol. Cell. Biochem.* 133–134, 193–220.
- Wallimann, T., Wyss, M., Brdiczka, D., Nicolay, K., and Eppenberger, H.M. (1992). Intracellular compartmentation, structure and function of creatine kinase isoenzymes in tissues with high and fluctuating energy demands: the “phosphocreatine circuit” for cellular energy homeostasis. *Biochem. J.* 281 (Pt 1), 21–40.
- Whitaker-Menezes, D., Martinez-Outschoorn, U.E., Flomenberg, N., Birbe, R.C., Witkiewicz, A.K., Howell, A., Pavlides, S., Tsigos, A., Ertel, A., Pestell, R.G., et al. (2011). Hyperactivation of oxidative mitochondrial metabolism in epithelial cancer cells in situ: visualizing the therapeutic effects of metformin in tumor tissue. *Cell Cycle* 10, 4047–4064.
- Wu, J., Hu, L., Wu, F., Zou, L., and He, T. (2017). Poor prognosis of hexokinase 2 overexpression in solid tumors of digestive system: a meta-analysis. *Oncotarget* 8.
- Yan, Y.-B. (2016). Creatine kinase in cell cycle regulation and cancer. *Amino Acids* 48, 1775–1784.
- Zarghami, N., Giai, M., Yu, H., Roagna, R., Ponzzone, R., Katsaros, D., Sismondi, P., and Diamandis, E.P. (1996). Creatine kinase BB isoenzyme levels in tumor cytosols and survival of breast cancer patients. *Br. J. Cancer* 73, 386–390.
- Zhang, Y., Li, H., Wang, X., Gao, X., and Liu, X. (2009). Regulation of T cell development and activation by creatine kinase B. *PLoS One* 4, e5000.
- Zhou, C.-F., Li, X.-B., Sun, H., Zhang, B., Han, Y.-S., Jiang, Y., Zhuang, Q.-L., Fang, J., and Wu, G.-H. Research Communication Pyruvate Kinase Type M2 Is Upregulated in Colorectal Cancer and Promotes Proliferation and Migration of Colon Cancer Cells.

Acknowledgements

This work has been partially supported by “TUT Institutional Development Program for 2016-2022” Graduate School in Biomedicine and Biotechnology receiving funding from the European Regional Development Fund under program ASTRA 2014-2020.4.01.16-0032 in Estonia.

Many people have influenced me personally and academically over the years that culminate in this thesis. This thesis is as much an attribute to them and their excellence as it is an example of my academic achievement.

First and foremost, I am extremely grateful to my supervisor, Dr. Tuuli Käämbre, for valuable suggestions, encouragement and patient guidance throughout my PhD study.

My sincere thanks also go to the collaborators from the Institute of Molecular and Cell Biology and Institute of Biomedicine and Translational Medicine at the University of Tartu for lending me their expertise to my scientific and technical problems. I would like to thank Prof. Toivo Maimets, Prof. Kalju Paju, Dr. Martin Pook and Indrek Teino for their help and insightful comments, but also for the questions which intended me to widen my research from various perspectives. Special thanks go to Nadežda Peet for exceptional helpfulness and creating such a positive working environment during her assistance in oxygraphic experiments.

I would like to thank all my colleagues from the Laboratory of Chemical Biology for stimulating discussions, continuous support and immense knowledge.

I am grateful to my course mates, Jekaterina, Valentina and Julia, for their help, our fruitful discussions and continuous support through this entire process.

This journey would not have been possible without the support of my family. The deepest gratitude goes to my mother, who has been a constant source of support and encouragement. My warmest thanks go to my husband and son, who have inspired me with their love and caring.

Abstract

Rearrangement of energy metabolism during differentiation of cancer cells

Tumor initiating or cancer stem cells are populations of cancer cells that can both self-renew and give rise to many cell types that constitute the tumor. These cells are considered to be responsible for tumor growth and development, reoccurrence of the disease after treatment, formation of metastasis and drug resistance. In the light of recent discoveries, the unique bioenergetic phenotype of cancer initiating cells may serve as an attractive target for more effective cancer therapy.

The aim of the current study was to uncover the relationship between cellular differentiation and the energy metabolism of cancer cells. The bioenergetic profiles of cancer cells in distinct differentiation states were characterized and compared. Three essential aspects of cellular bioenergetics were analyzed: oxidative phosphorylation, glycolysis and phosphotransfer network.

Human embryonal carcinoma stem cells as well as undifferentiated neuroblastoma and colon adenocarcinoma cells were found to share a common bioenergetic signature characterized by reduced oxidative metabolism compensated by increased glycolysis and shifted phosphotransfer towards adenylate kinase network. Cellular differentiation induced profound alterations in the energy producing and transferring pathways resulting in the phenotype similar to that in healthy cells. Adenylate kinase network was identified as an important player in the regulation of metabolic plasticity of cancer cells.

Lühikokkuvõte

Energiametabolismi ümberkorraldamine kasvajarakkude diferentseerimisel

Vähk on tuntud kui väga heterogeenne haigus. Üks ja sama kasvaja võib sisaldada erinevates proliferatsiooni ja diferentseerumise astmetes olevaid rakke. Vähem diferentseerunud kasvajakke, millel on oma populatsiooni säilitamise ja diferentseerumise võime, kutsutakse kasvaja tüvirakkudeks. Arvatakse, et just need rakud vastutavad kasvaja arengu, metastaseerumise, taastekkimise ja resistentsuse eest. Värskemad uuringud näitavad, et kasvaja tüvirakud on võimelised ümber korraldama oma ainevahetust nii, et saada rohkem energiat kiireks paljunemiseks ja levimiseks organismis. Seega on vähirakkude bioenergeetilise profiili uurimine uus võimalik lähenemine kasvajakprotsesside mõistmisele ning sellest lähtuvalt ka diagnoosimisele ja ravimisele. Kuna kasvaja tüvirakkudel on palju sarnasusi normaalsete tüvirakkudega, siis võib nende vastu suunatud ravi mõjutada negatiivselt normaalsete kudede uuenemist. Seega on väga oluline leida sellised tüvirakkude omadused, mis eristaksid neid nii normaalsetest tüvirakkudest kui ka rohkem diferentseerunud kasvajarakkudest.

Käesoleva doktoritöö eesmärgiks oli välja selgitada seosed kasvajarakkude energiametabolismi ja diferentseerumise vahel. Selleks iseloomustati energiametabolismi erinevate diferentseerumispotentsiaalidega rakkudel: inimese normaalsetes pluripotentsetes tüvirakkudes (H9), nullipotentsetes kartsinoomi tüvirakkudes (2102Ep), diferentseerumata ja diferentseerunud soole adenokartsinoomi (Caco-2) ja neuroblastoomi (Neuro-2A) rakkudes. Energiametabolismi iseloomustamiseks uuriti rakkude hapnikutarbimise võimet, glükoolüütilist aktiivsust ning adenülaat- (AK) ja kreatiinkinaasi (CK) energiaülekanne võrgustikku.

Töö esimeses pooles näidati, et normaalsetes ja kartsinoomi tüvirakkudes rakkude bioenergeetilised profiilid erinevad. Kasvaja tüvirakkudele olid iseloomulikud vähenenud hapnikutarbimise kiirus, suurenenud aeroobse glükolüüsi tase ning nihkunud energiaülekanne AK võrgustiku suunas. Doktoritöö tulemused näitasid, et hapnikutarbimise languse põhjuseks ei saa olla kahjustatud mitokondrid ega mitokondriaalse hingamisahela vähenenud aktiivsus. Mitokondriaalne võimekus ehk lisaenergia, mida rakud saavad kasutada stressi põhjustavate faktoritega toimetulemiseks, oli kartsinoomi tüvirakkudel isegi kõrgem kui normaalsetel tüvirakkudel. Loetletud eripärasused kartsinoomi ja normaalsete tüvirakkude bioenergeetikas aitavad paremini mõista kasvaja tüvirakke toetavaid mehhanisme ning nende põhjal on võimalik välja töötada uudseid meetodeid kasvaja tüvirakkude spetsiifiliseks eristamiseks normaalsetest rakkudest.

Järgnevalt uuriti muutusi energiametabolismis, mis järgnesid adenokartsinoomi ja neuroblastoomi rakkude diferentseerumisele. Tulemustest võib järeldada, et kasvajarakkude diferentseerumisega kaasnevad suured ümberkorraldused energiametabolismis. Eelkõige suureneb oksüdatiivse fosforüülimise osakaal energia tootmisel, millega kaasneb glükolüüsi vähenemine. Samuti toimuvad olulised ümberkorraldused AK ja CK energiaülekanne võrgustikes. Kui diferentseerumata rakud kasutavad peamiselt AK energiatranspordi rada energia homöostaasi säilitamisel, siis kasvajarakkude diferentseerumise käigus asendatakse AK poolt vahendatud rada CK rajaga. Varasemad uuringud näitavad, et soolevähi koes on CK aktiivsus langunud, mis on kompenseeritud suurenenud AK aktiivsusega. Kasvajarakkude diferentseerimine

võimaldas taastada rakkudes energiametabolismi profiili, mis sarnaneb normaalse koega. Seega on kasvajakude diferentseerimisel suur potentsiaal uute ravistrateegiate väljatöötamiseks.

Lisaks kasvaja poolt põhjustatud muutuste kirjeldamisele, on oluline mõista mehhanisme, mida kasvajakud kasutavad oma energiametabolismi säilitamiseks. Kuna meie eelnevad tulemused viitavad suurenenud AK ja CK rollile kasvajakude energiametabolismi ümberprogrammeerimisel, siis püstitati hüpotees, et kasvajakude kohandumine muutuvatele kasvutingimustele on seotud AK ja CK poolt katalüüsitud reaktsioonidega. Töö käigus leiti seos AK aktiivsuse ja glutamiini, ehk olulise süsiniku ja lämmastiku allika, kättesaadavuse vahel. Glutamiini puudumisel säilib soolevähi rakkudes kõrge glükolüütiline aktiivsus isegi peale rakkude diferentseerumist ning AK tõenäoliselt toetab seda. Kuid selleks, et välja selgitada täpsemat mehhanismi, mis seob glutamiini ja glükoosi metabolismi AK poolt katalüüsitud reaktsiooniga, on vaja läbi viia täiendavaid uuringuid.

Kokkuvõttes annab käesolev doktoritöö põhjaliku ülevaate kasvajakude diferentseerumise käigus toimuvatest ümberkorraldustest energiametabolismis. Need uuringud annavad väljundi ka onkoloogia-alastesse teadmistesse, mis aitavad paremini mõista kasvaja tekkimise ja arenemise mehhanisme ning seeläbi välja töötada senisest paremaid ravimeetodeid.

Appendix 1

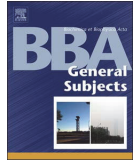
Publication I

Ounpuu, L., Klepinin, A., Pook, M., Teino, I., Peet, N., Paju, K., Tepp, K., Chekulayev, V., Shevchuk, I., Koks, S., Maimets, T., Kaambre, T. (2017). 2102Ep embryonal carcinoma cells have compromised respiration and shifted bioenergetic profile distinct from H9 human embryonic stem cells. *Biochim Biophys Acta Gen Subj.* 1861, 8, 2146–2154. DOI: 10.1016/j.bbagen.2017.05.020



Contents lists available at ScienceDirect

BBA - General Subjects

journal homepage: www.elsevier.com/locate/bbagen

2102Ep embryonal carcinoma cells have compromised respiration and shifted bioenergetic profile distinct from H9 human embryonic stem cells



Lyudmila Ounpuu^a, Aleksandr Klepinin^a, Martin Pook^b, Indrek Teino^b, Nadezda Peet^c, Kalju Paju^c, Kersti Tepp^a, Vladimir Chekulayev^a, Igor Shevchuk^a, Sulev Koks^b, Toivo Maimets^b, Tuuli Kaambre^{d,a,*}

^a Laboratory of Bioenergetics, National Institute of Chemical Physics and Biophysics, Akadeemia tee 23, 12618 Tallinn, Estonia

^b Department of Cell Biology, Institute of Molecular and Cell Biology, University of Tartu, Riia 23, 51010 Tartu, Estonia

^c Institute of Biomedicine and Translational Medicine, University of Tartu, Ravila 19, 50411 Tartu, Estonia

^d Tallinn University, Narva mnt 25, 10120 Tallinn, Estonia

ARTICLE INFO

Keywords:

Embryonal carcinoma
Human embryonic stem cells
Cellular bioenergetics

ABSTRACT

Recent studies have shown that cellular bioenergetics may be involved in stem cell differentiation. Considering that during cancerogenesis cells acquire numerous properties of stem cells, it is possible to assume that the energy metabolism in tumorigenic cells might be differently regulated. The aim of this study was to compare the mitochondrial bioenergetic profile of normal pluripotent human embryonic stem cells (hESC) and relatively nullipotent embryonal carcinoma cells (2102Ep cell line).

We examined three parameters related to cellular bioenergetics: phosphotransfer system, aerobic glycolysis, and oxygen consumption. Activities and expression levels of main enzymes that facilitate energy transfer were measured. The oxygen consumption rate studies were performed to investigate the respiratory capacity of cells.

2102Ep cells showed a shift in energy distribution towards adenylate kinase network. The total AK activity was almost 3 times higher in 2102Ep cells compared to hESCs (179.85 ± 5.73 vs 64.39 ± 2.55 mU/mg of protein) and the expression of AK2 was significantly higher in these cells, while CK was downregulated. 2102Ep cells displayed reduced levels of oxygen consumption and increased levels of aerobic glycolysis compared to hESCs. The compromised respiration of 2102Ep cells is not the result of increased mitochondrial mass, increased proton leak, and reduced respiratory reserve capacity of the cells or impairment of respiratory chain complexes. Our data showed that the bioenergetic profile of 2102Ep cells clearly distinguishes them from normal hESCs. This should be considered when this cell line is used as a reference, and highlight the importance of further research concerning energy metabolism of stem cells.

1. Introduction

There are increasing evidences that cancer could be considered as a stem cell disease [1]. As aging induces mutations in stem cells [1], it supports the idea of cancer stem cells (CSCs) evolving from different stem cell compartments. CSC has been defined as “a cell within a tumor that possesses the capacity to self-renew and to cause the heterogeneous lineages of cancer cells that comprise the tumor” [2]. It has been demonstrated that CSCs are involved in cancer onset and development,

distant metastasis, angiogenesis and drug resistance [3]. The development of specific strategies to eradicate highly malignant CSCs holds a great potential for cancer treatment [4,5]. In light of novel observations on how core metabolic properties of CSCs might contribute to tumor progression and resistance to conventional treatment, the cellular metabolism of CSCs may represent an attractive target for cancer therapy [6,7]. However, these therapies may cause toxicity to normal stem cells, which share many common features with CSCs [8]. In order to develop safe and effective cancer therapy, it is crucial to understand shared and

Abbreviations: ADP, adenosine diphosphate; AK, adenylate kinase; ANT, adenine nucleotide translocator; ATP, adenosine triphosphate; BSA, bovine serum albumin; CAT, carboxyatractyloside; CK, creatine kinase; CKB, brain-type creatine kinase; CKMT1A, creatine kinase, mitochondrial 1A; CKMT2, creatine kinase, mitochondrial 2; CS, citrate synthase; CSC, cancer stem cells; Cyt c, cytochrome c; ETC, electron transport chain; FBS, fetal bovine serum; FCC, flux control coefficient; FCCP, Carbonyl cyanide 4-(trifluoromethoxy)phenylhydrazone; hESCs, human embryonic stem cells; HK, hexokinase; hMSCs, human mesenchymal stem cells; MCA, metabolic control analysis; NEM, *N*-ethylmaleimide; OCR, oxygen consumption rate; OXPHOS, oxidative phosphorylation; RCI, respiratory control index; RCR, respiratory control ratio; ROS, reactive oxygen species; ROX, residual oxygen consumption; TCA cycle, tricarboxylic acid cycle; TMPD, *N,N,N',N'*-tetramethyl-*p*-phenylenediamine; VDAC, voltage dependent anion channel

* Corresponding author at: Laboratory of Bioenergetics, National Institute of Chemical Physics and Biophysics, Akadeemia tee 23, 12618 Tallinn, Estonia.

E-mail address: tuuli.kaambre@kbfi.ee (T. Kaambre).

<http://dx.doi.org/10.1016/j.bbagen.2017.05.020>

Received 30 January 2017; Received in revised form 17 May 2017; Accepted 23 May 2017

Available online 26 May 2017

0304-4165/© 2017 Elsevier B.V. All rights reserved.

distinguishing mechanisms that regulate proliferation in normal and cancer stem cells.

The bioenergetic profiles of various human progenitor and stem cells are just being understood. It is clear now, that energy metabolism plays an important role in the homeostasis and differentiation of stem cells. Differentiation of the cell is accompanied by changes in mitochondrial metabolism, activity, and organization of electron transport chain (ETC) complexes [9–11]. Moreover, recent studies have demonstrated that mitochondrial metabolism itself can influence the stemness maintenance and differentiation process [11,12]. Although stem cells contain fewer number and morphologically more immature mitochondria than differentiated cells [11], the ETC complexes within the inner membrane of the mitochondria are functionally active and mitochondria are able to consume oxygen and produce ATP from oxidative phosphorylation (OXPHOS) [12,13].

The reprogramming of energy metabolism is proposed as one of the hallmarks of cancer [14]. It has been shown that cancer cells are able to modulate their energy metabolism via aerobic glycolysis [15]. This inclination of cancer cells to use glycolysis even in the presence of oxygen characterizes also normal stem cells [16]. One of the mechanisms that explain high glycolytic rate in tumor cells at normoxic condition is Warburg-Pedersen model [17] where the association between glycolytic enzyme hexokinase (HK) and mitochondrial outer membrane enhances aerobic glycolysis in cancer cells. It has been demonstrated that HK bound to voltage dependent anion channel (VDAC) utilizes ATP produced during OXPHOS to catalyze the first reaction of glycolysis [17]. A similar mechanism may occur in stem cells, which also over-express HK enzymes [12].

Well-organized high-energy phosphoryl transfer system is required to mediate intracellular communication between ATP-consuming and ATP-producing cellular compartments and thus maintain normal growth and development of cell [18]. The main components of phosphotransfer system are adenylate kinase (AK) network, creatine kinase (CK) network and glycolysis [18]. CK network maintains normal phosphate levels in cells with high energy demands. Mitochondrial CK isoforms, CKMT1A and CKMT2, as well as cytosolic isoform, CKB, provide energy for various cellular processes [18]. AK1, the major cytosolic isoform, and AK2, localized in mitochondrial intermembrane space, have been recognized as the main facilitators of intracellular nucleotide exchange in cells with compromised CK network. AK4, enzymatically inactive isoform, has been proposed as a marker of poor clinical outcome for lung cancer [19].

Recent studies have shown that adenylate kinase and creatine kinase networks are involved in the differentiation of hematopoietic stem cells facilitating energy transfer and metabolic signaling required for developmental programming [20,21]. The cancerogenesis has been also associated with the reorganization of the phosphotransfer system. The creatine kinase system is significantly downregulated in various cancer types including breast cancer [22], Ehrlich ascites carcinoma [23], neuroblastoma [24], colorectal cancer [25] and prostate cancer [26]. On the contrary, AK levels were found to be elevated in several types of cancer [24,25]. However, the exact role of CK and AK enzymes in the regulation of cell stemness or cancer development remains elusive.

In the present study, we used 2102Ep cell line derived from a primary human testicular teratocarcinoma [27] as a CSC model. Described as relatively nullipotent, this cell line has been shown to express many of the identified markers of pluripotent hESCs [28], as well as, numerous oncogenes and has many potentially tumorigenic genomic alterations [29]. Embryonic stem cell-like gene expression signature has been found to be characteristic of poorly differentiated aggressive tumors [30,31]. With limited differentiation potential 2102Ep resembles these undifferentiated cancer cells that are often associated with poor prognosis of cancer patients. Embryonic stem cells represent the normal counterparts of embryonal carcinoma cells and together, these can be used as complementary tools for studying pluripotency, stem cell biology and cancer [32]. We examined differences between normal

human embryonic stem cells and 2102Ep cells in the three parameters related to cellular bioenergetics: phosphotransfer system, aerobic glycolysis, and oxygen consumption. In addition, we applied the metabolic control analysis to compare the effect of inhibition of different respiratory complexes on the respiratory efficiency in the two cell lines.

2. Material and methods

2.1. Cell cultures

2.1.1. 2102Ep cell line

The human embryonal carcinoma cell line 2102Ep (Cl.2/A6; GlobalStem) was routinely cultured in T75 (Greiner bio-one) flasks in high glucose Dulbecco's modified Eagle medium with L-glutamine, supplemented with 10% heat inactivated fetal bovine serum (FBS), penicillin (100 U/ml), streptomycin (100 µg/ml) and 50 µg/ml gentamicin. Cells were grown at high density to limit spontaneous differentiation [33] and maintained at 37 °C in a humidified incubator containing 5% CO₂ in the air.

2.1.2. H9 cell line

Pluripotent H9 human embryonic stem cells (WA09, National Stem Cell Bank, WiCell) were cultured on 6-well tissue culture plates (BD Biosciences) coated with Matrigel (BD Biosciences) in mTeSR1 media (STEMCELL Technologies) according to the manufacturer's specifications. The culture medium was changed daily. Cells were passaged mechanically with micropipette tip after 3–4 days and cultured in the presence of 5% CO₂ at 37 °C in humid conditions. Normal karyotype of the cells was confirmed by G-banding.

2.1.3. Oxygen consumption rate (OCR) study

The rates of oxygen consumption were measured at 25 °C using an Oxygraph-2k (Oroboros Instruments, Innsbruck, Austria). Measurements were performed in Mitomedium B solution supplemented with 5 mM glutamate, 2 mM malate and 1 mg/ml BSA. A suspension of cells (1×10^6 cells/ml) was placed in the oxygraph chamber, permeabilized with saponin (40 µg/ml) and allowed to equilibrate for 5 min. 10 mM succinate was added to initiate electron transport through Complex II. State 2 respiration was monitored and after that 2 mM ADP was added to evaluate state 3 respiration. Respiration rates were normalized to the total protein amount in the cells and expressed as nmol of O₂ consumed per/min/per mg of total protein (nmol / (min × mg)). Protein concentrations were determined using the Pierce BCA Protein Assay Kit.

The functional coupling between HK and mitochondria was measured as described earlier [25,34]. The functional activities of respiratory chain complexes were studied by substrate-inhibitor titration [25,35].

Mitochondrial contribution to the energy metabolism was measured in non-permeabilized cells. Following stabilization of endogenous routine respiration (ROUTINE) 2 µg/ml of oligomycin was added to inhibit ATP synthesis and induce the nonphosphorylating leak state (LEAK). Maximal uncoupled respiratory rates were determined with FCCP titration followed by inhibition of electron transfer by 10 µM antimycin A to measure residual oxygen consumption (ROX).

2.1.4. Metabolic control analysis (MCA)

In MCA, the degree of the control that a given enzyme exerts on the flux can be described quantitatively as a flux control coefficient (FCC). If the enzyme exerts an elevated control over the regulation of the metabolic pathway, then even a small change in the given enzyme activity will promote a significant variation in the pathway flux [36,37].

FCCs were determined for all mitochondrial ETC complexes, adenine nucleotide translocator (ANT) and inorganic phosphate carrier after their stepwise titration with specific pseudo irreversible inhibitors

upon direct activation of respiration by exogenously added ADP (at 2 mM). The following inhibitors were used: rotenone for Complex-I of the mitochondrial electron transport chain (ETC); atpenin A5 for Complex-II; antimycin A for Complex-III; sodium cyanide for Complex-IV; oligomycin for complex-V (ATP synthase); carboxyatractylidase (CAT) for ANT; and mersalyl for inorganic phosphate carrier.

2.1.5. Assays of enzymes activity

The enzyme activities were studied spectrophotometrically at 25 °C using a Cary 100 Bio UV–visible spectrophotometer. The activity of HK was measured as the total glucose phosphorylating capacity of whole cell extracts, using a standard glucose-6-phosphate dehydrogenase (G6PDH)-coupled spectrophotometric assay [38]. The activity of CK was measured by a coupled enzyme assay in the presence of di(adenosine-5') pentaphosphate (adenylate kinase inhibitor [39]), 20 mM phosphocreatine (PCr) and with 2 U/ml G6PDH and 2 U/ml HK as the coupled enzymes [40].

The total AK activity was also measured by a coupled enzyme assay [41]. In order to determine the specific activities of AK1 and AK2, lysates were incubated with AK1 inhibitor *N*-ethylmaleimide (NEM) for 1 h at 25 °C. AK2 activity was determined as the activity remaining after the NEM treatment. AK1 activity was calculated as total AK activity minus activity remaining after the NEM treatment.

The activity of citrate synthase (CS) was measured by monitoring the production of CoA from oxaloacetate together with acetyl-CoA. The thiol group of CoA reacts with 5,5'-dithiobis-(2-nitrobenzoic acid) (Ellman's reagent, DTNB) to produce a yellow-colored product which was observed by measuring the absorbance at 412 nm. Reactions were performed in 96-well plates containing 100 mM Tris-HCl pH 8.1, 0.3 mM AcCoA, 0.5 mM oxaloacetate and 0.1 mM DTNB using FLUOstar Omega plate-reader spectrophotometer (BMG Labtech).

2.1.6. Confocal imaging

2102Ep cells were seeded on glass coverslips in 12-well plates (Greiner bio-one) and allowed to adhere overnight. H9 cells were passaged onto Matrigel coated glass coverslips and cultured in 12-well plates for 3 days. Then, the growth medium was removed and cells were incubated with 200 nM MitoTracker Red CMXRos for 30 min at 37 °C to stain mitochondria. After staining, cells were fixed in 4% paraformaldehyde in PBS for 15 min at RT. Following permeabilization with ice-cold methanol for 20 min at RT, cells were incubated with 2% BSA in PBS for 1 h at RT, probed with specific primary antibodies against Oct-4 and incubated for 1 h at RT. After incubation, cells were washed with PBS and incubated with corresponding fluorescence-conjugated secondary antibodies. Finally, cells were incubated for 15 min at RT with 4',6-diamidino-2-phenylindole dihydrochloride (DAPI, Molecular Probes™) to visualize the cell nucleus. Cells were imaged by an Olympus FluoView FV1000 inverted laser scanning confocal microscope.

2.1.7. Isolation of RNA, cDNA synthesis, and qPCR

Total RNA from Ep2102 and hES cells was isolated using FavorPrep™ Blood/Cultured Cell. Total RNA Mini Kit (Favorgen Biotech Corporation) and quantitated using a Nanodrop spectrophotometer (ND-1000; Nanodrop). Following DNaseI (Thermo Fisher Scientific) treatment, reverse transcription was performed on 1 µg of total RNA with random hexamer primers using RevertAid RT Reverse Transcription Kit (Thermo Fisher Scientific) according to the manufacturer protocol. The synthesized cDNA was subjected to quantitative PCR analysis using 5 × HOT FIREPol® Probe Universal qPCR Mix (Solis BioDyne) and specific primers actin beta – Hs01060665_g1; hexokinase I – Hs00175976_m1; hexokinase II – Hs00606086_m1; creatine kinase brain-type HS00176484_m1; creatine kinase, mitochondrial 1B – Hs00179727_m1; creatine kinase, mitochondrial 2 – Hs00176502_m1, adenylate kinase 1 HS00176119_m1; adenylate kinase 2 HS01123132_g1; adenylate kinase 4 HS03405743_g1. All qPCR

experiments were performed on LightCycler 480 II Real-Time PCR System (Roche) with following conditions: 95 °C for 10 min followed by 40 cycles of 95 °C for 15 s and 60 °C for 1 min. PCR reactions were performed in triplicate for each of three independent experiments and included no reverse transcriptase and no template negative controls. Threshold cycles (Ct) were automatically calculated by LightCycler 480 software (Roche). Data were analyzed with the formula $2^{-\Delta\Delta Ct}$ [72], normalized to the endogenous control ActB and expressed as fold change over hESC samples.

2.1.8. Statistical analysis of data

All data points are presented as means ± standard error (SEM) from at least five separate experiments performed in duplicate. Significance was calculated by Student's *t*-test; differences between two data groups were considered to be statistically significant when $p < 0.05$.

3. Results

3.1. 2102Ep cells displayed elevated levels of adenylate kinase 2 (AK2) and reduced levels of creatine kinase (CK) compared to hESCs

2102Ep demonstrated a distinct expression pattern of key enzymes that are involved in cellular energy homeostasis (Fig. 1). The measurements of enzymatical activities further clarified the differences between hESC and 2102Ep cells. Compared to hESCs, the total creatine kinase activity was significantly decreased in 2102Ep cells (Table 1) in accordance with the down-regulation of creatine kinase mitochondrial (CKMT1A) and brain (CKB) isoforms (Fig. 1). Interestingly, both cell lines had very low expression of CKMT2 and the expression level of CKMT1A was significantly higher. This suggests CKMT1A to be the main isoform of mitochondrial CK expressed in these cells. Concomitantly, the total adenylate kinase activity was significantly increased in 2102Ep cells (Table 1) and was most probably associated with a nearly 2-fold higher expression level of AK2 isoform in 2102Ep cells than in hESC (Fig. 1). Although the expression of AK1 was lower in 2102Ep cells (Fig. 1), this was not reflected on its enzymatical activity (Table 1). We observed no statistical difference in the expression levels of AK4 between two cell lines (Fig. 1).

3.2. The respiration is compromised in 2102Ep cells compared to hESCs

To characterize the ability of cells to consume oxygen we performed OCR studies. The intactness of mitochondrial outer and inner membranes was controlled by standard mitochondrial membrane integrity test (Fig. 2A) [42]. The addition of cytochrome *c* (8 µM) had no effect

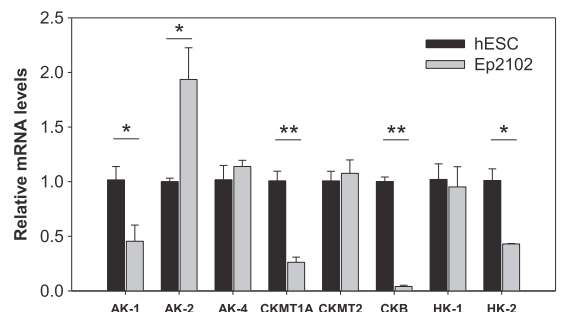


Fig. 1. Comparison of the mRNA expression levels of key enzymes involved in cellular energy homeostasis in hESCs and 2102Ep cells. Expression of the indicated mRNA was quantified using qPCR. Data were normalized to β -actin mRNA and expressed as a fold change relative to hESCs. The results are means ± SEM of three individual studies. * $p < 0.05$ and ** $p < 0.005$.

Table 1
The activity of HK, CK, and CS in hESCs and 2102Ep cells.

	Enzyme activities, mU/mg protein		p-Values
	hESC mean ± SEM	2102Ep mean ± SEM	
Hexokinase	67.28 ± 2.75	71.46 ± 7.91	0.64
Creatine kinase	159.84 ± 3.70	12.75 ± 2.15	< 0.0001
Citrate synthase	52.26 ± 3.07	64.77 ± 4.26	0.08
Total adenylate kinase (AK)	64.39 ± 2.55	179.85 ± 5.73	< 0.001
AK1	28.77 ± 1.6 (46% ^a)	37.44 ± 3.86 (21%)	0.1
AK2	33.10 ± 1.00 (54%)	142.42 ± 3.29 (79%)	< 0.001

^a % from the total AK activity.

on oxygen consumption rate, while the addition of carboxyatractyloside (1 μ M) decreased the respiration rate to the basal level indicating the intactness of outer and inner mitochondrial membranes. In order to ensure the quality of the cells, this test was performed prior to every experiment.

State 2 (in the absence of ADP) and state 3 (in the presence of ADP) respiration rates were determined and compared between these two cell lines. State 3 respiration rate in 2102Ep cells was remarkably lower than in hESCs (5.04 ± 0.37 versus 7.45 ± 0.58 , $p = 0.01$) (Fig. 2B). Respiratory control ratios (RCRs) were calculated as the ratios between state 2 and state 3 respiration. Because of reduced state 3 respiration, RCR was two times lower in the 2102Ep cells (1.98 ± 0.10 versus 3.99 ± 0.36 , $p = 0.005$) (Fig. 2C).

3.3. Mitochondrial contribution to the energy metabolism of hESCs and 2102Ep cells

For the understanding of mitochondrial contribution to the energy metabolism of hESC and 2102Ep cell lines, we analyzed OCR response of these cells to the combination of inhibitors (oligomycin, antimycin) and uncoupler of OXPHOS (FCCP) (Fig. 3A, B). After monitoring

routine respiration, oligomycin, the inhibitor of ATP synthase, was added to uncouple the ATP-linked respiration from the proton leak. As shown in Fig. 3C, 50% of routine respiration (state 2 respiration measured without permeabilization of the cell membrane) was dedicated to ATP production. The proton leak appears to be very similar in these two cell lines, accounting approximately 25% of the cellular respiration rate, indicating that the suppressed respiration of 2102Ep cells is not due to the decreased proton leak. After addition of oligomycin, the maximal respiratory rate was determined by FCCP treatment. FCCP is a protonophore that uncouples electron transport and mitochondrial respiration from ATP synthesis by dissipating the proton gradient. The addition of FCCP resulted in an increase of oxygen consumption levels in both cell lines with a more pronounced response in 2102Ep cells. The difference between oxygen consumption rate following FCCP treatment and State 2 respiration rate represents the respiratory capacity of these cells. We observed that the mitochondrial respiratory capacity was higher for 2102Ep cells when compared with hESCs (Fig. 3C). The addition of mitochondrial Complex I and III inhibitors rotenone and antimycin reduced respiration rates in both cell lines, although this effect was significantly more pronounced in 2102Ep cells (Fig. 3B).

3.4. 2102Ep demonstrated stronger coupling between HK and OXPHOS than hESCs

To examine if reduced level of oxygen consumption is associated with increased level of glycolysis in 2102Ep cells, we compared the activity and expression levels of HK, an enzyme that catalyzes the first reaction of glycolysis, between these two cell lines. Although 2102Ep cells had a 2-fold decrease in HK2 mRNA level, the total HK activity was similar between studied cell lines (Fig. 1, Table 1).

To evaluate the coupling between HK and OXPHOS, we investigated the effect of glucose on cellular respiration (Fig. 4). It can be seen that addition of 0.1 mM ATP increased the respiration rate due to the generation of a large flux of ADP from ATPases in hESCs. The effect of glucose on the oxygen consumption was characterized by glucose index (I_{glu}), which represents the degree of glucose-stimulated respiration

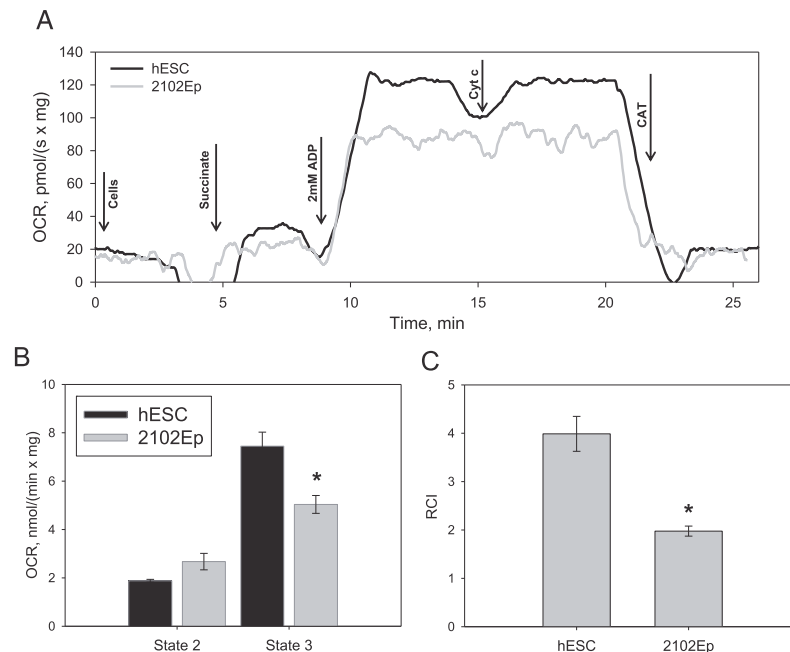


Fig. 2. Respiratory properties of hESC and 2102Ep cells. (A) Mitochondrial membranes integrity validation test. Adenosine diphosphate, ADP; cytochrome c, Cyt c; carboxyatractyloside, CAT. (B) State 2 and state 3 respiration rates. All rates were normalized to total protein concentration in the same samples. (C) Respiratory control indexes (RCIs). RCI was calculated as the ratios between state 2 and state 3 rates. All data are mean \pm SEM of 5–6 independent experiments. * $p < 0.05$.

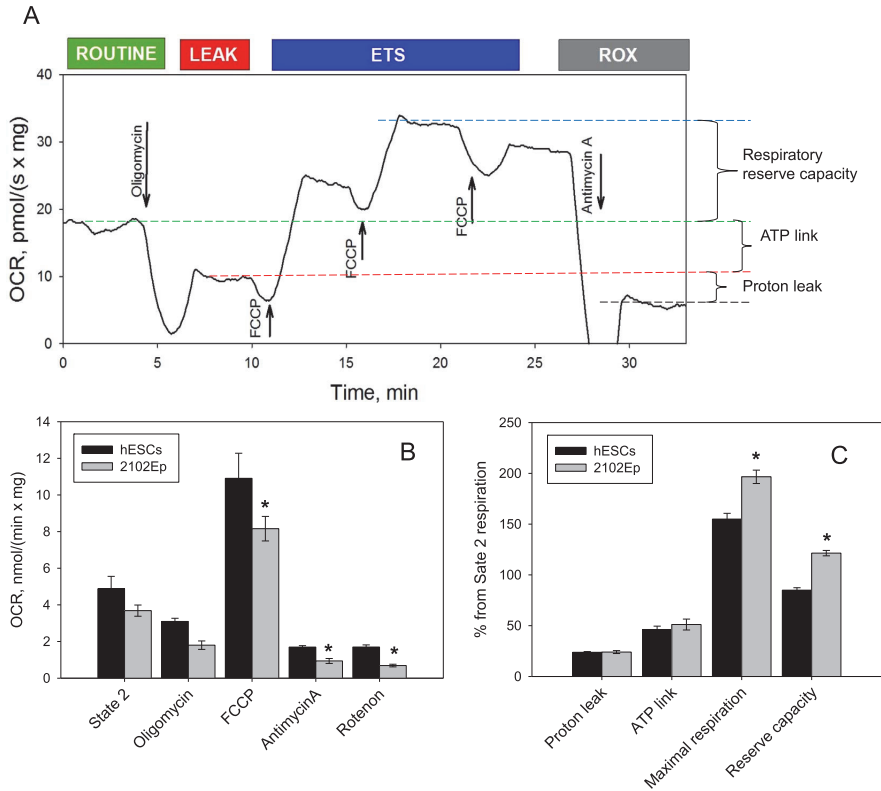


Fig. 3. Assessment of mitochondrial function in hESCs and 2102Ep cells. (A) Representative respirometric trace with schematic representation of the mitochondrial function assay. Arrows indicate the titrations into the oxygraph chamber. Maximal respiratory rate was determined with FCCP titration. Maximal uncoupled respiration was reached at 0.5 μ M FCCP followed by inhibition of electron transfer (ETS) by antimycin A to measure residual oxygen consumption (ROX). (B) Quantitative analysis of mitochondrial OCR readings. (C) Functional properties of mitochondrial respiration. Proton leak was calculated as $(V_{LEAK} - V_{ROX}) / V_{ROUTINE}$; ATP-linked respiration: $(V_{ROUTINE} - V_{LEAK}) / V_{ROUTINE}$; maximal respiration: $(V_{FCCP} - V_{ROX}) / V_{ROUTINE}$; respiratory reserve capacity: $(V_{FCCP} - V_{ROUTINE}) / V_{ROUTINE}$.

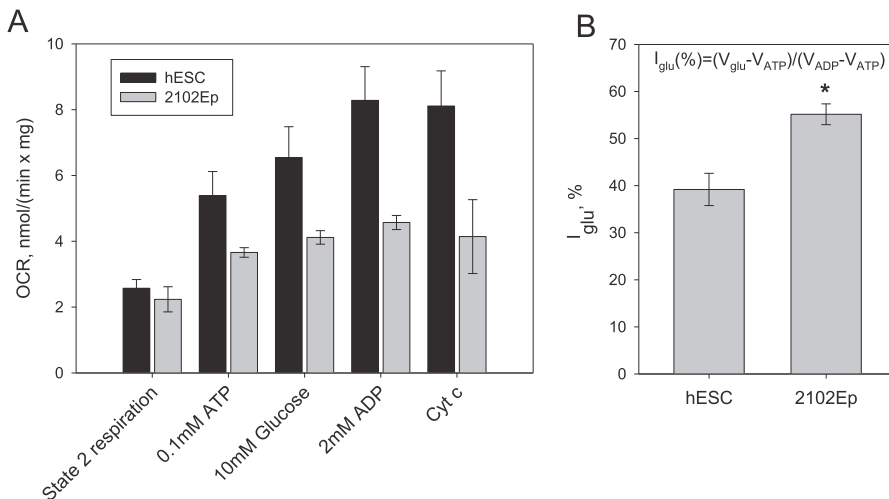


Fig. 4. Effect of exogenously added glucose on the rate of oxygen consumption. The effect of glucose was estimated as a degree of glucose-mediated respiration compared to State 3 respiration and expressed as the glucose index (I_{glu}): $I_{glu}(\%) = (V_{glu} - V_{ATP}) / (V_{ADP} - V_{ATP})$. Results represent means \pm SEM, n = 5. The difference in the mean values of the two groups is statistically significant, *p < 0.05. Cytochrome c, Cyt c.

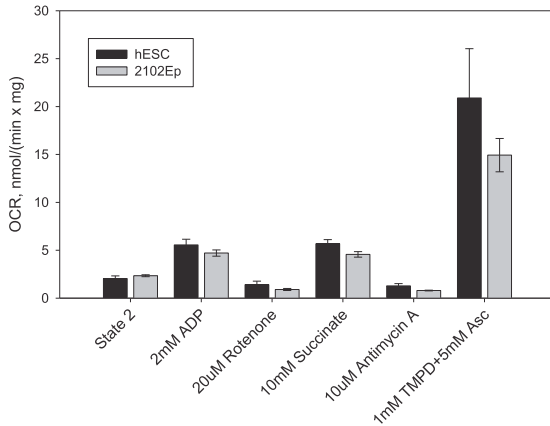


Fig. 5. Functional activity of respiratory chain complexes. The Complex IV-dependent respiration was calculated as $V_{\text{TMPD/Asc}} - V_{\text{TMPD/Asc} + \text{NaCN}}$ where $V_{\text{TMPD/Asc}}$ and $V_{\text{TMPD} + \text{NaCN}}$ are TMPD-stimulated respiration rates before and after addition of NaCN. Results represent means \pm SEM, $n = 5$. Asc – ascorbate, TMPD - N,N,N',N' -tetramethyl- p -phenylenediamine, CI, CII, CIII, and CIV – Complexes I, II, III, and IV, respectively. Bars are SEM.

compared to maximal ADP-stimulated respiration. The I_{glu} calculated for 2102Ep cells was considerably higher compared to hESCs, $55.16 \pm 2.21\%$ versus $40.18 \pm 4.64\%$, respectively ($p = 0.06$), suggesting that coupling between HK reactions and OXPHOS are more pronounced in 2102Ep cells (Fig. 4B). These results suggest that 2102Ep cells prefer more aerobic glycolysis to produce ATP than hESC.

3.5. hESCs and 2102Ep have a functional mitochondrial respiratory chain

In order to identify mechanisms of mitochondrial respiratory chain that could account for the lower oxygen consumption rate in 2102Ep, we examined the functional activity of respiratory chain complexes I–IV and ATP-synthase in both cell types. Our data demonstrated that all complexes within the mitochondrial respiratory chain of hESCs and 2102Ep cells were functionally active and their activities were equivalent in both cell lines (Fig. 5). Firstly, ADP-stimulated respiration was blocked by rotenone (20 μM , Complex I inhibitor), restored by addition of succinate (10 mM, Complex II substrate) and then, inhibited again by antimycin A (10 μM , Complex III inhibitor), indicating the functional activity of Complexes I, II and III. Finally, the functional activity of Complex IV was confirmed by the addition of electron donors ascorbic acid (5 mM) and N,N,N',N' -tetramethyl- p -phenylenediamine (TMPD, 1 mM), which strongly enhanced oxygen consumption in both cell types (Fig. 5).

The morphological features of hESC and 2102Ep cells were examined by confocal microscopy (Fig. 6). Although both cell lines expressed pluripotency marker Oct-4 and contained some spontaneously differentiated cells, there were several differences in cell morphology. While hESCs grow as colonies and display high nucleus to cytoplasm ratio, 2102Ep cells grow as a monolayer and contain considerably larger volumes of cytoplasm. Consistent with previous reports [11], hESCs display punctuate mitochondria with predominantly perinuclear localization, whereas in 2102Ep cells mitochondria localize randomly in the cytoplasm (Fig. 6). To ensure that alterations in mitochondrial respiration rates were not due to differences in mitochondrial content, the CS activity assay was performed. Our results (Table 1) indicated a similar mitochondrial mass in both cell lines.

3.6. Metabolic control analysis revealed the differences of regulation of cellular respiration in 2102Ep and hESCs

To further analyze mitochondrial respiration in hESCs and 2102Ep cells, the sensitivity of mitochondrial respiratory chain complexes to specific inhibitors was measured and the degree of control that each individual complex exerts on whole respiration chain was evaluated using MCA method [43]. Flux control coefficients (FCC) for mitochondrial complexes I–IV, ATP-synthase, adenine nucleotide translocator (ANT) and phosphate carrier (Pi) are summarized in Table 2. Our results showed that the key sites for the regulation of respiration are Complex I (FCC = 0.76), and Complex IV (FCC = 1.02) in hESCs. In 2102Ep cells, Complex II (FCC = 0.75) and Complex IV (FCC = 1.24) are the main regulators, since FCC values for other complexes were considerably lower (Table 2). It was impossible to determine FCC for Complex III in hESCs, because of the high sensitivity of these cells to Complex III inhibition. Beyond 0.15 nM of antimycin A, the inhibition was suddenly increased and the rate of respiration dropped sharply.

Our results indicated a notable difference in the control exerted by the phosphorylating system of OXPHOS constituted by the ATP synthase, ANT and Pi carrier in 2102Ep and hESCs. The FCC for ANT in 2102Ep cells exceeded 8 times the value obtained for hESCs (FCC = 0.62 versus FCC = 0.07). On the contrary, the FCC for Pi carrier was significantly lower in 2102Ep cells (FCC = 0.03 versus FCC = 0.26). The FCC value estimated for ATP synthase was 3 times higher in 2102Ep cells (FCC = 0.63) compared to hESCs (FCC = 0.22).

The total FCCs values for both cell types exceeded significantly the theoretic value for linear systems, which is considered to be close to 1 [44]. 2102Ep cells had higher total FCC values (FCC = 3.98) than hESCs (FCC > 2.7). Altogether, these results demonstrate that the role of respiratory chain complexes and ATP synthase in energy metabolism of 2102Ep cells differ considerably from that in normal stem cells.

4. Discussion

Cancer stem cells may acquire numerous properties of normal stem cells including their ability to self-renew, relative quiescence, expression of the same surface markers and activation of the same cell signaling pathways [45]. The specific depletion of CSC that represents a promising approach in clinical cancer therapy is challenging due to this similarity. Therefore, it is necessary to discover cellular or metabolic features that could help to distinguish CSCs from normal stem cells. In order to elucidate the possible differences, we have chosen normal hESC (H9) to compare with embryonal carcinoma cells (2102Ep) that express similar pluripotency-associated marker proteins but have limited differentiation ability [46].

In normal cells, the oxidative phosphorylation is closely linked to phosphotransfer systems where adenylate kinase and creatine kinase networks transport ATP from mitochondria to ATP-consumption sites [18]. We have demonstrated that the expression and the activity of several major components of the phosphotransfer system vary notably between 2102Ep cells and hESCs. In the current study, the deficiency of CK network was accompanied by the up-regulation of AK network in 2102Ep cells. The significant decrease of CK levels has been previously reported upon the transformation of skeletal muscle into sarcoma [47]. Several reports have indicated reduced levels of CK in brain cancer, colon cancer, prostate cancer and other malignancies [22,48]. The current findings about the expression and activity of different AK isoforms during cancerogenesis are contradictory. Although the increased expression of AK2 has been found in breast CSC [49] and prostate cancer cells [50], another study states that AK2 is rather a negative regulator of tumor growth [51]. On the other hand, it has been reported that the up-regulation of AK2 provides the energy required for the proliferation of hematopoietic stem cells [52] and plays an important role in communication between mitochondria and nucleus [18]. AK2

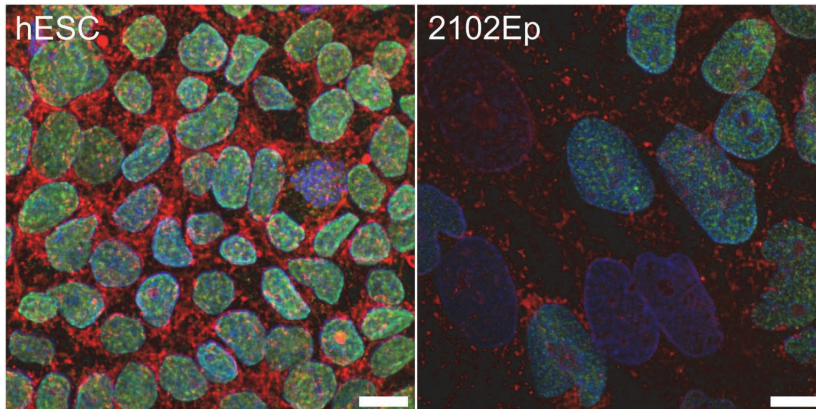


Fig. 6. Immunocytochemical analysis of Oct-4 (green) and MitoTracker Red (red) in hESC and 2102Ep cells. Nuclei are stained with DAPI (blue). Scale bars, 10 μ m.

Table 2

Flux control coefficients (FCC) of respiratory chain complexes for hESCs and 2102Ep cells.

ETC component	Inhibitor	hESCs, FCC	2102Ep, FCC
Complex I	Rotenone	0.76	0.40
Complex II	Atpenin A5	0.37	0.75
Complex III	Antimycin A	NA	0.31
Complex IV	Na cyanide	1.02	1.24
ATP synthase	Oligomycin	0.22	0.63
ANT	Carboxyatractyloside	0.07	0.62
Pi carrier	Mersalyl	0.26	0.03

deficiency impairs embryonic development and causes hematopoietic defects indicating the significance of AK2 in the energy metabolism of normal stem cells [52,53]. Further studies are needed to find out how AK2 expression and its compartmentalization influence cellular proliferation. A brief analysis of data from The Cancer Genome Atlas (TCGA) using the cBioPortal shows genomic alterations (amplification, deletion, or base pair mutation) in phosphotransfer systems in many cancers (Fig. 1S [54,55]). The most frequent alteration was detected in breast cancer xenografts where 48% of tumors exhibited amplified number of AK2 and HK2 suggesting that tumor cells with elevated levels of AK2 and HK2 may be one of the key players in cancer development and progression. A closer look at specific AK2 and HK2 alterations across various tumors reveals that amplification is the most common genomic alteration of AK2 while HK2 might be either amplified or mutated (Table 1S).

In agreement with previous reports, our results demonstrated that both normal and cancer stem cells have functional mitochondria. Although CSCs are often considered to be a glycolytic cell type, many recent reports identify oxidative metabolism as the preferred energy production mechanism in various CSCs [19,56]. Moreover, it has been shown that functional mitochondria are crucial for the maintenance of CSC phenotype [19,49]. Enhanced mitochondrial function of CSCs has been associated with tumor growth [57], increased metastatic potential [58] and resistance to chemotherapy [59].

Our results showed that 2102Ep cells consume lower levels of oxygen than normal stem cells. The reduced respiration rate may indicate that the mitochondrial respiratory chain does not operate sufficiently to generate an effective proton gradient. However, our results demonstrated that reduced mitochondrial respiration in 2102Ep cells was not the result of the impairment of respiratory chain complexes because all mitochondrial respiratory complexes were functionally active and their activities were equivalent in both cell lines. No differences were found between the rates of proton leak in studied cell lines. Mitochondria are functioning in the vast majority of cells at a basal

energy level that is required for cell survival and normal performance. The term “reserve respiratory capacity” is used to characterize the additional capacity available in cells to produce energy in response to certain conditions or increased stress [60]. One possible reason for the elevated reserve respiratory capacity in 2102Ep cells could be the increase of substrate entry into the TCA cycle [61]. In support of this hypothesis, it has been shown that TCA cycle intermediates are enriched in another (NTERA2) human embryonal carcinoma cell line [62].

We applied MCA to identify target reactions that control respiratory chain activity in 2102Ep cells and hESCs. Our results from MCA provided indirect evidence to conclude that the complexes II and IV share larger control strength over respiration in 2102Ep than in hESCs. Complex I exerted larger control over respiration in hESCs. Interestingly, Complex I has been shown to play an important role in cellular differentiation by generating reactive oxygen species (ROS) that stimulate muscle cell differentiation [63]. Taking into account that 2102Ep cells exhibit reduced ability to differentiate; Complex I in these cells may have distinct functional features compared to hESCs.

Completely different control patterns were also obtained for ATP synthase and its associated substrate suppliers, Pi carrier, and ANT. It has long been known that the coupling of ATP synthesis to oxygen consumption is not perfect due to the proton leak across the inner membrane of mitochondria [64]. Two groups of mitochondrial proteins contribute significantly to proton leak, uncoupling proteins and the adenine nucleotide translocator [65]. In current work the FCC for ANT was considerably higher in 2102Ep cells, showing that ANT exerts a higher degree of control over respiration and may play an important role in the regulation of proton leak in these cells. This is supported by the recent finding that the regulation of mitochondrial proton leak depends on the metabolic conditions [66]. Thus, it can be assumed that the regulation of proton leak could be also distinctly mediated in cells with different cellular metabolic states. However, additional research is needed to control this hypothesis.

The total FCCs were higher than expected for both hESCs and 2102Ep cells, contradicting the summation theorem of MCA according to which the sum of the FCCs of the enzymes of a metabolic pathway should be equal to 1. High total FCCs in both cell lines might be the result of branched pathways or direct substrate channeling between the protein (super)complexes [44]. Very little is known about the organization of respiratory chain in stem cells. It has been shown that the differentiation of human mesenchymal stem cells (hMSCs) is accompanied by the increased mitochondrial biogenesis and formation of supercomplexes [10,67]. Hoffmann et al. has confirmed the presence of several supercomplexes in hMSCs, although the number of supramolecular assemblies was significantly reduced compared with

differentiated cells [10]. It has been shown that in mitochondria with impaired respiration, ATP synthase and ANT may operate in the opposite direction compared with normal cells generating high ATP level and reverse proton gradient [68]. Definitely, the role of mitochondrial biogenesis and OXPHOS organization in the regulation of cellular differentiation and cancer development represents an important direction for future research.

Rapidly proliferating hESCs and CSCs are forced to adapt their cellular metabolism to meet their demand for energy and increased biosynthesis of macromolecules [69]. The Warburg effect represents one of the most common adaptive mechanisms which is acquired by highly proliferative and malignant cells to support their metabolic needs [70]. While the majority of normal differentiated cells use glycolysis followed by aerobic oxidation of pyruvate in the mitochondria to eventually produce ATP, highly proliferating cells prefer glycolysis followed by lactic acid fermentation during the process called “aerobic glycolysis” or “Warburg effect” [70]. Although aerobic glycolysis provides less ATP per molecule of glucose, it produces energy much faster and provides many intermediates for the production of proteins, lipids, and nucleotides [71]. In order to compare the level of aerobic glycolysis in our experimental models (Warburg-Pedersen) we evaluated the effect of exogenously added glucose on the cellular respiration. Our results showed up-regulation of aerobic glycolysis in 2102Ep compared to hESCs.

Altogether, our results confirm that the embryonal carcinoma 2102Ep cells display distinct bioenergetic profile compared to normal hESCs. The shift in energy distribution towards AK network, alterations in the regulation of respiratory chain as well as suppressed respiration may serve as indicators of tumorigenic stem cell. In addition, as differences in bioenergetic profile indicate different regulation of various cellular processes, this data should be taken into account for future use of these cell lines as in vitro stem cell or cancer stem cell models. Clearly, further extensive characterization of bioenergetics of normal and cancer cells is necessary in order to extend our knowledge of the mechanisms behind the cellular proliferation and differentiation. Ultimately, this will help to develop an effective treatment that would selectively target CSCs sparing normal stem cells and, thus, reducing side effects of conventional anti-cancer therapy.

5. Conclusions

Current study shed light on several aspects of energy metabolism in normal and tumorigenic stem cells. Our results showed that the bioenergetic profile of 2102Ep cells clearly distinguishes them from normal hESCs. Reduced oxygen consumption, increased aerobic glycolysis and shifted energy metabolism towards AK network represented the bioenergetic signature of this carcinoma cell line. Present and future studies will potentially aid in the understanding of metabolic properties of stem cells and establishment of effective strategies for identifying cells with increased tumorigenic potential.

Funding

The work of LO, AK, KT, NT, VC, IS and TK was supported by institutional research funding IUT23-1 of the Estonian Research Council. The work of MP, IT and TM was supported by a grant PUT0374 from the Estonian Research Council. This work of NP, KP and SK was supported by institutional research funding IUT20-46 of the Estonian Research Council.

Transparency Document

The <http://dx.doi.org/10.1016/j.bbagen.2017.05.020> associated with this article can be found, in online version.

Acknowledgements

The authors are thankful to Annika Trei for culturing the hESC.

Appendix A. Supplementary data

Supplementary data to this article can be found online at <http://dx.doi.org/10.1016/j.bbagen.2017.05.020>.

References

- [1] P.D. Adams, H. Jasper, K.L. Rudolph, Aging-induced stem cell mutations as drivers for disease and cancer, *Cell Stem Cell* 16 (6) (2015) 601–612.
- [2] M.F. Clarke, et al., Cancer stem cells—perspectives on current status and future directions: AACR Workshop on cancer stem cells, *Cancer Res.* 66 (19) (2006) 9339–9344.
- [3] C. Fanali, et al., Cancer stem cells in colorectal cancer from pathogenesis to therapy: controversies and perspectives, *World J. Gastroenterol.* 20 (2014) 923–942.
- [4] D.L. Dragu, et al., Therapies targeting cancer stem cells: current trends and future challenges, *World J. Stem Cells* 7 (2015) 1185–1201.
- [5] S.J. Vidal, et al., Targeting cancer stem cells to suppress acquired chemotherapy resistance, *Oncogene* 33 (2014) 4451–4463.
- [6] Y.A. Shen, et al., Metabolic reprogramming orchestrates cancer stem cell properties in nasopharyngeal carcinoma, *Cell Cycle* 14 (1) (2015) 86–98.
- [7] U.D. Kahlert, et al., Targeting cancer stem-like cells in glioblastoma and colorectal cancer through metabolic pathways, *Int. J. Cancer* 140 (1) (2017) 10–22.
- [8] M. Shackleton, Normal stem cells and cancer stem cells: similar and different, *Semin. Cancer Biol.* 20 (2010) 85–92.
- [9] S. Han, et al., Mitochondrial biogenesis and energy production in differentiating murine stem cells: a functional metabolic study, *Cell. Reprogram.* 16 (2014) 84–90.
- [10] A.D. Hofmann, et al., OXPHOS supercomplexes as a hallmark of the mitochondrial phenotype of adipogenic differentiated human MSCs, *PLoS One* 7 (4) (2012) e35160.
- [11] I. Vega-Naredo, et al., Mitochondrial metabolism directs stemness and differentiation in P19 embryonal carcinoma stem cells, *Cell Death Differ.* 21 (2014) 1560–1574.
- [12] S. Varum, et al., Enhancement of human embryonic stem cell pluripotency through inhibition of the mitochondrial respiratory chain, *Stem Cell Res.* 3 (2009) 142–156.
- [13] J. Zhang, et al., UCP2 regulates energy metabolism and differentiation potential of human pluripotent stem cells, *EMBO J.* 30 (2011) 4860–4873.
- [14] D. Hanahan, Robert A. Weinberg, Hallmarks of cancer: the next generation, *Cell* 144 (2011) 646–674.
- [15] O. Warburg, On respiratory impairment in cancer cells, *Science* 124 (3215) (1956) 269–270.
- [16] C. Hu, et al., Energy metabolism plays a critical role in stem cell maintenance and differentiation, *Int. J. Mol. Sci.* 17 (2016).
- [17] P.L. Pedersen, Warburg, me and hexokinase 2: multiple discoveries of key molecular events underlying one of cancers' most common phenotypes, the “Warburg Effect”, i.e., elevated glycolysis in the presence of oxygen, *J. Bioenerg. Biomembr.* 39 (2007) 211–222.
- [18] P.P. Dzeja, A. Terzic, Phosphotransfer networks and cellular energetics, *J. Exp. Biol.* 206 (2003) 2039–2047.
- [19] M. Janiszewska, et al., Imp2 controls oxidative phosphorylation and is crucial for preserving glioblastoma cancer stem cells, *Genes Dev.* 26 (2012) 1926–1944.
- [20] S. Chung, et al., Developmental restructuring of the creatine kinase system integrates mitochondrial energetics with stem cell cardiogenesis, *Ann. N. Y. Acad. Sci.* 1147 (2008) 254–263.
- [21] P.P. Dzeja, et al., Developmental enhancement of adenylate kinase-AMPK metabolic signaling axis supports stem cell cardiac differentiation, *PLoS One* 6 (2011) e19300.
- [22] H. Pan, et al., Low serum creatine kinase levels in breast cancer patients: a case-control study, *PLoS One* 8 (4) (2013) e62112.
- [23] S. Bera, et al., Enzymes of creatine biosynthesis, arginine and methionine metabolism in normal and malignant cells, *FEBS J.* 275 (2008) 5899–5909.
- [24] A. Klepinin, et al., Comparative analysis of some aspects of mitochondrial metabolism in differentiated and undifferentiated neuroblastoma cells, *J. Bioenerg. Biomembr.* 46 (2014) 17–31.
- [25] V. Chekulayev, et al., Metabolic remodeling in human colorectal cancer and surrounding tissues: alterations in regulation of mitochondrial respiration and metabolic fluxes, *Biochem. Biophys. Rep.* 4 (2015) 111–125.
- [26] R. Amamoto, et al., The expression of ubiquitous mitochondrial creatine kinase is downregulated as prostate cancer progression, *J. Cancer* 7 (2016) 50–59.
- [27] P.W. Andrews, et al., Cell-surface antigens of a clonal human embryonal carcinoma cell line: morphological and antigenic differentiation in culture, *Int. J. Cancer* 29 (5) (1982) 523–531.
- [28] R. Josephson, et al., Qualification of embryonal carcinoma 2102Ep as a reference for human embryonic stem cell research, *Stem Cells* 25 (2007) 437–446.
- [29] O. Hovatta, et al., A teratocarcinoma-like human embryonic stem cell (hESC) line and four hESC lines reveal potentially oncogenic genomic changes, *PLoS One* 5 (2010) e10263.
- [30] I. Ben-Porath, et al., An embryonic stem cell-like gene expression signature in poorly differentiated aggressive human tumors, *Nat. Genet.* 40 (5) (2008) 499–507.
- [31] D.J. Wong, et al., Module map of stem cell genes guides creation of epithelial cancer

- stem cells, *Cell Stem Cell* 2 (4) (2008) 333–344.
- [32] P.W. Andrews, et al., Embryonic stem (ES) cells and embryonal carcinoma (EC) cells: opposite sides of the same coin, *Biochem. Soc. Trans.* 33 (Pt 6) (2005) 1526–1530.
- [33] P.W. Andrews, Human embryonal carcinoma cells in culture do not synthesize fibronectin until they differentiate, *Int. J. Cancer* 30 (5) (1982) 567–571.
- [34] M. Eimre, et al., Distinct organization of energy metabolism in HL-1 cardiac cell line and cardiomyocytes, *Biochim. Biophys. Acta* 1777 (6) (2008) 514–524.
- [35] M. Puurand, et al., Deficiency of the complex I of the mitochondrial respiratory chain but improved adenylate control over succinate-dependent respiration are human gastric cancer-specific phenomena, *Mol. Cell. Biochem.* 370 (1–2) (2012) 69–78.
- [36] D. Fell, Understanding the control of metabolism, in: K. Snell (Ed.), *Frontiers in Metabolism*, 2 Portland Press, London, Miami, 1997(xii, 301 pp.).
- [37] K. Tepp, et al., Metabolic control analysis of integrated energy metabolism in permeabilized cardiomyocytes - experimental study, *Acta Biochim. Pol.* 57 (2010) 421–430.
- [38] S. Biswas, et al., Selective inhibition of mitochondrial respiration and glycolysis in human leukemic leukocytes by methylglyoxal, *Biochem. J.* (1997) 343–348.
- [39] G.E. Lienhard, I.I. Secemski, P 1,P 5 -Di(adenosine-5')pentaphosphate, a potent multisubstrate inhibitor of adenylate kinase, *J. Biol. Chem.* 248 (1973) 1121–1123.
- [40] C. Monge, et al., Comparative analysis of the bioenergetics of adult cardiomyocytes and nonbeating HL-1 cells: respiratory chain activities, glycolytic enzyme profiles, and metabolic fluxes, *Can. J. Physiol. Pharmacol.* 87 (2009) 318–326.
- [41] P.P. Dzeja, et al., Adenylate kinase-catalyzed phosphotransfer in the myocardium: increased contribution in heart failure, *Circ. Res.* 84 (1999) 1137–1143.
- [42] D. Pesta, E. Gnaiger, High-resolution respirometry: OXPHOS protocols for human cells and permeabilized fibers from small biopsies of human muscle, *Methods Mol. Biol.* 810 (2012) 25–58.
- [43] R. Moreno-Sanchez, et al., Metabolic control analysis: a tool for designing strategies to manipulate metabolic pathways, *J. Biomed. Biotechnol.* 2008 (2008) 30.
- [44] B.N. Kholodenko, O.V. Demin, H.V. Westerhoff, "Channelled" pathways can be more sensitive to specific regulatory signals, *FEBS Lett.* 320 (1) (1993) 75–78.
- [45] T. Reya, et al., Stem cells, cancer, and cancer stem cells, *Nature* 414 (2001) 105–111.
- [46] K.I. Matthaei, P.W. Andrews, D.L. Bronson, Retinoic acid fails to induce differentiation in human teratocarcinoma cell lines that express high levels of a cellular receptor protein, *Exp. Cell Res.* 143 (2) (1983) 471–474.
- [47] S. Patra, et al., Progressive decrease of phosphocreatine, creatine and creatine kinase in skeletal muscle upon transformation to sarcoma, *FEBS J.* 275 (2008) 3236–3247.
- [48] J. Joseph, A. Cardesa, J. Carreras, Creatine kinase activity and isoenzymes in lung, colon and liver carcinomas, *Br. J. Cancer* 76 (1997) 600–605.
- [49] R. Lamb, et al., Mitochondrial mass, a new metabolic biomarker for stem-like cancer cells: understanding WNT/FGF-driven anabolic signaling, *Oncotarget* 6 (2015) 30453–30471.
- [50] M. Hail, et al., AdenylateKinase: an oncodevelopmental marker in an animal model for human prostatic cancer, *Clin. Chem.* 3110 (1985) 1689–1691.
- [51] H. Kim, et al., The DUSP26 phosphatase activator adenylate kinase 2 regulates FADD phosphorylation and cell growth, *Nat. Commun.* 5 (2014) 3351.
- [52] C. Lagresle-Peyrou, et al., Human adenylate kinase 2 deficiency causes a profound hematopoietic defect associated with sensorineural deafness, *Nat. Genet.* 41 (2009) 106–111.
- [53] K. Fujisawa, et al., Adenylate kinase isozyme 2 is essential for growth and development of *Drosophila melanogaster*, *Comp. Biochem. Physiol. B Biochem. Mol. Biol.* 153 (2009) 29–38.
- [54] J. Gao, et al., Integrative analysis of complex cancer genomics and clinical profiles using the cBioPortal, *Sci. Signal.* 6 (269) (2013) pl1.
- [55] E. Cerami, et al., The cBio cancer genomics portal: an open platform for exploring multidimensional cancer genomics data, *Cancer Discov.* 2 (5) (2012) 401–404.
- [56] A. Pastò, et al., Cancer stem cells from epithelial ovarian cancer patients privilege oxidative phosphorylation, and resist glucose deprivation, *Oncotarget* 5 (2014) 4305–4319.
- [57] A.F. Salem, et al., Mitochondrial biogenesis in epithelial cancer cells promotes breast cancer tumor growth and confers autophagy resistance, *Cell Cycle* 11 (2012) 4174–4180.
- [58] V.S. LeBleu, et al., PGC-1 α mediates mitochondrial biogenesis and oxidative phosphorylation in cancer cells to promote metastasis, *Nat. Cell Biol.* 16 (2014) 992–1003 (1–15).
- [59] G. Farnie, F. Sotgia, M.P. Lisanti, High mitochondrial mass identifies a sub-population of stem-like cancer cells that are chemo-resistant, *Oncotarget* 6 (2015) 30472–30486.
- [60] C. Desler, et al., Is there a link between mitochondrial reserve respiratory capacity and aging? *J. Aging. Res.* 2012 (2012) 192503.
- [61] J. Pflieger, M. He, M. Abdellatif, Mitochondrial complex II is a source of the reserve respiratory capacity that is regulated by metabolic sensors and promotes cell survival, *Cell Death Dis.* 6 (2015) e1835.
- [62] R. Abu Dawud, et al., Human embryonic stem cells and embryonal carcinoma cells have overlapping and distinct metabolic signatures, *PLoS One* 7 (6) (2012) e39896.
- [63] S. Lee, et al., Mitochondrial H₂O₂ generated from electron transport chain complex I stimulates muscle differentiation, *Cell Res.* 21 (5) (2011) 817–834.
- [64] J.A. Stuart, et al., Mitochondrial proton leak and the uncoupling proteins, *J. Bioenerg. Biomembr.* 31 (1999) 517–525.
- [65] M. Jastroch, et al., Mitochondrial proton and electron leaks, *Essays Biochem.* 47 (2010) 53–67.
- [66] S. Cardoso, et al., UCP2 and ANT differently modulate proton-leak in brain mitochondria of long-term hyperglycemic and recurrent hypoglycemic rats, *J. Bioenerg. Biomembr.* 45 (2013) 397–407.
- [67] C.T. Chen, et al., Coordinated changes of mitochondrial biogenesis and antioxidant enzymes during osteogenic differentiation of human mesenchymal stem cells, *Stem Cells* 26 (4) (2008) 960–968.
- [68] A. Chevrollier, et al., Adenine nucleotide translocase 2 is a key mitochondrial protein in cancer metabolism, *Biochim. Biophys. Acta* 1807 (6) (2011) 562–567.
- [69] H. Jang, et al., Metabolism in embryonic and cancer stemness, *Arch. Pharm. Res.* 38 (2015) 381–388.
- [70] J.A. Gaspar, et al., Unique metabolic features of stem cells, cardiomyocytes, and their progenitors, *Circ. Res.* 114 (2014) 1346–1360.
- [71] S.Y. Lunt, M.G. Vander Heiden, Aerobic glycolysis: meeting the metabolic requirements of cell proliferation, *Annu. Rev. Cell Dev. Biol.* 27 (2011) 441–464.
- [72] K.J. Livak, T.D. Schmittgen, Analysis of relative gene expression data using real-time quantitative PCR and the 2⁻ $\Delta\Delta$ CT Method, *Methods* 25 (4) (2001) 402–408, <http://dx.doi.org/10.1006/meth.2001.1262>.

Appendix 2

Publication II

Klepinina, L., Klepinin, A., Truu, L., Chekulayev, V., Kuus, K., Teino, I., Pook, M., Maimets, T., Kaambre, T. (2021). Colon cancer cell differentiation by sodium butyrate modulates metabolic plasticity of Caco-2 cells via alteration of phosphotransfer network. *PLOS ONE* 16(1): e0245348. DOI: 10.1371/journal.pone.0245348

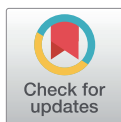
RESEARCH ARTICLE

Colon cancer cell differentiation by sodium butyrate modulates metabolic plasticity of Caco-2 cells via alteration of phosphotransfer network

Ljudmila Klepinina^{1*}, Aleksandr Klepinin¹, Laura Truu¹, Vladimir Chekulayev¹, Heiki Vija², Kaisa Kuus³, Indrek Teino³, Martin Pook³, Toivo Maimets³, Tuuli Kaambre¹

1 Laboratory of Chemical Biology, National Institute of Chemical Physics and Biophysics, Tallinn, Estonia, **2** Laboratory of Environmental Toxicology, National Institute of Chemical Physics and Biophysics, Tallinn, Estonia, **3** Department of Cell Biology, Institute of Molecular and Cell Biology, University of Tartu, Tartu, Estonia

* ljudmila.ounpuu@gmail.com



OPEN ACCESS

Citation: Klepinina L, Klepinin A, Truu L, Chekulayev V, Vija H, Kuus K, et al. (2021) Colon cancer cell differentiation by sodium butyrate modulates metabolic plasticity of Caco-2 cells via alteration of phosphotransfer network. *PLoS ONE* 16(1): e0245348. <https://doi.org/10.1371/journal.pone.0245348>

Editor: Joseph Najbauer, University of Pécs Medical School, HUNGARY

Received: June 26, 2020

Accepted: December 28, 2020

Published: January 20, 2021

Peer Review History: PLOS recognizes the benefits of transparency in the peer review process; therefore, we enable the publication of all of the content of peer review and author responses alongside final, published articles. The editorial history of this article is available here: <https://doi.org/10.1371/journal.pone.0245348>

Copyright: © 2021 Klepinina et al. This is an open access article distributed under the terms of the [Creative Commons Attribution License](https://creativecommons.org/licenses/by/4.0/), which permits unrestricted use, distribution, and reproduction in any medium, provided the original author and source are credited.

Data Availability Statement: All relevant data are within the manuscript and its [Supporting Information](#) files.

Abstract

The ability of butyrate to promote differentiation of cancer cells has important implication for colorectal cancer (CRC) prevention and therapy. In this study, we examined the effect of sodium butyrate (NaBT) on the energy metabolism of colon adenocarcinoma Caco-2 cells coupled with their differentiation. NaBT increased the activity of alkaline phosphatase indicating differentiation of Caco-2 cells. Changes in the expression of pluripotency-associated markers OCT4, NANOG and SOX2 were characterized during the induced differentiation at mRNA level along with the measures that allowed distinguishing the expression of different transcript variants. The functional activity of mitochondria was studied by high-resolution respirometry. Glycolytic pathway and phosphotransfer network were analyzed using enzymatical assays. The treatment of Caco-2 cells with NaBT increased production of ATP by oxidative phosphorylation, enhanced mitochondrial spare respiratory capacity and caused rearrangement of the cellular phosphotransfer networks. The flexibility of phosphotransfer networks depended on the availability of glutamine, but not glucose in the cell growth medium. These changes were accompanied by suppressed cell proliferation and altered gene expression of the main pluripotency-associated transcription factors. This study supports the view that modulating cell metabolism through NaBT can be an effective strategy for treating CRC. Our data indicate a close relationship between the phosphotransfer performance and metabolic plasticity of CRC, which is associated with the cell differentiation state.

Introduction

Colorectal cancer originates from the epithelial cells lining the large intestine. A rapid cell turnover is important for the growth of normal colonic epithelium. Stem cells continuously

Funding: This work was supported by the institutional research funding IUT23-1 of the Estonian Ministry of Education and Research.

Competing interests: The authors have declared that no competing interests exist.

proliferate in the base of the colonic crypt producing transit cells that migrate toward the upper part of the crypt, acquire the differentiated phenotype and finally undergo apoptosis [1]. Increased alkaline phosphatase activity has been shown to indicate differentiation of colon and colon cancer cells [2–6]. Since cancer cells often lack features of terminally differentiated cells, it has been proposed that tumor cells might arise from undifferentiated stem/progenitor cells. Alternatively, cancer cells can undergo progressive dedifferentiation into cells with “stem-like” properties known as cancer stem cells (CSC) [7,8]. Moreover, CSCs might use the same molecular pathways to facilitate self-renewal as normal stem cells. The increased expression of self-renewal regulatory factors important in cell pluripotent state such as OCT4, NANOG and SOX2 was detected in various types of cancers [9,10]. In clinical studies, the expression of these stem cell markers has been found to correlate with poor differentiation, advanced disease stages and worse overall survival in various cancers [11]. The OCT4 gene can generate several transcripts and isoforms by alternative splicing and these are differentially expressed in pluripotent and non-pluripotent cells [12]. In general, OCT4A together with OCT4B1 are highly expressed in embryonic stem and embryonic carcinoma cells and down-regulated after differentiation, while OCT4B is mainly the transcript expressed in somatic tumor cells [12]. Besides, OCT4B1 has been also found to be highly expressed in gastric, bladder, brain and colorectal cancers [13–16]. The expression of OCT4B4, which sequence is very similar to OCT4B, has been reported in embryonic carcinoma cells [17]. Additionally, there are OCT4 pseudogenes, which have been shown to be expressed in cancers. Those transcripts together with the different splice variants from the main gene make it difficult to detect the OCT4 expression level [18,19]. Aberrant NANOG expression has been also reported in many types of cancer including germline tumors, breast, prostate and colorectal cancers [20–22]. There are two different NANOG transcripts that can be expressed from the main gene [23] together with the transcripts from NANOG gene tandem duplication (NANOGP1) and NANOG pseudogenes [24]. The expression of SOX2 has been associated with cancer stem-like properties in skin, bladder and colorectal cancers [25–27].

The differentiation of colonic epithelial cells relies on numerous determinants including growth factors, hormones, vitamins as well as intestinal microbiota-derived metabolites such as short-chain fatty acids (SCFAs) [28]. Butyrate, which is present at relatively high concentrations (mM) in the colon lumen, is one of the most abundant SCFA produced by bacterial fermentation of dietary fibers. This metabolite exerts multiple beneficial effects on the intestinal homeostasis. Being the main energy source for normal colonocytes, butyrate also promotes proliferation of colonic epithelial cells, modulates immune and inflammatory responses, improves intestinal barrier function, and stimulates mucus secretion increasing vascular flow and motility [29]. More recently, attention has been given to butyrate due to its ability to suppress the *in vitro* proliferation of colon carcinoma cells. The anti-carcinogenic effect of butyrate has been attributed to its function as a histone deacetylase (HDAC) inhibitor. In various cancer cell lines, HDAC inhibitors suppress cell proliferation via cell cycle arrest, induce differentiation and apoptosis, reduce angiogenesis and modulate immune response [30].

The opposing effects of butyrate on the proliferation of normal versus cancerous colon cells has been explained by the “Warburg phenotype” of cancer cells [31]. Normally differentiated colon cells rely primarily on mitochondrial oxidative phosphorylation (OXPHOS) for energy production. Butyrate is metabolized in the β -oxidation pathway to acetyl-CoA, which enters the tricarboxylic acid (TCA) cycle and is used for ATP generation. The tendency of cancer cells to enhance glucose metabolism through aerobic glycolysis (Warburg effect) leads to diminished use of OXPHOS and butyrate as a substrate. Unmetabolized butyrate accumulates in the cell nucleus and functions as an HDAC inhibitor to control genes that inhibit cell proliferation and increase apoptosis [31].

Several studies demonstrated that butyrate could affect cancer cell proliferation by acting on individual enzymes of the glycolytic and OXPHOS pathways. Butyrate has been shown to increase oxidative pathway and/or decrease glycolytic metabolism in lung tumor cells (H460), colorectal adenocarcinoma cells (HT29, Caco-2, HCT116) and breast cancer cells (MCF-7, T47-D, MDA-MB231). This was correlated either with suppressed proliferation or induced differentiation or both together [32–36].

Although much is known about the rearrangements in energy producing pathways that occur during malignant transformation, the way how the energy is being transported within the cancer cell remains largely undiscovered. Creatine kinase (CK) and adenylate kinase (AK) that transfer phosphoryl groups between creatine phosphate, ADP, ATP and AMP are considered to facilitate the intracellular energetic communication. CK and AK phosphotransfer networks are defined as circuits of enzymes catalyzing sequential series of reversible transphosphorylation reactions linking ATP production and consumption sites in the cell (reviewed in [37]). It is noteworthy to mention that the phosphotransfer network of cell undergoes profound alterations during cancer development. Our previous studies revealed elevated AK activity and downregulated CK network in several tumors including human colorectal and breast cancer tissues, mouse neuroblastoma (Neuro-2A) and human embryonal carcinoma cells [38–40]. It has been proposed that diminished CK network can be partly compensated by other phosphotransfer enzymes, such as AK and glycolytic networks [41]. An important role for AK is emerging in cancer. AK4 has been reported to promote lung cancer progression and metastasis as well as modulate anti-cancer drug sensitivity in HeLa cells [42,43]. Recently, AK6 was proposed to be a potent modulator of metabolic reprogramming by regulating lactate dehydrogenase A (LDHA) activity in colon cancer stem cells [44]. Moreover, different AK isoforms have a prognostic biomarker potential for various cancer types (S1 Table).

Since SCFAs can alter the cellular metabolism of cancer cells, we hypothesized that treatment with sodium butyrate (NaBT) may reverse cancer-induced changes in phosphotransfer network of colon adenocarcinoma (Caco-2) cells including AK pathway. In addition to evidence supporting this hypothesis, we found that the flexibility of phosphotransfer networks depends on the availability of key metabolic substrates. The differentiation of Caco-2 cells was determined by increased alkaline phosphatase activity. In addition, NaBT-treatment resulted in the enhanced oxidative metabolism along with the changes in gene expression of the main pluripotency-associated transcription factors. Altogether, this indicates the link between regulation of phosphotransfer system and metabolic plasticity of cancer cells associated with the cell differentiation state.

Materials and methods

Patients and tissue samples

Human colorectal cancer and adjacent normal tissues were obtained from eight colorectal cancer patients between 55–87 years old, who underwent surgery at the North Estonia Medical Centre (Tallinn, Estonia). The adjacent normal tissue specimens were collected from an incision > 5 cm away from the carcinoma sites. Immediately after surgery, tissue samples were collected into RNAlater solution, frozen in the liquid nitrogen and kept at -80°C.

The pathological information of all patients was obtained from the Oncology and Hematology Clinic of the North Estonia Medical Centre. All patients examined had primary tumors and had not received prior radiation or chemotherapy. The study was approved by the Medical Research Ethics Committee (National Institute for Health Development, Tallinn) and conducted in compliance with the Declaration of Helsinki and the European Convention on Human Rights and Biomedicine. Written informed consent was obtained from all patients.

Cell culture and cell lines

The established Caco-2 cell line was obtained from American Type Tissue Culture Collection; HTB-37TM; p5). Cells were maintained in Eagle's minimum essential medium (Corning), supplemented with 10% fetal bovine serum (Gibco), 1% non-essential amino acids 100X (Corning), 100 U·ml⁻¹ penicillin (Gibco), 100 µg·ml⁻¹ streptomycin (Gibco) and 50 µg·ml⁻¹ gentamicin (Gibco) at 37°C in a humidified incubator supplied with 5% CO₂. Cells were sub-cultured every 3 days by mild trypsinization and seeded at a density of 20 000 cells·cm⁻². The viability of cells was around 95% according to trypan blue exclusion test. Cells were counted using a Bürker-Türk counting chamber. The maximal passage number of the cells used in the study was 20 and PCR based mycoplasma testing (see Supplementary) was used to confirm no mycoplasma contamination in the cell culture.

Human embryonic stem cells (WA09, National Stem Cell Bank, WiCell; received Feb-2020, p25) were cultured on 6-well tissue culture plates (BD Biosciences) coated with Matrigel (BD Biosciences) in mTeSR1 media (STEMCELL Technologies) according to the manufacturer's specifications. The culture medium was changed daily. Cells were passaged mechanically with micropipette tip after 3–4 days and cultured in the presence of 5% CO₂ at 37°C in humid conditions. The maximal passage number of the cells used in the study was 70 and the normal karyotype of the cells was routinely confirmed by G-banding.

Cell viability and cytotoxicity assay

Cells were grown on 6 and 96-well plates. 24 h after plating, cells were incubated with various concentrations of NaBT (Acros Organics) for 24, 48 or 72 h. NaBT solution was prepared immediately before use by dissolving NaBT powder in complete growth medium. After each treatment, cell viability was assessed using MTT assay as described previously [45] and trypan blue test [46]. The cytotoxicity was assayed by lactate dehydrogenase (LDH) release after NaBT treatment. LDH activity was measured in both floating dead cells and viable adherent cells by using a standard kinetic determination [47]. The cytotoxicity was calculated as LDH activity in culture medium divided by total LDH activity.

Quantitative RT-PCR, semi-quantitative RT-PCR and enzymatic digestion

RNA from Caco-2 cells, frozen human colorectal cancer and adjacent normal samples was extracted with the RNeasy Mini Kit (QIAGEN Sciences) followed by DNase I treatment (Thermo Fisher Scientific). Synthesis of cDNA was performed with RevertAid First Strand cDNA Synthesis Kit using oligo(dT)₁₈ primer (Thermo Fisher Scientific). Quantitative RT-PCR was performed using Maxima SYBR Green/ROX qPCR Master Mix (Thermo Fisher Scientific), specific primers (S2 and S4 Tables) and real-time PCR machine LightCycler 480 (Roche). Semi-quantitative RT-PCR was carried out with FIREPol Master Mix (Solis BioDyne) and gene-specific primers (S4 and S5 Tables). PCR products were analyzed on 2% agarose gel electrophoresis. Images were obtained and band intensities were quantified with Biospectrum 510 Imaging System (UVP, LLC). To distinguish between OCT4A and its pseudogene expression, the approximately 500 bp band was excised from agarose gel, followed by purification of DNA with FavorPrep GEL/PCR Purification Mini Kit (Favorgen). Recovered DNA was subjected to 5 units of ApaI (Thermo Fisher Scientific) digestion overnight followed by separation on 2% agarose gel electrophoresis and imaging. Transcripts were identified by size, based on the previously published results with these primers. The respective areas were selected as rows to summarize the results for different transcripts in the figures.

High-resolution respirometry

Mitochondrial respiration was measured in intact cells by means of high-resolution respirometry using the Oroboros® Oxygraph-2K (Oroboros Instruments, Innsbruck, Austria). The DATLAB 5 software (Oroboros Instruments) was used for real-time data acquisition and subsequent data analysis. Measurements were performed at 25°C in the respiration medium comprising 110 mM sucrose, 60 mM K-lactobionate, 0.5 mM EGTA, 3 mM MgCl₂·6H₂O, 20 mM taurine, 3 mM KH₂PO₄, 20 mM HEPES, adjusted to pH 7.1 with KOH and supplemented with 2 mg·ml⁻¹ bovine serum albumin free from essential fatty acids (Sigma), 0.5 mM DTT and 9.6 µg/ml leupeptin. The rates of oxygen consumption were normalized to cell number (nmol of O₂·min⁻¹·10⁻⁶ cells). To measure the oxygen consumption through different segments of the respiratory chain and analyze basic respiratory properties, cells were treated with the combination of substrates, uncouplers and inhibitors of respiration as depicted in [S1 Fig](#).

Mitochondrial membrane potential

Caco-2 cells were seeded into black clear-bottom 96-well plates (Greiner Bio-One) at a density of 3 000 cells per well. The next day the growth medium was changed to the medium containing 1 mM NaBT and cells were incubated for 48 h at 37°C in a humidified incubator supplied with 5% CO₂. After treatment, the mitochondrial membrane potential was measured using the fluorescent dye tetramethylrhodamine methyl ester (TMRE). Cells were incubated with 20 nM TMRE in complete growth medium at 37°C for 30 min protected from light. The medium was removed, and cells were washed 3 times with PBS to remove background fluorescence from the cell culture medium. 100 µl of PBS was added into each well, and fluorescence intensities were measured on a FLUOstar Omega microplate reader (BMG Labtech) (excitation: 550 nm and emission: 590 nm). In order to exclude any possible impact of the plasma membrane potential on the fluorescence intensities, each assay was performed in parallel as above plus 10 µM of FCCP, which disrupts the mitochondrial membrane potential. After measurements, PBS was removed, and cells were lysed with 1% SDS solution in PBS. Protein concentrations were determined by Pierce BCA Protein Assay Kit according to the manufacturer recommendations. All data were expressed as the total TMRE fluorescence minus FCCP-treated TMRE fluorescence and normalized to protein content.

Immunofluorescence analysis

Cells were seeded onto glass coverslips at a density of 1.7·10⁴ cells·cm⁻² in 12-well plates (Greiner Bio-one) overnight and treated with 1 mM NaBT for 48 h. For mitochondria staining, 200 nM MitoTracker Red CMXRos (Invitrogen) was added into culture medium for 30 min before fixing with 4% paraformaldehyde in PBS for 10 min at room temperature (RT). Fixed cells were washed with PBS and permeabilized with 0.1% Triton X-100 in PBS for 10 min. After washing with PBS, the coverslips were incubated with anti-beta tubulin antibody (ab6046, Abcam) in 2% BSA/PBS overnight at 4°C. Thereafter, these were washed with PBS, followed by incubation with Alexa Fluor 488 conjugated anti-rabbit antibody (ab96899, Abcam) for 1 h at RT. After washing 3X with PBS, the coverslips were mounted with ProLong Gold antifade reagent containing 4',6-diamidino-2-phenylindole dihydrochloride (DAPI, Thermo Fisher Scientific). Cells were examined under Olympus FluoView FV10i-W inverted laser scanning confocal microscope.

Preparation of cell lysates

The cell pellets were re-suspended in ice-cold lysis buffer containing 20 mM MOPS pH 8.0, 20 mM MgCl₂·6H₂O, 10 mM glucose, 200 mM NaCl, 10 mM EDTA-Na₂, 0.25% Triton-X, and protease inhibitor cocktail (Roche). Cell lysates were homogenized using a Retsch Mixer Mill (Retsch) at 25

Hz for 2 min and centrifuged at 12,000 rcf for 20 min at 4°C. The supernatants were used for enzymatic assays. Protein concentrations were determined by Pierce BCA Protein Assay Kit according to the manufacturer recommendations using bovine serum albumin (BSA) as a standard.

Enzymatic activity assays

Enzymatic activities were measured spectrophotometrically in cell lysates at 25°C with a FLUOstar Omega microplate reader. Alkaline phosphatase (ALP) activity was determined with *p*-nitrophenyl phosphate (pNPP) as a substrate using a modification of the published method [48]. The assay mixture contained 0.1 M Tris-HCl pH 9.8, 5 mM MgCl₂ and 2 mM pNPP. The activity was associated with a decrease in absorbance at 405 nm. Specific activity was calculated by using an extinction coefficient 6.22 mM⁻¹cm⁻¹. Citrate synthase (CS) activity was determined by measuring the rate of thionitrobenzoic acid production at 412 nm [49]. Hexokinase (HK) activity was determined using a standard glucose-6-phosphate dehydrogenase (G6PDH)-coupled spectrophotometric assay [50]. Lactate dehydrogenase and pyruvate kinase activities were quantified by measuring the decrease in absorbance of NADH at 340 nm [47,51]. CK and AK activities were measured by an enzyme-coupled spectrophotometric assay in the direction of ATP formation as described earlier [52,53]. All enzymatic activities were normalized per mg of cell protein.

Nucleotide measurements

ATP level and ATP/ADP ratio were determined by ultra-performance liquid chromatography (UPLC) as described previously [54] with some modification. Briefly, after quick growth medium removal, cells were rinsed with saline solution, quenched with 0.6 M ice-cold HClO₄ and immediately frozen in liquid nitrogen. After cell collection, samples were centrifuged at 10,000 rcf for 5 min at 4°C. The supernatant was neutralized with 2 M KHCO₃ and the pellet was used in protein assay. To remove salt, samples were centrifuged at 10,000 rcf for 15 min at 4°C. Nucleotides in the supernatant were separated on a reversed-phase C18 column Separon SGX 5 μm 3x150 mm (Tessek, Czech Republic) with the Waters Acquity UPLC equipped with a PDA detector. A phosphate buffer (100 mM) with tetrabutylammonium sulfate (10 mM) and methanol mixture (water:methanol; 60:40% (v:v)) was used as mobile phase at 0.6 mL·min⁻¹ flow rate. Gradient elution was applied and during 9 min all nucleotides were completely separated. To estimate ATP production through mitochondrial respiration and glycolysis, we measured ATP/ADP ratio in the presence of OXPHOS inhibitors (rotenone, antimycin A and oligomycin 1 μg/mL) or glycolysis [2-deoxyglucose (DOG) 6mM], as described previously [55]. The ATP levels were normalized per mg of cell protein.

Statistical analysis

Data analysis was performed using SigmaPlot software. Results are expressed as means ± SEM. Statistical comparisons between control group and treated cells were made by two-tailed Student's *t* test for unpaired samples. To assess differences between multiple groups, a 2-way analysis of variance (ANOVA) was applied. The Turkey test was used for post-hoc analysis. The statistical analysis was conducted at 95% confidence level. A *P* value less than 0.05 was considered statistically significant.

Results

Incubation of cells with 1 mM NaBT for 48 h induced cell differentiation without any toxic effect

In this study, we evaluated a possible relationship between cellular differentiation and energy metabolism in colon cancer cells. To avoid any interferences caused by cytotoxicity, we first

validated the best experimental conditions to study effects of NaBT on cellular bioenergetics. Caco-2 cells were treated with various concentrations of NaBT for 24, 48 and 72 hours. The viability of metabolically active cells was estimated by MTT assay (Fig 1A). The viability of the treated cells is presented relative to that of the untreated cells (control), which is regarded as 100% cell viability. In addition, the cytotoxic effect of NaBT was assayed by lactate dehydrogenase (LDH) release. As expected, treatment with NaBT induced time and dose-dependent inhibition of cell growth (Fig 1A). Treatment of cells for 24 hours was not enough to reveal inhibitory effect of NaBT on the cell growth since the doubling time of Caco-2 monolayer cell culture is approximately 32 hours (ATCC). Gradual inhibition of cell growth was observed after 48 hours of incubation. The viability of cells was $90\pm 2\%$ with 1 mM NaBT, $73\pm 7\%$ with 2 mM, $56\pm 10\%$ with 5 mM and $37\pm 3\%$ with 10 mM. Longer incubation with NaBT (72 hours) resulted in more prominent effect on the viability. Specifically, cell viability of $85\pm 6\%$, $68\pm 9\%$, $39\pm 5\%$ and $17\pm 4\%$ were observed for 1, 2, 5 and 10 mM NaBT, respectively. The cytotoxic effect of NaBT appeared after 48 h of treatment at concentrations above 2 mM (Fig 1B and S2 Fig). When the incubation was extended to 72 hours, the cytotoxicity of NaBT was also observed at 2 mM concentration. In contrast, 1 mM NaBT was non-toxic for Caco-2 cells at all studied time points.

The inhibition of cell growth was also accompanied by increased ALP activity (Fig 1C), a well-established marker of colon cell differentiation [56]. After 48 h of incubation with 1 mM NaBT, the ALP activity increased almost 10 times compared with untreated control. Furthermore, treated cells resembled epithelial-like cells with a polygonal shape and had more regular dimensions compared to cells cultured in the absence of NaBT (Fig 2). Thus, the incubation of cells with 1 mM NaBT for 48 h was sufficient to induce cell differentiation without any notable toxic effect, and this treatment protocol was used in subsequent experiments.

Treatment with NaBT affected expression of stem cell markers OCT4 and SOX2 but not NANOG

As treatment with 1 mM NaBT for 48 h induced changes in Caco-2 cell growth and increased ALP activity, pointing to cancer cell differentiation, we decided to analyze the expression pattern of main pluripotency-associated stem cell markers to indicate the presence of putative cancer stem cells and also characterize the possible splice variants of OCT4 and NANOG which expression could be modulated by the epigenetic changes induced by NaBT. The expression of OCT4, NANOG and SOX2 was detected in Caco-2 cells at mRNA level (S3 Fig) and the change in relative expression was semi-quantitatively measured from band intensity levels (Fig 3). To examine the expression pattern of different splice variants of OCT4 in Caco-2 cells, we used primers that were previously described to specifically amplify OCT4A, OCT4B and OCT4B1 [12]. In order to verify the expression of OCT4A, we used restriction analysis with *ApaI* for the amplified OCT4A product as only the true OCT4A product contains this restriction site [57]. Interestingly, OCT4A transcript was found to be expressed only after treatment with NaBT and the control cells did mainly express transcripts from OCT4 pseudogenes that were non-specifically amplified with the previously published OCT4A primers (S3B Fig). In order to confirm the expression changes for OCT4A we designed new primers, which specifically detected OCT4A. With the subsequent quantitative RT-PCR analysis we confirmed increased OCT4A expression after NaBT treatment (Fig 4). Additionally, we detected the expression of OCT4B1 variant, while OCT4B variant was missing (S3A and S5 Figs). In human embryonic stem cells (hESCs, cell line WA09), OCT4B appeared as a double band (S3A Fig) where the shorter product points to the existence of OCT4B4 transcript [17] that was also detected from Caco-2 cells (S5 Fig). Semi-quantitative densitometric analysis of

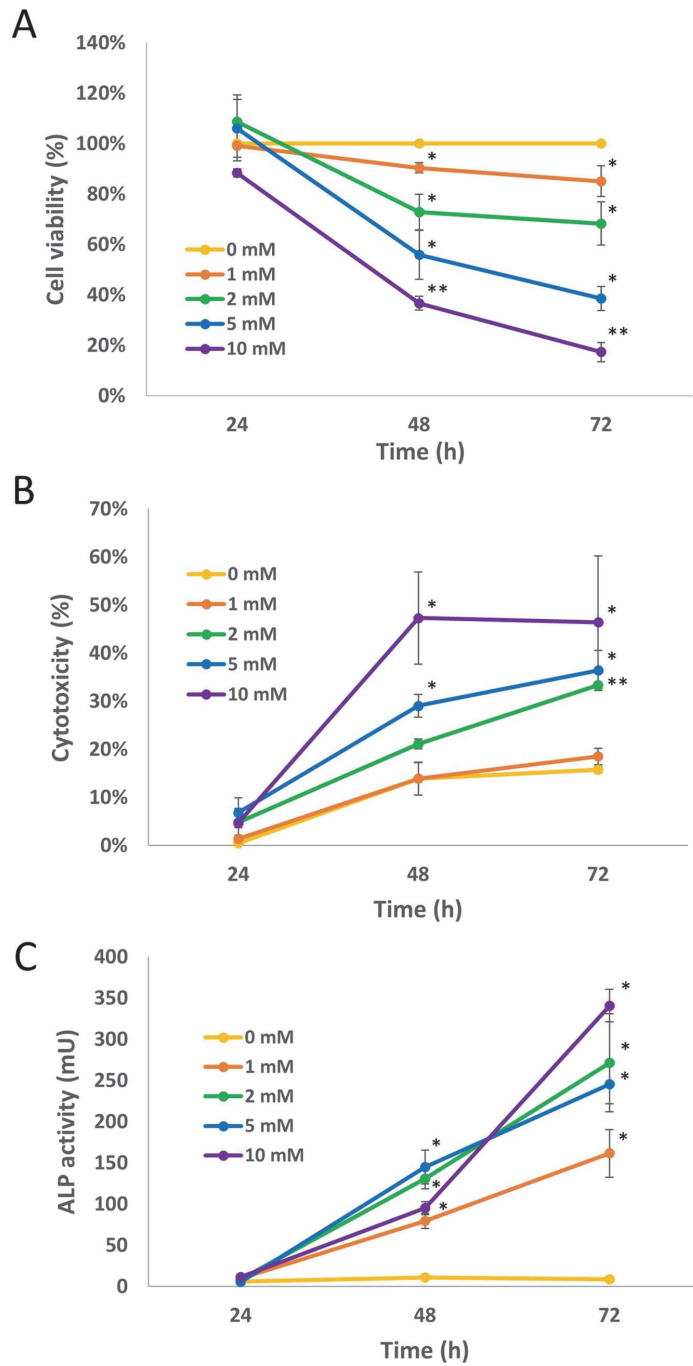


Fig 1. Caco-2 cell culture sensitivity and differentiation response to sodium butyrate (NaBT). Cells were incubated in the presence of various concentrations of NaBT for 24, 48 or 72 hours. (A): The viability of cells was analyzed by MTT assay. (B): Cytotoxicity was estimated by measurement of lactate dehydrogenase release after treatment with NaBT. (C) Alkaline phosphatase (ALP) activity assay was used to estimate differentiation status of the cells. Data are presented as mean \pm SEM (n = 3–5). *P < 0.01; **p < 0.001 (ANOVA followed by Tukey post-hoc test).

<https://doi.org/10.1371/journal.pone.0245348.g001>

OCT4B4 band intensities revealed that this transcript is more expressed after treatment with NaBT (Fig 3). Unfortunately, we were not able to confirm this by quantitative RT-PCR due to lack of suitable specific primers. We also checked for NANOG expression in hESCs and Caco-2 cells (S3A Fig). Although both transcripts from NANOG (NANOG1, NANOG2) were detected in Caco-2 cells, the expression of NANOG2 was prevailing and no differences were noted after treatment with NaBT. In embryonic stem cells, only NANOG1 transcript was observed. Interestingly, we did not detect changes in the expression of SOX2 after differentiation of Caco-2 cells with NaBT (Figs 3 and 4).

Next, we were interested to find out which variants of the analyzed stem cell markers are expressed in primary colorectal tumors. We used colorectal tumor tissue samples together with the control samples taken from the surrounding normal tissue of the same patient and characterized the expression of the same pluripotency-associated stem cell markers in this material (S4A Fig). The general OCT4A primers amplified a product that was more abundant in some of the analyzed tumor samples compared with normal tissue, but at the same time there were samples that did not show this tendency. Verification of OCT4A with ApaI restriction analysis showed that most of the amplified products (excluding sample 6) were OCT4 pseudogenes and together with semi-quantitative measurements of this band and quantitative RT-PCR with OCT4A specific primers we can suggest the increased expression of OCT4 pseudogenes in colorectal cancer (Figs 3, 4 and S4B). OCT4B1 expression was detected showing no

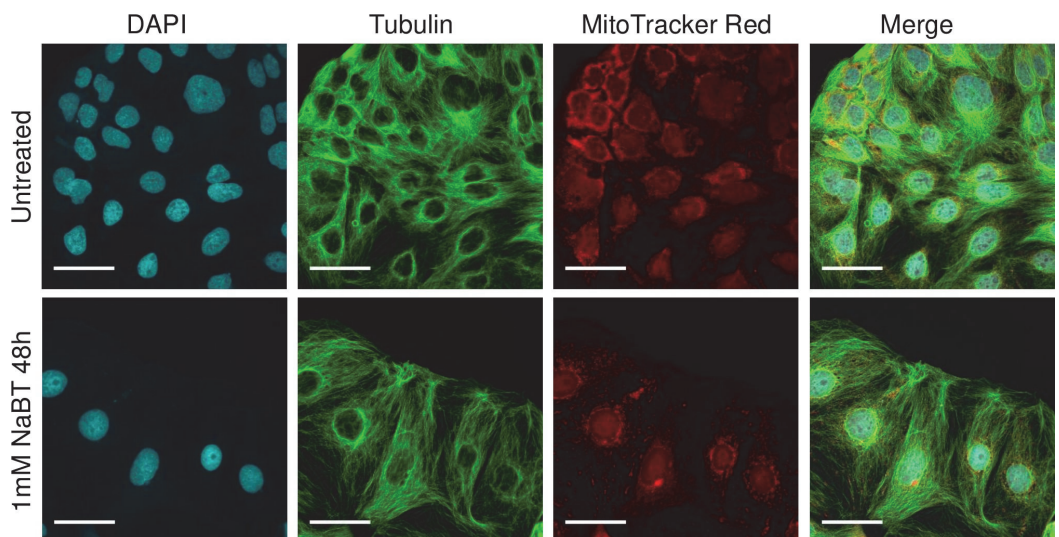


Fig 2. Confocal microscopy of untreated and sodium butyrate (NaBT)-treated Caco-2 cells. Morphological changes of cells occur after treatment of cells for 48h with 1mM NaBT. Cells were stained with MitoTracker (red), anti-whole tubulin (green) and DAPI (blue). For all the above, representative images are shown. Scale bars: 50 μ m.

<https://doi.org/10.1371/journal.pone.0245348.g002>

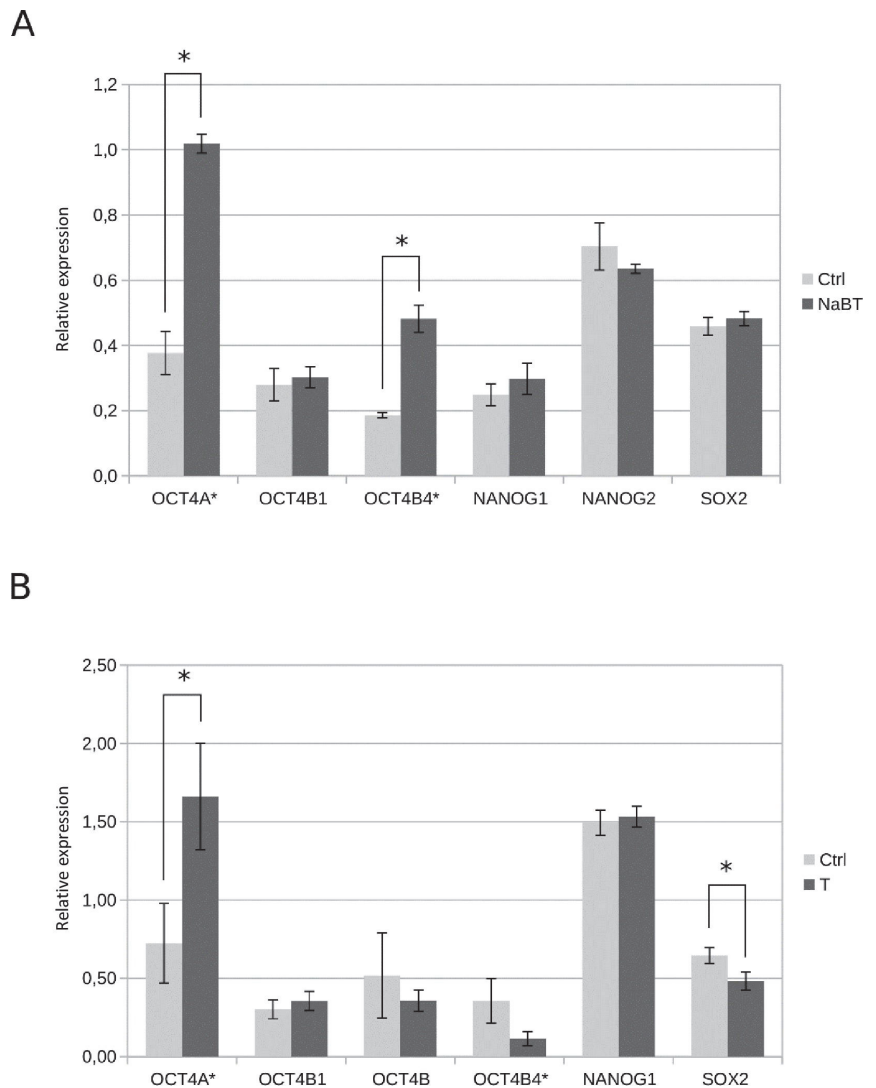


Fig 3. Semi-quantitative densitometric analysis of pluripotency-associated transcription factors. (A): Densitometric band intensity measurements from [S3A Fig](#) showing the relative changes between NaBT-treated (1mM, 48h) Caco-2 cells (NaBT) and without treatment (Ctrl) (B): Densitometric band intensity measurements from [S4A Fig](#) showing relative changes between primary colorectal tumor samples (T) and adjacent normal tissue samples (Ctrl). Data are presented as mean \pm SEM (* $p < 0.05$, Student's t test).

<https://doi.org/10.1371/journal.pone.0245348.g003>

evident changes between tumor and normal tissue samples ([Fig 3](#)) and OCT4B together with OCT4B4 was showing variable expression pattern between the analyzed patient tissue samples ([Fig 3](#) and [S4A Fig](#)). Interestingly, we did not see expression of NANOG transcript variant 2 (NANOG2) in primary tissue samples, while the expression of variant NANOG1 was present

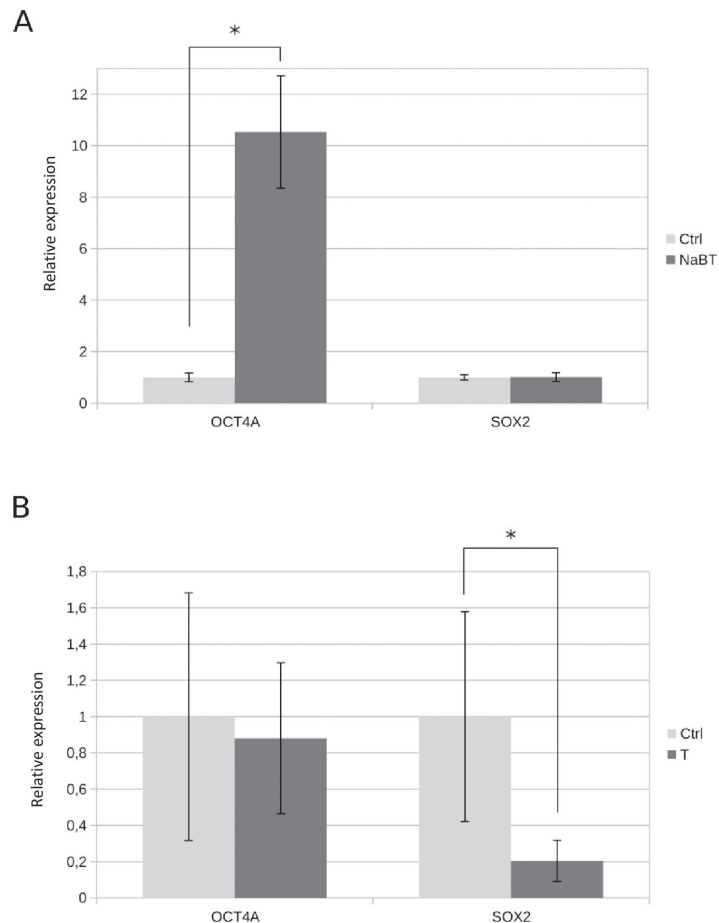


Fig 4. Quantitative RT-PCR analysis of pluripotency-associated transcription factors OCT4A and SOX2. (A): Relative gene expression in Caco-2 cells treated for 48h with 1 mM sodium butyrate (NaBT) or without treatment (Ctrl). (B): Relative gene expression in primary colorectal tumor samples (T) and adjacent normal tissue samples (Ctrl). Data are presented as mean \pm SEM (* $p < 0.05$, Student's t test).

<https://doi.org/10.1371/journal.pone.0245348.g004>

without evident changes in all the samples (Fig 3 and S4A Fig). Surprisingly, the expression of SOX2 was more detected in normal samples and most tumor tissue samples had less SOX2 expressed than in adjacent normal tissue (Figs 3, 4 and S4A).

Treatment of cells with NaBT increased oxidative metabolism

Caco-2 cells displayed mixed profile of small punctate and elongated mitochondria (Fig 2). Treatment of cells with 1 mM NaBT did not induce any drastic changes in mitochondria morphology, total mitochondrial mass or mitochondrial membrane potential (Fig 2 and S6 Fig).

To investigate whether NaBT affects mitochondria on the functional level, we measured the rates of oxygen consumption by Caco-2 cells using high-resolution respirometry (S1A Fig).

The ability of cells growing with or without NaBT to consume oxygen was measured in the absence or presence of NaBT in the respiratory medium (Fig 5A and 5B). We also used substrates specific for the mitochondrial complex I (5 mM glutamate and 2 mM malate) and complex II (10 mM succinate) to assess the impact of individual electron transfer system components on the overall respiratory performance of cells. In the absence of butyrate in the respiratory medium, treated cells and cells growing without NaBT displayed similar rates of oxygen consumption (Fig 5A). However, the supplementation of respiratory medium with 5 mM NaBT resulted in significantly increased respiration rates only in 48h NaBT pre-treated cells with each substrate tested suggesting that butyrate is used as a substrate for an oxidative metabolism in more differentiated colon cancer cells (Fig 5B).

To analyze the impact of NaBT on the key parameters of mitochondrial respiration, we measured oxygen consumption rates in non-permeabilized Caco-2 cells using mitochondrial stress test protocol (S1 Fig). No significant difference was observed in the routine respiration, proton leak or ATP-coupled respiration (Fig 5C). However, the maximal respiration rate following addition of uncoupling agent (FCCP) and spare respiratory capacity were significantly higher in NaBT-treated cells compared with untreated control cells, indicating that treated cells are more adaptable to cellular stress. Furthermore, the increased non-mitochondrial residual oxygen consumption (ROX) after treatment of cells with NaBT may indicate that NaBT can activate alternative oxidases or promote other oxygen consuming processes in cell cytosol.

To estimate the contribution of glycolysis and oxidative phosphorylation to ATP production, we measured the amount of ATP and the ratio of ATP/ADP in cells treated with inhibitors of OXPHOS (rotenone, antimycin A and oligomycin) or glycolysis [2-deoxyglucose (DOG)] (Fig 5D and 5E). The total ATP level as well as the ratio of ATP/ADP did not differ between NaBT-treated and untreated control cells. We found that in both experimental groups, most of ATP was generated by glycolytic pathway. However, the level of ATP produced by OXPHOS was increased and the amount of ATP generated by glycolysis was slightly decreased after incubation of cells with NaBT (Fig 5E). Namely, untreated cells produced $33 \pm 1\%$ of total ATP by OXPHOS, while $67 \pm 1\%$ of ATP was derived from glycolysis. After treatment with NaBT, $44 \pm 3\%$ and $56 \pm 2\%$ of ATP was produced by OXPHOS and glycolysis, respectively. In addition, enzyme assay study showed that the activities of glycolytic enzymes lactate dehydrogenase and pyruvate kinase were decreased in NaBT-treated cells (Fig 6A–6D). Altogether, these results suggest that differentiation of Caco-2 cells with NaBT induced a shift from glycolytic to more oxidative metabolism.

Rearrangement of phosphotransfer system in response to NaBT treatment and changing microenvironmental conditions

To test whether there is a relationship between NaBT-induced changes in energy metabolism and a phosphotransfer system of cells, we measured the specific activities of CK, AK and glycolytic enzymes (Figs 6 and 7). As glutamine can be an alternative energy source for tumor cells (Fig 7A), we evaluated the changes in phosphotransfer system also in the glutamine-free media.

The reduced levels of glycolysis-derived ATP suggested that treatment of cells with NaBT might lead to disturbances in the glycolytic pathway. To investigate this, the activity of HK, an important regulator of earlier stages of glycolytic flux, was measured. The middle stage of glycolysis was evaluated by pyruvate kinase (PYK) activity and the end phase was estimated by LDH activity. The HK activity remained the same in all experimental groups (Fig 6E and 6F). However, both PYK and LDH activities were significantly decreased after treatment of cells

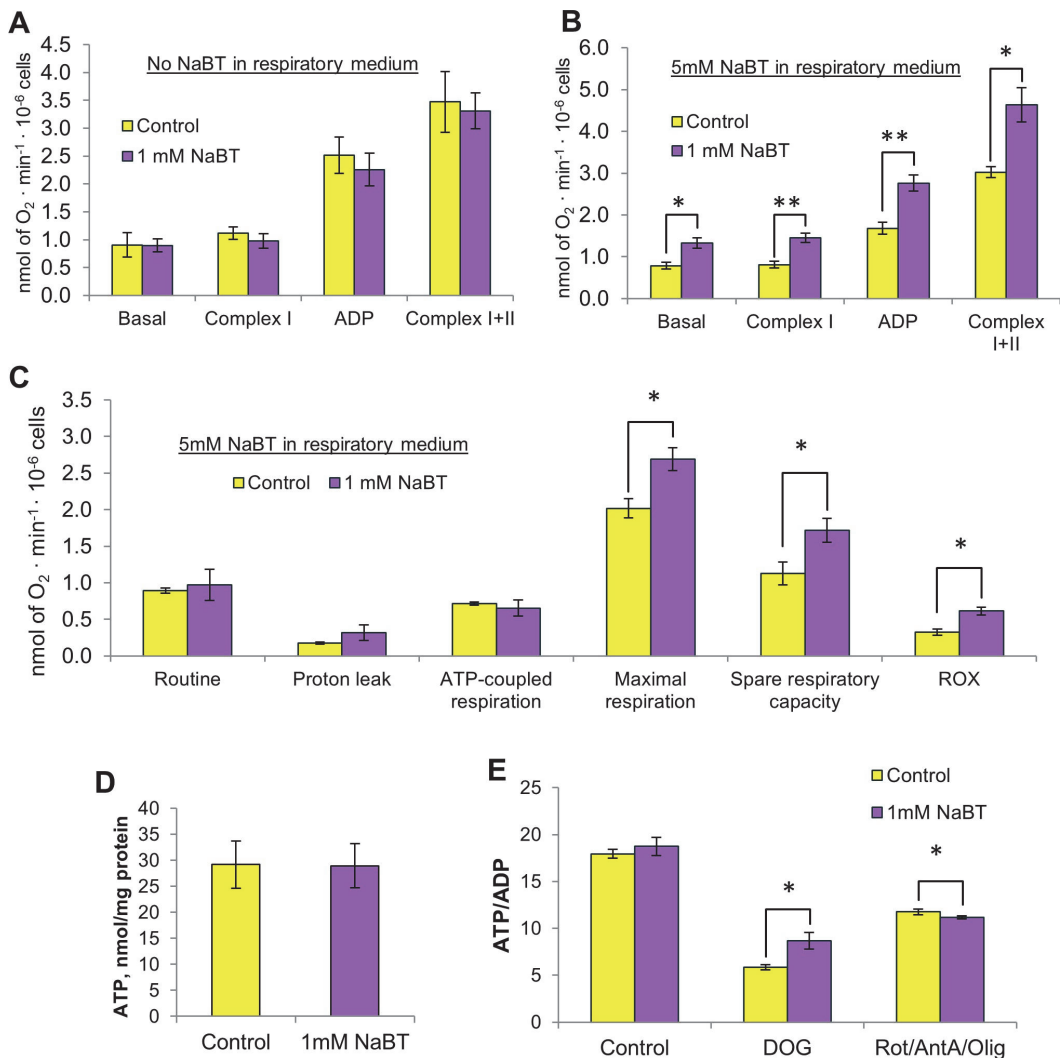


Fig 5. 48-hour pre-treatment with sodium butyrate induced an increase in oxidative metabolism of Caco-2 cells. (A): Oxygen consumption rates in the absence of sodium butyrate in the respiratory medium were measured using high-resolution respirometry. (B): Oxygen consumption rates in the presence of sodium butyrate. (C): Parameters of mitochondrial respiration obtained using mitochondrial stress test protocol. (D): ATP concentration measured by UPLC. (E): Effect of glycolysis and OXPHOS inhibition on the ATP/ADP ratio. All data are presented as mean \pm SEM ($n = 3-5$; * $p < 0.05$, Student's t test). AntA-antimycin A, CS-citrate synthase, DOG- 2-deoxyglucose, NaBT-sodium butyrate, Olig-oligomycin, Rot-rotenone.

<https://doi.org/10.1371/journal.pone.0245348.g005>

with NaBT in the presence of glutamine in the growth media (Fig 6A–6C). Interestingly, PYK activity did not change after NaBT-treatment in glutamine free media. In contrast, LDH activity was decreased after NaBT treatment in glutamine-free media containing lower levels of glucose (5 mM), while supplementation of glutamine-free media with higher glucose concentration (25 mM) resulted in similar levels of LDH activity in treated and untreated cells. These

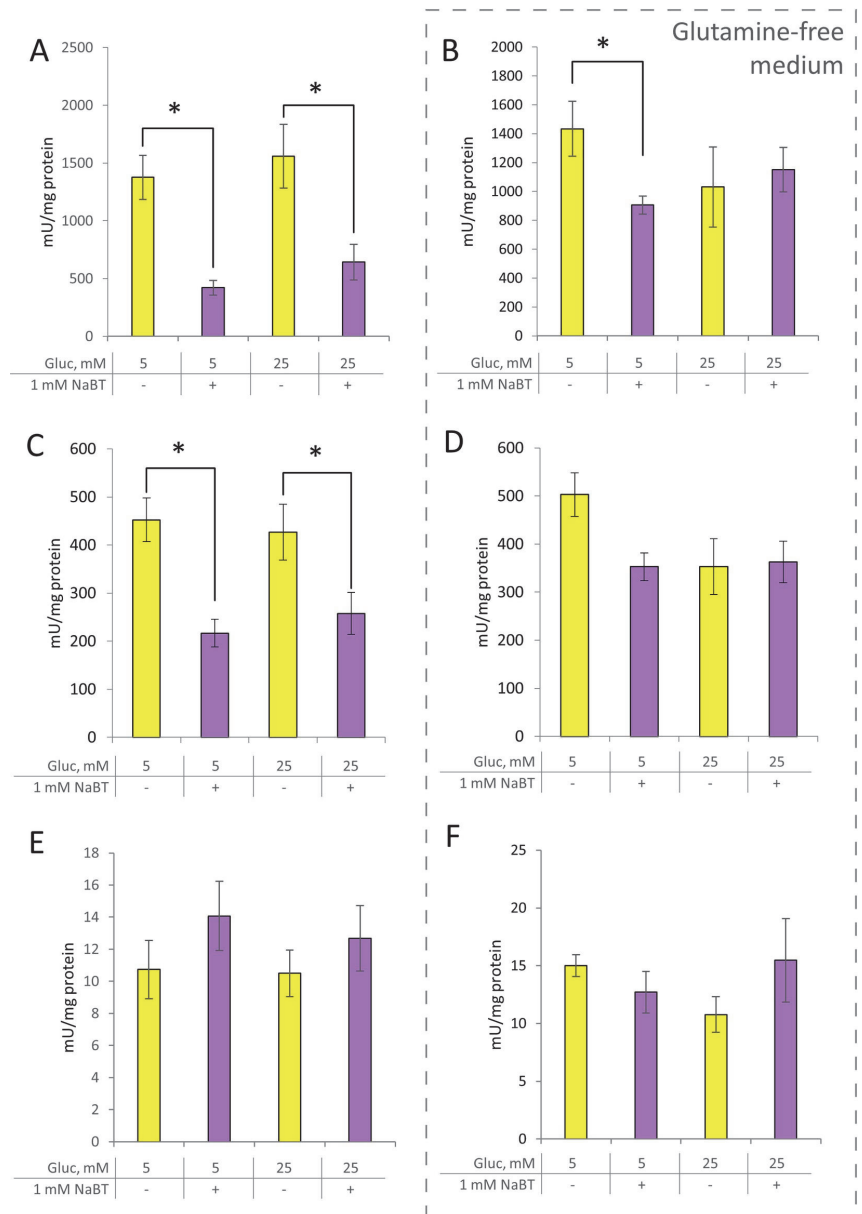


Fig 6. Effect of sodium butyrate on the activity of main glycolytic enzymes. (A, B): Lactate dehydrogenase activity (C,D): Pyruvate kinase activity. (E,F): Hexokinase activity. B,D,F—cells were grown in glutamine-free medium. All data are presented as mean \pm SEM (n = 3–5; *p < 0.05, ANOVA followed by Turkey post hoc test). Gluc—glucose, NaBT—sodium butyrate.

<https://doi.org/10.1371/journal.pone.0245348.g006>

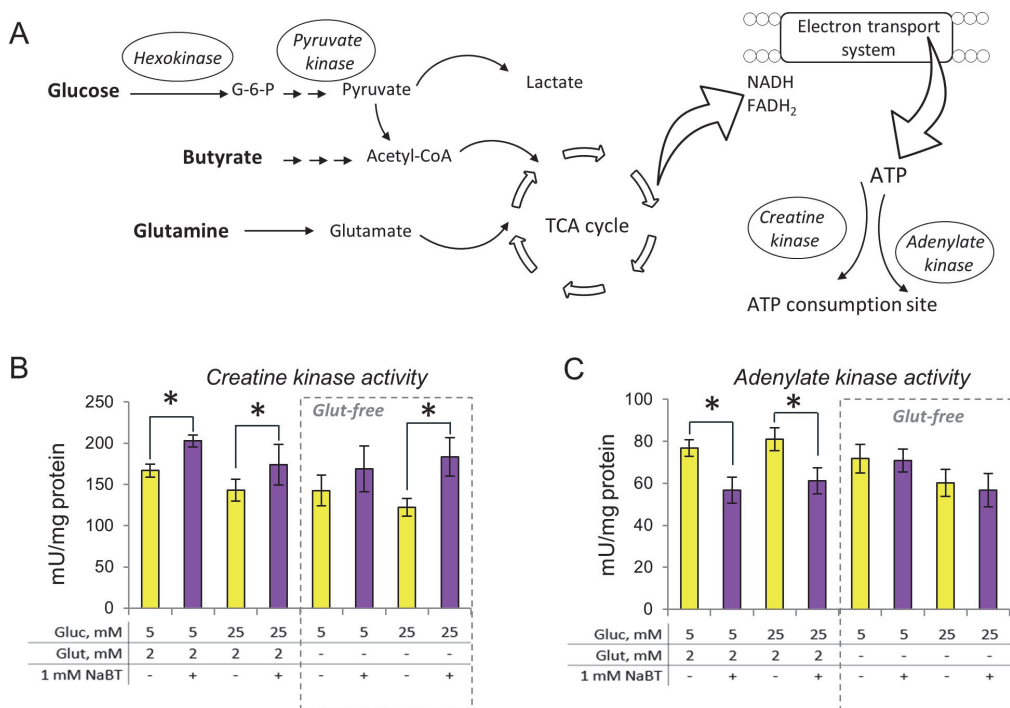


Fig 7. Rearrangement of phosphotransfer system after treatment of Caco-2 cells with sodium butyrate. (A): Schematic representation of main pathways analyzed. (B): Creatine kinase activity. (C): Adenylate kinase activity. All data are presented as mean \pm SEM ($n = 3-5$; * $p < 0.05$, ANOVA followed by Tukey post hoc test). AK—adenylate kinase, CK—creatine kinase, G-6-P—glucose-6-phosphate, Gluc—glucose, Glut—glutamine, NaBT—sodium butyrate, TCA—tricarboxylic acid.

<https://doi.org/10.1371/journal.pone.0245348.g007>

results suggested that in Caco-2 cells, butyrate affects later stages of glycolytic pathway, rather than earlier stages.

The activity of CK was increased and the activity of AK was decreased after differentiation with NaBT in the presence of glucose (5 mM) and glutamine. An increase in glucose concentration did not affect AK and CK activities (Fig 7B and 7C). The pattern of CK activity remained similar in glutamine-free media as the activities increased after cell incubation with NaBT regardless of glutamine or glucose availability in the growth medium. In contrast, the suppressive effect of NaBT on AK activity disappeared in glutamine-free media. Altogether, the results suggest that NaBT, in the presence of glutamine and glucose, can modulate cancer-induced changes in the phosphotransfer system.

Discussion

Although conventional chemotherapy is the main treatment strategy for cancer, the lack of sensitivity and the development of resistance to currently available drugs limit significantly the efficiency of existent therapies [58]. Cancer stem cells, which demonstrate unique metabolic flexibility, are considered to be the reason for tumor relapse and metastasis and were shown to exhibit a remarkable resistance to chemo- and radiotherapy [59]. Reactivation of endogenous differentiation programs that would make cancer cells more amenable to treatment using

conventional therapeutic approaches appears to be one of the promising strategies for targeting CSCs in colon cancer [60]. Thus, the ability of butyrate and its derivatives to act as epigenetic modulators and promote differentiation of cancer cells has important implication for cancer prevention and therapy.

Currently, the identification of CSCs relies mostly on the expression of CSC surface markers. Numerous cell surface markers have been proposed for colon CSCs including CD133, CD44, LGR5, EpCAM, ALDH etc. The variability of CSC surface markers creates a necessity to identify more putative markers for colon CSCs. Factors regulating pluripotent stem cell renewal such as OCT4, SOX2 or NANOG, have potential for CSC identification [61,62], but one has to take into account the existence of different splice variants and expressed pseudogenes for OCT4 and NANOG. We aimed to characterize the expression of the main pluripotency-associated genes in colorectal cancer and distinguish it from the expression of relevant pseudogenes. In order to follow the differentiation status of butyrate-treated cells, we used alkaline phosphatase activity, which is a widely accepted differentiation marker for colon and colon cancer cells [2–6]. As quantitative RT-PCR is challenging and cannot be used sometimes to distinguish between different transcript variants or expressed pseudogenes, our study also includes semi-quantitative analysis of expressed transcripts. We aimed to reveal the major pattern and track possible changes in the expression of CSC markers at RNA level. Firstly, we used semi-quantitative densitometric measurements to quantify band intensities of respective transcripts and then chose targets, which showed differences between analyzed samples to be additionally validated by quantitative RT-PCR, if possible. We did not see any major differences in the expression of NANOG transcripts between butyrate treated and un-treated Caco-2 cells or between primary tumor and normal tissue samples. Apart from OCT4A/OCT4 pseudogenes and an increase in the expression of OCT4B4 transcript after butyrate treatment in Caco-2 cells, there were no apparent changes detected for OCT4B or OCT4B1. It was surprising to find out that NaBT induced OCT4A expression in Caco-2 cells. Along with this, transcription of OCT4A was mainly missing from tumor samples and instead elevated expression of OCT4 pseudogenes was detected, which coincides well with a previous study on colorectal cancer tissue [16]. Interestingly, decreased expression of SOX2 was noted in tumor samples compared with the respective control tissue samples, while there were no significant changes in the expression of SOX2 after NaBT treatment on Caco-2 cells. Previously, expression of SOX2 has been shown to be associated with CSC phenotype in colorectal cancer and lower levels of SOX2 expression have been suggested to associate prognosis for relapse-free survival [25] and forced expression of OCT4 and SOX2 has been shown to induce CSCs properties including sphere formation, chemoresistance and tumorigenicity [63]. Therefore, our results showing the opposite in tumor samples for SOX2 are challenging new studies to be conducted to find out more about SOX2 expression. Of note, we also found that some of the published SOX2 primers we tested were actually amplifying non-specific transcripts and we had to test several before choosing the ones that worked logically for human embryonic stem cells and cancer cells. Although rather speculative, our results showing that treatment with sodium butyrate induces OCT4A expression in differentiating colorectal Caco-2 cells could mark the phenotype of endodermal differentiation as it is known that induced expression of OCT4 can promote this type of differentiation under certain conditions [64]. Interestingly, it has been also noted that sodium butyrate supports endodermal differentiation [65–67]. Alternatively, the induced expression of OCT4A after NaBT treatment may reflect partial reprogramming in some of the cancer cells. The latter may not be preferable and should be further studied in the context of cancer stem cells, differentiation and cell survival. As the analyzed primary tumor samples expressed transcripts from pseudogenes and at the same time it was possible to induce OCT4A expression with sodium butyrate in differentiating Caco-2 cells, it gives OCT4A a new

possible role in colorectal cancer cells regulating the differentiation state and underscores the need of careful distinguishing between OCT4A and the relevant pseudogenes in future studies.

Enormous metabolic plasticity of cancer cells allows them to survive in severe environmental conditions that would be harmful to most normal cells. Cancer cells of the same tumor might use predominantly glycolysis or OXPHOS for energy production depending on nutrient availability within a given intertumoral compartment [68]. In contrast to normal cells, cancer cells often enhance glycolytic flux that supports cells with sufficient level of energy and intermediates for the biosynthetic pathways required for rapidly proliferating cells [69]. In the current paper, we show that about 70% of ATP produced by Caco-2 cells is derived from glycolysis while only 30% comes from the OXPHOS. Treatment of cells with NaBT allowed us to shift energy metabolism towards more oxidative metabolism, where butyrate is used as a preferred substrate for OXPHOS. Similar results were previously obtained using lung, breast and colon cancer cell lines [32–36]. Moreover, we found that butyrate not only increase OXPHOS but also non-mitochondrial residual oxygen consumption. Increased non-mitochondrial oxidation may be related with elevated intracellular levels of reactive oxygen species (ROS). It was demonstrated that butyrate can increase ROS levels more than 40% in hepatocellular carcinoma cells [70]. There are two possible mechanism how can butyrate effect on intracellular ROS level. Firstly, by decreasing flux through pentose phosphate shunt as a result decrease NADPH level [35,36,71]. Secondly, by alteration of Thioredoxin-1 expression [72]. In addition, our experiments revealed reduced glycolytic flux in Caco-2 cells after treatment with NaBT. Unaltered HK activity and decreased PYK and LDH activities suggested that NaBT affected the later stages of glycolytic pathway, rather than the earlier steps. These results are in contrast with studies by Amoêdo et al, who observed significantly increased HK activity and unchanged PYK and LDH activities after treatment of H460 lung cancer cells with NaBT [32]. Consequently, we assume that different cancer cell lines might respond in an individual manner to NaBT depending on the metabolic phenotype of utilized cell type; this has been also pointed out by other investigators [34].

In our previous studies, we observed the rearrangement of phosphotransfer network induced by malignant transformation of cancer cells [38–40]. Interestingly, increased AK and decreased CK activities were observed in cancer compared to control samples [38–40]. Here, we show that treatment of Caco-2 cells with NaBT may reverse cancer-induced changes in the phosphotransfer system as treated cells displayed increased CK activity and decreased AK activity. One possible way how butyrate may affect phosphotransfer network involves activation of AMP-dependent kinase (AMPK). Butyrate has been reported to modulate the energy metabolism of the cell by altering the phosphorylation status of AMPK directly or indirectly [73]. The AMPK can be activated by changes in the intracellular ATP/ADP ratio. Once activated, AMPK stimulates catabolic pathways to generate ATP, while turning off energy-consuming anabolic pathways [74]. In the cell, the level of ATP and ADP is monitored by the AK that catalyzes the conversion of ADP to ATP and AMP. Because of the AK reaction, even slight changes in ATP concentration lead to the drastic increase of cellular AMP concentration resulting in the AMPK activation [75]. Whether altered AK network in NaBT-treated cells is a consequence or a cause of AMPK activation needs to be determined.

In the current work, we showed that the response of phosphotransfer system to the butyrate treatment is modulated by the availability of glutamine in the growth medium. Glutamine is an important substrate and signaling molecule for intestinal epithelial proliferation and colonic crypt expansion [76]. In addition, glutamine may serve as an alternate fuel for cancer cells [68]. However, it is unknown whether the availability of different energy sources including glutamine and butyrate may alter phosphotransfer network of the cell. This study provides the first step toward clarification of this gap. Although the CK network responded to NaBT-

treatment similarly in the presence and in the absence of glutamine, notable changes were observed in the AK activity. The suppressive effect of NaBT on the AK activity disappeared during glutamine deprivation. The supplementation of glutamine-free medium with additional glucose resulted in decreased AK activity in both NaBT-treated and untreated Caco-2 cells. Future studies are required to define how AK network interferes with glucose and glutamine metabolism. In addition, the suppressive effect of NaBT on PYK and LDH activities was also abolished after treatment of cells with additional glucose in the absence of glutamine. A potential explanation for this phenomenon is the adaptation of cellular energy pathways to glutamine deprivation. The removal of glutamine from the growth medium alters cellular and mitochondrial NADH and NAD⁺ ratios [77]. In order to cope with emerged imbalance, cancer cells may keep high glycolytic rate including high PYK and LDH activities. Collectively, our results link rearrangements in phosphotransfer network with metabolic alterations induced by NaBT treatment.

To our knowledge, this is the first study to describe the alterations in the phosphotransfer network induced by butyrate treatment of colon cancer cells. Our data indicate a close interplay between the phosphotransfer networks and metabolic plasticity of CRC, which is associated with the cell differentiation state. Further studies are needed to clarify the mechanisms behind the butyrate-mediated changes in AK network and its dependence on the glutamine and glucose availability.

Supporting information

S1 Fig. Schematic depiction of the oxygraphy protocols employed in the current study. (PPTX)

S2 Fig. The effect of NaBT on the survival of Caco-2 cells in trypan blue excluding test: Exposure time was 48 hours. Bars are SEM (n = 3); *** $p < 0.001$ (Student's t test). (PPTX)

S3 Fig. Expression of pluripotency-associated transcription factors in Caco-2 cells after 48h treatment with 1 mM sodium butyrate. (A): Detection of main OCT4 spliced variants, transcripts from NANOG1, NANOG2 and SOX2. GAPDH was used for loading control. OCT4A* primers can also amplify transcripts from OCT4 pseudogenes. OCT4B/B1 primers allow detection of OCT4 variant OCT4B4* (B): Restriction analysis of OCT4A* PCR product with ApaI showing 204 bp and 291bp fragments in the presence of OCT4A and 496bp product representative of OCT4 pseudogenes. (TIF)

S4 Fig. Expression of pluripotency-associated transcription factors in primary colorectal tumor (T) and adjacent tissue (Ctrl) samples. (A): Detection of main OCT4 spliced variants, transcripts from NANOG1, NANOG2 and SOX2. GAPDH was used for loading control. OCT4A* primers can also amplify transcripts from OCT4 pseudogenes. OCT4B/B1 primers allow detection of OCT4 variant OCT4B4* (B): Restriction analysis of OCT4A* PCR product with ApaI showing 204 bp and 291bp fragments in the presence of OCT4A and 496bp product representative of OCT4 pseudogenes. (TIF)

S5 Fig. OCT4B/B1 primers allow detection of OCT4 variant OCT4B4. OCT4B1 product is 492 bp, OCT4B is 267 bp and OCT4B4 product is 239 bp. OCT4B1 is highly expressed in human embryonic stem cells (hESC) together with both OCT4B and OCT4B4 transcripts. Caco-2 cells express OCT4B1 and OCT4B4, but not the OCT4B variant. In colorectal tumor and respective control samples the expression of OCT4B4 and OCT4B varies while OCT4B1 is

expressed on low level.
(PPTX)

S6 Fig. Effect of sodium butyrate on the mitochondrial mass and membrane potential. (A): Specific citrate synthase activity. (B,C): Mitochondrial membrane potential was assayed by TMRE and MitoTracker Red staining using fluorescence microplate reader. Data presented as mean \pm SEM (n = 5). NaBT–sodium butyrate.
(PPTX)

S1 Table. Changes in the AK isoforms in cancer cells and tissues described in the literature.
(DOCX)

S2 Table. Primers and product sizes in quantitative RT-PCR.
(DOCX)

S3 Table. Quantitative RT-PCR amplification program.
(DOCX)

S4 Table. Primers and product sizes in semi-quantitative RT-PCR.
(DOCX)

S5 Table. Semi-quantitative RT-PCR amplification programs.
(DOCX)

S1 File.
(PDF)

S1 Raw images.
(PDF)

Author Contributions

Conceptualization: Ljudmila Klepinina, Aleksandr Klepinin, Martin Pook.

Data curation: Ljudmila Klepinina, Aleksandr Klepinin.

Formal analysis: Ljudmila Klepinina, Aleksandr Klepinin, Laura Truu, Kaisa Kuus, Indrek Teino, Martin Pook.

Funding acquisition: Tuuli Kaambre.

Investigation: Ljudmila Klepinina, Indrek Teino, Martin Pook.

Methodology: Ljudmila Klepinina, Aleksandr Klepinin, Heiki Vija, Kaisa Kuus, Indrek Teino, Martin Pook.

Resources: Toivo Maimets, Tuuli Kaambre.

Validation: Ljudmila Klepinina, Aleksandr Klepinin.

Writing – original draft: Ljudmila Klepinina, Vladimir Chekulayev, Martin Pook.

Writing – review & editing: Ljudmila Klepinina, Aleksandr Klepinin, Laura Truu, Vladimir Chekulayev, Indrek Teino, Martin Pook, Toivo Maimets, Tuuli Kaambre.

References

1. Barker N. Adult intestinal stem cells: Critical drivers of epithelial homeostasis and regeneration. Vol. 15, Nature Reviews Molecular Cell Biology. 2014. p. 19–33. <https://doi.org/10.1038/nrm3721> PMID: [24326621](https://pubmed.ncbi.nlm.nih.gov/24326621/)

2. Yamamoto N, Yasuda K. PURIFICATION AND IMMUNOHISTOCHEMICAL STUDY OF ALKALINE PHOSPHATASE IN BOVINE KIDNEY. *Acta Histochem Cytochem.* 1973; 6(2):107–16.
3. Chung YS, Song IS, Erickson RH, Sleisenger MH, Kim YS. Effect of Growth and Sodium Butyrate on Brush Border Membrane-associated Hydrolases in Human Colorectal Cancer Cell Lines. *Cancer Res.* 1985; 45(7).
4. Henthorn PS, Raducha M, Kadesch T, Weiss MJ, Harris H. Sequence and characterization of the human intestinal alkaline phosphatase gene. *J Biol Chem.* 1988; 263(24):12011–9. PMID: [2841341](https://pubmed.ncbi.nlm.nih.gov/2841341/)
5. Matsumoto H, Erickson RH, Gum JR, Yoshioka M, Gum E, Kim YS. Biosynthesis of alkaline phosphatase during differentiation of the human colon cancer cell line Caco-2. *Gastroenterology* [Internet]. 1990; 98(5 PART 1):1199–207. [https://doi.org/10.1016/0016-5085\(90\)90334-w](https://doi.org/10.1016/0016-5085(90)90334-w) PMID: [2323513](https://pubmed.ncbi.nlm.nih.gov/2323513/)
6. Herz F, Schermer A, Halwer M, Bogart LH. Alkaline phosphatase in HT-29, a human colon cancer cell line: Influence of sodium butyrate and hyperosmolality. *Arch Biochem Biophys.* 1981 Sep 1; 210(2):581–91. [https://doi.org/10.1016/0003-9861\(81\)90224-1](https://doi.org/10.1016/0003-9861(81)90224-1) PMID: [7305346](https://pubmed.ncbi.nlm.nih.gov/7305346/)
7. Reya T, Morrison SJ, Clarke MF, Weissman IL. Stem cells, cancer, and cancer stem cells. *Nature.* 2001 Nov; 414(6859):105–11. <https://doi.org/10.1038/35102167> PMID: [11689955](https://pubmed.ncbi.nlm.nih.gov/11689955/)
8. Friedmann-Morvinski D, Verma IM. Dedifferentiation and reprogramming: Origins of cancer stem cells. Vol. 15, *EMBO Reports.* Nature Publishing Group; 2014. p. 244–53. <https://doi.org/10.1002/embr.201338254> PMID: [24531722](https://pubmed.ncbi.nlm.nih.gov/24531722/)
9. Ben-Porath I, Thomson MW, Carey VJ, Ge R, Bell GW, Regev A, et al. An embryonic stem cell-like gene expression signature in poorly differentiated aggressive human tumors. *Nat Genet.* 2008 May; 40(5):499–507. <https://doi.org/10.1038/ng.127> PMID: [18443585](https://pubmed.ncbi.nlm.nih.gov/18443585/)
10. Amini S, Fathi F, Mobalegi J, Sofimajidpour H, Ghadimi T. The expressions of stem cell markers: Oct4, Nanog, Sox2, nucleostemin, Bmi, Zfx, Tcf1, Tbx3, Dppa4, and Esrrb in bladder, colon, and prostate cancer, and certain cancer cell lines. *Anat Cell Biol.* 2014 Mar; 47(1):1–11. <https://doi.org/10.5115/acb.2014.47.1.1> PMID: [24693477](https://pubmed.ncbi.nlm.nih.gov/24693477/)
11. Yang F, Zhang J, Yang H. OCT4, SOX2, and NANOG positive expression correlates with poor differentiation, advanced disease stages, and worse overall survival in HER2+ breast cancer patients. *Onco Targets Ther.* 2018; 11:7873–81. <https://doi.org/10.2147/OTT.S173522> PMID: [30464534](https://pubmed.ncbi.nlm.nih.gov/30464534/)
12. Atlasi Y, Mowla SJ, Ziaee SAM, Gokhale PJ, Andrews PW. OCT4 spliced variants are differentially expressed in human pluripotent and nonpluripotent cells. *Stem Cells.* 2008 Dec; 26(12):3068–74. <https://doi.org/10.1634/stemcells.2008-0530> PMID: [18787205](https://pubmed.ncbi.nlm.nih.gov/18787205/)
13. Asadi MH, Khalifeh K, Mowla SJ. OCT4 spliced variants are highly expressed in brain cancer tissues and inhibition of OCT4B1 causes G2/M arrest in brain cancer cells. *J Neurooncol.* 2016 Dec; 130(3):455–63. <https://doi.org/10.1007/s11060-016-2255-1> PMID: [27585657](https://pubmed.ncbi.nlm.nih.gov/27585657/)
14. Asadi MH, Mowla SJ, Fathi F, Aleyasin A, Asadzadeh J, Atlasi Y. OCT4B1, a novel spliced variant of OCT4, is highly expressed in gastric cancer and acts as an antiapoptotic factor. *Int J Cancer.* 2011 Jun; 128(11):2645–52. <https://doi.org/10.1002/ijc.25643> PMID: [20824712](https://pubmed.ncbi.nlm.nih.gov/20824712/)
15. Asadzadeh J, Asadi MH, Shakhssalim N, Rafiee M-R, Kalhor HR, Tavallaei M, et al. A plausible anti-apoptotic role of up-regulated OCT4B1 in bladder tumors. *Urol J.* 2012; 9(3):574–80. PMID: [22903480](https://pubmed.ncbi.nlm.nih.gov/22903480/)
16. Gazouli M, Roubelakis MG, Theodoropoulos GE, Papaliou J, Vaiopoulou A, Pappa KI, et al. OCT4 spliced variant OCT4B1 is expressed in human colorectal cancer. *Mol Carcinog.* 2012 Feb; 51(2):165–73. <https://doi.org/10.1002/mc.20773> PMID: [21480394](https://pubmed.ncbi.nlm.nih.gov/21480394/)
17. Poursani EM, Mehravar M, Soltani BM, Mowla SJ. Novel variant of OCT4B4 is differentially expressed in human embryonic stem and embryonic carcinoma cells. *Gene.* 2017 Sep; 627:369–72. <https://doi.org/10.1016/j.gene.2017.06.032> PMID: [28633916](https://pubmed.ncbi.nlm.nih.gov/28633916/)
18. Wang X, Dai J. Concise review: isoforms of OCT4 contribute to the confusing diversity in stem cell biology. *Stem Cells.* 2010 May; 28(5):885–93. <https://doi.org/10.1002/stem.419> PMID: [20333750](https://pubmed.ncbi.nlm.nih.gov/20333750/)
19. Suo G, Han J, Wang X, Zhang J, Zhao Y, Zhao Y, et al. Oct4 pseudogenes are transcribed in cancers. *Biochem Biophys Res Commun.* 2005 Dec; 337(4):1047–51. <https://doi.org/10.1016/j.bbrc.2005.09.157> PMID: [16229821](https://pubmed.ncbi.nlm.nih.gov/16229821/)
20. Ezeh UI, Turek PJ, Reijo RA, Clark AT. Human embryonic stem cell genes OCT4, NANOG, STELLAR, and GDF3 are expressed in both seminoma and breast carcinoma. *Cancer.* 2005 Nov; 104(10):2255–65. <https://doi.org/10.1002/cncr.21432> PMID: [16228988](https://pubmed.ncbi.nlm.nih.gov/16228988/)
21. Meng H-M, Zheng P, Wang X-Y, Liu C, Sui H-M, Wu S-J, et al. Over-expression of Nanog predicts tumor progression and poor prognosis in colorectal cancer. *Cancer Biol Ther.* 2010 Feb; 9(4):295–302. <https://doi.org/10.4161/cbt.9.4.10666> PMID: [20026903](https://pubmed.ncbi.nlm.nih.gov/20026903/)
22. Jeter CR, Liu B, Liu X, Chen X, Liu C, Calhoun-Davis T, et al. NANOG promotes cancer stem cell characteristics and prostate cancer resistance to androgen deprivation. *Oncogene.* 2011 Sep; 30(36):3833–45. <https://doi.org/10.1038/onc.2011.114> PMID: [21499299](https://pubmed.ncbi.nlm.nih.gov/21499299/)

23. Kim JS, Kim J, Kim BS, Chung HY, Lee YY, Park CS, et al. Identification and functional characterization of an alternative splice variant within the fourth exon of human nanog. *Exp Mol Med*. 2005 Dec; 37(6):601–7. <https://doi.org/10.1038/emm.2005.73> PMID: 16391521
24. Eberle I, Pless B, Braun M, Dinger T, Marschalek R. Transcriptional properties of human NANOG1 and NANOG2 in acute leukemic cells. *Nucleic Acids Res*. 2010 Sep; 38(16):5384–95. <https://doi.org/10.1093/nar/gkq307> PMID: 20427424
25. Takeda K, Mizushima T, Yokoyama Y, Hirose H, Wu X, Qian Y, et al. Sox2 is associated with cancer stem-like properties in colorectal cancer. *Sci Rep*. 2018 Dec; 8(1):17639. <https://doi.org/10.1038/s41598-018-36251-0> PMID: 30518951
26. Boumahdi S, Driessens G, Lapouge G, Rorive S, Nassar D, Le Mercier M, et al. SOX2 controls tumour initiation and cancer stem-cell functions in squamous-cell carcinoma. *Nature*. 2014 Jul; 511(7508):246–50. <https://doi.org/10.1038/nature13305> PMID: 24909994
27. Zhu F, Qian W, Zhang H, Liang Y, Wu M, Zhang Y, et al. SOX2 Is a Marker for Stem-like Tumor Cells in Bladder Cancer. *Stem Cell Reports*. 2017 Aug; 9(2):429–37. <https://doi.org/10.1016/j.stemcr.2017.07.004> PMID: 28793245
28. Kaiko GE, Ryu SH, Koues OI, Pearce EL, Oltz EM, Stappenbeck Correspondence TS. The Colonic Crypt Protects Stem Cells from Microbiota-Derived Metabolites. *Cell*. 2016;165. <https://doi.org/10.1016/j.cell.2016.01.020> PMID: 26924576
29. Gonçalves P, Martel F. Butyrate and Colorectal Cancer: The Role of Butyrate Transport. *Curr Drug Metab*. 2013 Nov; 14(9):994–1008. <https://doi.org/10.2174/1389200211314090006> PMID: 24160296
30. Eckschlager T, Pich J, Stiborova M, Hrabeta J. Histone deacetylase inhibitors as anticancer drugs. Vol. 18, *International Journal of Molecular Sciences*. MDPI AG; 2017. <https://doi.org/10.3390/ijms18071414> PMID: 28671573
31. Donohoe DR, Collins LB, Wali A, Bigler R, Sun W, Bultman SJ. The Warburg effect dictates the mechanism of butyrate-mediated histone acetylation and cell proliferation. *Mol Cell*. 2012 Nov; 48(4):612–26. <https://doi.org/10.1016/j.molcel.2012.08.033> PMID: 23063526
32. Amoêdo ND, Rodrigues MF, Pezzuto P, Galina A, da Costa RM, de Almeida FCL, et al. Energy Metabolism in H460 Lung Cancer Cells: Effects of Histone Deacetylase Inhibitors. Kowaltowski AJ, editor. *PLoS One*. 2011 Jul; 6(7):e22264. <https://doi.org/10.1371/journal.pone.0022264> PMID: 21789245
33. Alcarraz-Vizán G, Boren J, Lee W-NP, Cascante M. Histone deacetylase inhibition results in a common metabolic profile associated with HT29 differentiation. *Metabolomics*. 2010 Jun; 6(2):229–37. <https://doi.org/10.1007/s11306-009-0192-0> PMID: 20445757
34. Rodrigues MF, Carvalho É, Pezzuto P, Rumjanek FD, Amoêdo ND. Reciprocal Modulation of Histone Deacetylase Inhibitors Sodium Butyrate and Trichostatin A on the Energy Metabolism of Breast Cancer Cells. *J Cell Biochem*. 2015 May; 116(5):797–808. <https://doi.org/10.1002/jcb.25036> PMID: 25510910
35. Blouin J-M, Penot G, Collinet M, Nacfer M, Forest C, Laurent-Puig P, et al. Butyrate elicits a metabolic switch in human colon cancer cells by targeting the pyruvate dehydrogenase complex. *Int J Cancer*. 2011 Jun; 128(11):2591–601. <https://doi.org/10.1002/ijc.25599> PMID: 20715114
36. Li Q, Cao L, Tian Y, Zhang P, Ding C, Lu W, et al. Butyrate Suppresses the Proliferation of Colorectal Cancer Cells via Targeting Pyruvate Kinase M2 and Metabolic Reprogramming. *Mol Cell Proteomics*. 2018 Aug; 17(8):1531–45. <https://doi.org/10.1074/mcp.RA118.000752> PMID: 29739823
37. Dzeja PP, Terzic A. Phosphotransfer networks and cellular energetics. *J Exp Biol*. 2003 Jun; 206(Pt 12):2039–47. <https://doi.org/10.1242/jeb.00426> PMID: 12756286
38. Chekulayev V, Mado K, Shevchuk I, Koit A, Kaldma A, Klepinin A, et al. Metabolic remodeling in human colorectal cancer and surrounding tissues: alterations in regulation of mitochondrial respiration and metabolic fluxes. *Biochem Biophys Reports*. 2015 Dec; 4:111–25. <https://doi.org/10.1016/j.bbrep.2015.08.020> PMID: 29124194
39. Klepinin A, Ounpuu L, Guzun R, Chekulayev V, Timohhina N, Tepp K, et al. Simple oxygraphic analysis for the presence of adenylate kinase 1 and 2 in normal and tumor cells. *J Bioenerg Biomembr*. 2016 Oct; 48(5):531–48. <https://doi.org/10.1007/s10863-016-9687-3> PMID: 27854030
40. Ounpuu L, Klepinin A, Pook M, Teino I, Peet N, Paju K, et al. 2102Ep embryonal carcinoma cells have compromised respiration and shifted bioenergetic profile distinct from H9 human embryonic stem cells. *Biochim Biophys Acta Gen Subj*. 2017 Aug; 1861(8):2146–54. <https://doi.org/10.1016/j.bbagen.2017.05.020> PMID: 28552560
41. Dzeja PP, Terzic A, Wieringa B. Phosphotransfer dynamics in skeletal muscle from creatine kinase gene-deleted mice. Vols. 256–257, *Molecular and Cellular Biochemistry*. Springer Netherlands; 2004. p. 13–27. <https://doi.org/10.1023/b:mcbi.0000009856.23646.38> PMID: 14977167
42. Jan Y-H, Tsai H-Y, Yang C-J, Huang M-S, Yang Y-F, Lai T-C, et al. Adenylate Kinase-4 Is a Marker of Poor Clinical Outcomes That Promotes Metastasis of Lung Cancer by Downregulating the Transcription

- Factor ATF3. *Cancer Res.* 2012 Oct; 72(19):5119–29. <https://doi.org/10.1158/0008-5472.CAN-12-1842> PMID: 23002211
43. Fujisawa K, Terai S, Takami T, Yamamoto N, Yamasaki T, Matsumoto T, et al. Modulation of anti-cancer drug sensitivity through the regulation of mitochondrial activity by adenylate kinase 4. *J Exp Clin Cancer Res.* 2016 Dec; 35(1):48. <https://doi.org/10.1186/s13046-016-0322-2> PMID: 26980435
 44. Ji Y, Yang C, Tang Z, Yang Y, Tian Y, Yao H, et al. Adenylate kinase hCINAP determines self-renewal of colorectal cancer stem cells by facilitating LDHA phosphorylation. *Nat Commun.* 2017 May; 8:15308. <https://doi.org/10.1038/ncomms15308> PMID: 28516914
 45. Mosmann T. Rapid colorimetric assay for cellular growth and survival: application to proliferation and cytotoxicity assays. *J Immunol Methods.* 1983 Dec; 65(1–2):55–63. [https://doi.org/10.1016/0022-1759\(83\)90303-4](https://doi.org/10.1016/0022-1759(83)90303-4) PMID: 6606682
 46. Strober W. Trypan Blue Exclusion Test of Cell Viability. In: *Current Protocols in Immunology*. Hoboken, NJ, USA: John Wiley & Sons, Inc.; 2001. p. Appendix 3B. <https://doi.org/10.1002/0471142735.ima03bs21> PMID: 18432654
 47. Pesce A, McKay RH, Stolzenbach F, Cahn RD, Kaplan NO. The comparative enzymology of lactic dehydrogenases. I. Properties of the crystalline beef and chicken enzymes. *J Biol Chem.* 1964 Jun; 239:1753–61. PMID: 14213346
 48. Sabokbar A, Millett PJ, Myer B, Rushton N. A rapid, quantitative assay for measuring alkaline phosphatase activity in osteoblastic cells in vitro. *Bone Miner.* 1994; 27(1):57–67. [https://doi.org/10.1016/s0169-6009\(08\)80187-0](https://doi.org/10.1016/s0169-6009(08)80187-0) PMID: 7849547
 49. Cormio A, Guerra F, Cormio G, Pesce V, Fracasso F, Loizzi V, et al. The PGC-1 α -dependent pathway of mitochondrial biogenesis is upregulated in type I endometrial cancer. *Biochem Biophys Res Commun.* 2009 Dec; 390(4):1182–5. <https://doi.org/10.1016/j.bbrc.2009.10.114> PMID: 19861117
 50. Robey RB, Raval BJ, Ma J, Santos AV. Thrombin is a novel regulator of hexokinase activity in mesangial cells. *Kidney Int.* 2000 Jun; 57(6):2308–18. <https://doi.org/10.1046/j.1523-1755.2000.00091.x> PMID: 10844601
 51. Ainsworth S, MacFarlane N. A kinetic study of rabbit muscle pyruvate kinase. *Biochem J.* 1973 Feb; 131(2):223–36. <https://doi.org/10.1042/bj1310223> PMID: 4737316
 52. Dzeja PP, Vitkevicius KT, Redfield MM, Burnett JC, Terzic A. Adenylate kinase-catalyzed phosphotransfer in the myocardium: increased contribution in heart failure. *Circ Res.* 1999 May; 84(10):1137–43. <https://doi.org/10.1161/01.res.84.10.1137> PMID: 10347088
 53. Monge C, Beraud N, Tepp K, Pelloux S, Chahboun S, Kaambre T, et al. Comparative analysis of the bioenergetics of adult cardiomyocytes and nonbeating HL-1 cells: respiratory chain activities, glycolytic enzyme profiles, and metabolic fluxes. *Can J Physiol Pharmacol.* 2009 Apr; 87(4):318–26. <https://doi.org/10.1139/Y09-018> PMID: 19370085
 54. Wang F, Zhang S, Vuckovic I, Jeon R, Lerman A, Folmes CD, et al. Glycolytic Stimulation Is Not a Requirement for M2 Macrophage Differentiation. *Cell Metab.* 2018 Sep; 28(3):463–475.e4. <https://doi.org/10.1016/j.cmet.2018.08.012> PMID: 30184486
 55. Dzeja PP, Bortolon R, Perez-Terzic C, Holmuhamedov EL, Terzic A. Energetic communication between mitochondria and nucleus directed by catalyzed phosphotransfer. *Proc Natl Acad Sci U S A.* 2002 Jul; 99(15):10156–61. <https://doi.org/10.1073/pnas.152259999> PMID: 12119406
 56. Shin J, Carr A, Corner GA, Tögel L, Dávaos-Salas M, Tran H, et al. The Intestinal Epithelial Cell Differentiation Marker Intestinal Alkaline Phosphatase (ALPI) Is Selectively Induced by Histone Deacetylase Inhibitors (HDACi) in Colon Cancer Cells in a Kruppel-like Factor 5 (KLF5)-dependent Manner. *J Biol Chem.* 2014; 289(36):25306. <https://doi.org/10.1074/jbc.M114.557546> PMID: 25037223
 57. Panagopoulos I, Möller E, Isaksson M, Mertens F. A PCR/restriction digestion assay for the detection of the transcript variants 1 and 2 of POU5F1. *Genes Chromosom Cancer.* 2008 Jun; 47(6):521–9. <https://doi.org/10.1002/gcc.20555> PMID: 18335506
 58. Phi LTH, Sari IN, Yang Y-G, Lee S-H, Jun N, Kim KS, et al. Cancer Stem Cells (CSCs) in Drug Resistance and their Therapeutic Implications in Cancer Treatment. *Stem Cells Int.* 2018; 2018:5416923. <https://doi.org/10.1155/2018/5416923> PMID: 29681949
 59. Pattabiraman DR, Weinberg RA. Tackling the cancer stem cells-what challenges do they pose? Vol. 13, *Nature Reviews Drug Discovery*. Nature Publishing Group; 2014. p. 497–512. <https://doi.org/10.1038/nrd4253> PMID: 24981363
 60. Ordóñez-Morán P, Dafflon C, Imajo M, Nishida E, Huelsken J. HOXA5 Counteracts Stem Cell Traits by Inhibiting Wnt Signaling in Colorectal Cancer. *Cancer Cell.* 2015 Dec; 28(6):815–29. <https://doi.org/10.1016/j.ccell.2015.11.001> PMID: 26678341


61. Voutsadakis IA. The pluripotency network in colorectal cancer pathogenesis and prognosis: An update. Vol. 12, *Biomarkers in Medicine*. Future Medicine Ltd.; 2018. p. 653–65. <https://doi.org/10.2217/bmm-2017-0369> PMID: [29944017](https://pubmed.ncbi.nlm.nih.gov/29944017/)
62. Izumi D, Ishimoto T, Sakamoto Y, Miyamoto Y, Baba H. Molecular insights into colorectal cancer stem cell regulation by environmental factors. *J Cancer Metastasis Treat*. 2015; 1(3):156.
63. Oshima N, Yamada Y, Nagayama S, Kawada K, Hasegawa S, Okabe H, et al. Induction of cancer stem cell properties in colon cancer cells by defined factors. *PLoS One*. 2014 Jul; 9(7):e101735. <https://doi.org/10.1371/journal.pone.0101735> PMID: [25006808](https://pubmed.ncbi.nlm.nih.gov/25006808/)
64. Niwa H, Miyazaki JI, Smith AG. Quantitative expression of Oct-3/4 defines differentiation, dedifferentiation or self-renewal of ES cells. *Nat Genet*. 2000 Apr; 24(4):372–6. <https://doi.org/10.1038/74199> PMID: [10742100](https://pubmed.ncbi.nlm.nih.gov/10742100/)
65. Jiang J, Au M, Lu K, Eshpeter A, Korbitt G, Fisk G, et al. Generation of Insulin-Producing Islet-Like Clusters from Human Embryonic Stem Cells. *Stem Cells*. 2007 Aug; 25(8):1940–53. <https://doi.org/10.1634/stemcells.2006-0761> PMID: [17510217](https://pubmed.ncbi.nlm.nih.gov/17510217/)
66. Rambhatla L, Chiu CP, Kundu P, Peng Y, Carpenter MK. Generation of hepatocyte-like cells from human embryonic stem cells. *Cell Transplant*. 2003; 12(1):1–11. <https://doi.org/10.10372/00000003783985179> PMID: [12693659](https://pubmed.ncbi.nlm.nih.gov/12693659/)
67. Tzur G, Levy A, Meiri E, Barad O, Spector Y, Bentwich Z, et al. MicroRNA expression patterns and function in endodermal differentiation of human embryonic stem cells. *PLoS One*. 2008 Nov; 3(11). <https://doi.org/10.1371/journal.pone.00003726> PMID: [19015728](https://pubmed.ncbi.nlm.nih.gov/19015728/)
68. Martinez-Outschoorn UE, Peiris-Pagés M, Pestell RG, Sotgia F, Lisanti MP. Cancer metabolism: a therapeutic perspective. *Nat Rev Clin Oncol*. 2017 Jan; 14(1):11–31. <https://doi.org/10.1038/nrclinonc.2016.60> PMID: [27141887](https://pubmed.ncbi.nlm.nih.gov/27141887/)
69. DeBerardinis RJ, Chandel NS. Fundamentals of cancer metabolism. *Sci Adv*. 2016 May; 2(5): e1600200. <https://doi.org/10.1126/sciadv.1600200> PMID: [27386546](https://pubmed.ncbi.nlm.nih.gov/27386546/)
70. Pant K, Saraya A, Venugopal SK. Oxidative stress plays a key role in butyrate-mediated autophagy via Akt/mTOR pathway in hepatoma cells. *Chem Biol Interact*. 2017 Aug 1; 273:99–106. <https://doi.org/10.1016/j.cbi.2017.06.001> PMID: [28600122](https://pubmed.ncbi.nlm.nih.gov/28600122/)
71. Patra KC, Hay N. The pentose phosphate pathway and cancer. Vol. 39, *Trends in Biochemical Sciences*. Elsevier Ltd; 2014. p. 347–54. <https://doi.org/10.1016/j.tibs.2014.06.005> PMID: [25037503](https://pubmed.ncbi.nlm.nih.gov/25037503/)
72. Wang W, Fang D, Zhang H, Xue J, Wangchuk D, Du J, et al. Sodium Butyrate Selectively Kills Cancer Cells and Inhibits Migration in Colorectal Cancer by Targeting Thioredoxin-1. *Onco Targets Ther [Internet]*. 2020 May 27; Volume 13:4691–704. <https://doi.org/10.2147/OTT.S235575> PMID: [32547098](https://pubmed.ncbi.nlm.nih.gov/32547098/)
73. Peng L, Li Z-R, Green RS, Holzman IR, Lin J. Butyrate Enhances the Intestinal Barrier by Facilitating Tight Junction Assembly via Activation of AMP-Activated Protein Kinase in Caco-2 Cell Monolayers. *J Nutr*. 2009 Sep; 139(9):1619–25. <https://doi.org/10.3945/jn.109.104638> PMID: [19625695](https://pubmed.ncbi.nlm.nih.gov/19625695/)
74. Garcia D, Shaw RJ. AMPK: Mechanisms of Cellular Energy Sensing and Restoration of Metabolic Balance. *Mol Cell*. 2017 Jun; 66(6):789–800. <https://doi.org/10.1016/j.molcel.2017.05.032> PMID: [28622524](https://pubmed.ncbi.nlm.nih.gov/28622524/)
75. Hardie DG. Minireview: The AMP-Activated Protein Kinase Cascade: The Key Sensor of Cellular Energy Status. Vol. 144, *Endocrinology*. 2003. p. 5179–83. <https://doi.org/10.1210/en.2003-0982> PMID: [12960015](https://pubmed.ncbi.nlm.nih.gov/12960015/)
76. Moore SR, Guedes MM, Costa TB, Vallance J, Maier EA, Betz KJ, et al. Glutamine and alanyl-glutamine promote crypt expansion and mTOR signaling in murine enteroids. *Am J Physiol Gastrointest Liver Physiol*. 2015 May; 308(10):G831–9. <https://doi.org/10.1152/ajpgi.00422.2014> PMID: [25792564](https://pubmed.ncbi.nlm.nih.gov/25792564/)
77. Fan J, Kamphorst JJ, Mathew R, Chung MK, White E, Shlomi T, et al. Glutamine-driven oxidative phosphorylation is a major ATP source in transformed mammalian cells in both normoxia and hypoxia. *Mol Syst Biol*. 2013 Dec; 9:712. <https://doi.org/10.1038/msb.2013.65> PMID: [24301801](https://pubmed.ncbi.nlm.nih.gov/24301801/)

Appendix 3

Publication III

Klepinin, A., **Ounpuu, L.**, Guzun, R., Chekulayev, V., Timohhina, N., Tepp, K., Shevchuk, I., Schlattner, U., Kaambre, T. (2016). Simple oxygraphic analysis for the presence of adenylate kinase 1 and 2 in normal and tumor cells. *J Bioenerg Biomembr.* 48, 5, 531–548. DOI: 10.1007/s10863-016-9687-3

Simple oxygraphic analysis for the presence of adenylate kinase 1 and 2 in normal and tumor cells

Aleksandr Klepinin¹ · Lyudmila Ounpuu¹ · Rita Guzun^{2,3} · Vladimir Chekulayev¹ · Natalja Timohhina¹ · Kersti Tepp¹ · Igor Shevchuk¹ · Uwe Schlattner^{2,3} · Tuuli Kaambre^{1,4} 

Received: 28 June 2016 / Accepted: 31 October 2016 / Published online: 17 November 2016
© Springer Science+Business Media New York 2016

Abstract The adenylate kinase (AK) isoforms network plays an important role in the intracellular energy transfer processes, the maintenance of energy homeostasis, and it is a major player in AMP metabolic signaling circuits in some highly-differentiated cells. For this purpose, a rapid and sensitive method was developed that enables to estimate directly and semi-quantitatively the distribution between cytosolic AK1 and mitochondrial AK2 localized in the intermembrane space, both in isolated cells and tissue samples (biopsy material). Experiments were performed on isolated rat mitochondria or permeabilized material, including undifferentiated and differentiated neuroblastoma Neuro-2a cells, HL-1 cells, isolated rat heart cardiomyocytes as well as on human breast cancer post-operative samples. In these samples, the presence of AK1 and AK2 could be detected by high-resolution respirometry due to the functional coupling of these enzymes with ATP synthesis. By eliminating extra-mitochondrial ADP with an excess of pyruvate kinase and its substrate phosphoenolpyruvate, the coupling of the AK reaction with mitochondrial ATP synthesis could be quantified for total AK and mitochondrial AK2 as a specific AK index. In contrast to the creatine kinase pathway,

the AK phosphotransfer pathway is up-regulated in murine neuroblastoma and HL-1 sarcoma cells and in these malignant cells expression of AK2 is higher than AK1. Differentiated Neuro-2a neuroblastoma cells exhibited considerably higher OXPHOS capacity than undifferentiated cells, and this was associated with a remarkable decrease in their AK activity. The respirometric method also revealed a considerable difference in mitochondrial affinity for AMP between non-transformed cells and tumor cells.

Keywords Adenylate kinase · Cardiomyocytes; mitochondria · Neuroblastoma · Breast cancer

Introduction

Adenylate kinases (AKs) are members of an evolutionary conserved family of enzymes that catalyze the phosphoryl transfer between adenylates ($\text{AMP} + \text{ATP} \leftrightarrow 2\text{ADP}$) and could facilitate the intracellular energetic communication (Carrasco et al. 2001; Dzeja and Terzic 2009; Dzeja and Terzic 2003). The main function of AK is to maintain the cellular energy state through regulation of nucleotide ratios in different intracellular compartments (Dzeja and Terzic 2009). AK(s) also mediate intracellular AMP signaling, e.g. via the membrane metabolic sensor ATP-sensitive potassium channel, the energy-sensing AMP-activated protein kinase (AMPK), and other AMP-sensitive metabolic enzymes which collectively form a key metabolic sensing system to regulate a number of vital cellular processes (Dzeja and Terzic 2009; Dzeja et al. 2007; Dyck and Lopaschuk 2006). For example, regulation of AMPK by AMP is involved in its tumor suppressor functions under energy-poor conditions in several types of tumors (Dasgupta and Chhipa 2016; Hardie and Alessi 2013; Shackelford and Shaw 2009). In cells, AMPK

Electronic supplementary material The online version of this article (doi:10.1007/s10863-016-9687-3) contains supplementary material, which is available to authorized users.

✉ Tuuli Kaambre
tuuli.kaambre@kbfi.ee

¹ Laboratory of Bioenergetics, National Institute of Chemical Physics and Biophysics, Akadeemia tee 23, 12618 Tallinn, Estonia

² Laboratory of Fundamental and Applied Bioenergetics, Univ. Grenoble Alpes, Grenoble, France

³ Inserm, U1055, Grenoble, France

⁴ Tallinn University, Tallinn, Estonia

is activated through increased AK-catalyzed AMP generation or suppression of AMP removal catalyzed by 5'-nucleotidase (5'-NT) and AMP-deaminase (AMPD¹) which all regulate cellular AMP concentration (Dzeja and Terzic 2009; Plaideau et al. 2014; Plaideau et al. 2012).

The AK family includes nine major isoforms (AK1 - AK9), and several sub-forms with distinct intracellular localization and kinetic properties (Amiri et al. 2013; Dzeja and Terzic 2009; Panayiotou et al. 2014). These isoenzymes support specific cellular processes ranging from muscle contraction, electrical activity, cell motility, unfolded protein response and mitochondrial energetics (Burkart et al. 2011; Zhang et al. 2014). Different isoforms of AK have been found in distinct cell compartments such as cell membranes, cytosol, mitochondria and also nucleus, thereby creating an integrated phosphotransfer network. Tissues with high energy demand, such as brain, heart and skeletal muscles are rich in AK1, the major isoform located in the cytosol (Tanabe et al. 1993). In striated muscle cells (e.g., cardiomyocytes (Noma 2005)), AK1 contributes to energy transfer from ATP-producing sites (mitochondria) to the ATP-consuming sites (actomyosin) (Dzeja et al. 1999). Mitochondria harbor three different isoforms: AK2 in the intermembrane space and AK3 and AK4 in the matrix. AK2 is predominantly expressed in liver, kidney, spleen, large intestine and stomach (Tanabe et al. 1993). Due to its localization at the mitochondria/cytosol interface, AK2 plays a unique role in the regulation of energy transfer between these two compartments and cellular energy homeostasis in general (Gellerich 1992). AK3, which uses GTP instead of ATP, is expressed in all tissues except red blood cells. AK4 is expressed mainly in kidney, brain, heart, and liver, however it is unsure whether it functions as a kinase (Liu et al. 2009). Expression of AK1, AK2 and AK4 is regulated and shows a certain tissue-specificity, while AK3 is ubiquitously expressed and can be considered as a housekeeping enzyme.

AK2 and enzymatically-inactive AK4 are considered (Eimre et al. 2008; Liu et al. 2009) to be the components of the Mitochondrial Interactosome - a large mitochondrial

transmembrane complex consisting of ATP-synthasome, mitochondrial creatine kinase (MtCK), voltage dependent anion channel (VDAC), and some protein factors which regulate the mitochondrial outer membrane (MOM) permeability by interacting with VDAC from the cytosolic side (Guzun et al. 2012; Martel et al. 2014). It was reported that within this mitochondrial supercomplex, AK4 interacted with mitochondrial ADP/ATP-translocase which protected the neural cells against oxidative stress (Liu et al. 2009). The mitochondrial supercomplex may also include some cytosolic hexokinase (HK) isoforms HK-1 or -2 (Mathupala et al. 2006) which in hepatomas bind to mitochondria and use mitochondrially produced ATP, where up to ~50% of total ATP provided by AK2 (Nelson and Kabir 1985).

For a long time, the main function of AK has been associated solely with efficient transfer and equilibrium of high-energy phosphates in different micro-compartments within the cell. During the last decade, several new functions of AK have been identified. Firstly, AK has an important role in cell proliferation where AK1 associated with the mitotic spindle apparatus, to supply energy for cell division (Dzeja et al. 2011). Secondly, AK2 plays an important role in differentiation of neural, cardiac and haematopoietic stem cells, by providing the energy required for cell cycle, DNA synthesis and repair (Dzeja and Terzic 2009; Inouye et al. 1998; Zhang et al. 2014; Tanimura et al. 2014). Adipocyte differentiation was also shown to be associated with a remarkable increase in the levels of AK2 (Burkart et al. 2011). Thirdly, mitochondrially-associated AK2 is one of the components of the apoptotic complex where AK2 released into cytosol initiates cell death (Lee et al. 2007; Mather and Rottenberg 2001).

Deficiencies of AK expression or mutations in AK genes are associated with several diseases such as hemolytic anemia, reticular dysgenesis and ciliary dyskinesia (Dzeja and Terzic 2009). Park et al. (Park et al. 2012) have reported that AK1 could play a neuropathogenic role in Alzheimer's disease due to hyperphosphorylation of tau proteins. In cells, AK is functionally coupled to mitochondrial oxidative phosphorylation (OXPHOS), where during cellular stress conditions a small decrease in ATP induces a large increase in AMP which stimulates OXPHOS through AK-catalyzed ADP regeneration in mitochondria (Dzeja and Terzic 2009). This is in particular true for highly-differentiated cells such as adult cardiomyocytes (CM) and hepatocytes (Gellerich 1992), but has also been found for some sarcoma cells and other neoplasms (Chekulayev et al. 2015; Eimre et al. 2008; Klepinin et al. 2014). Previous studies have shown that increased AK expression, associated with changes in the expression profile of creatine kinase (CK) isoforms (Chekulayev et al. 2015; Greengard et al. 1980; Patra et al. 2012), can promote tumor progression. Moreover, in human prostate cancer (Hall et al. 1985) it was shown that AK may serve as an onco-

¹ Abbreviations:

AK, adenylate kinase; AMPD, AMP deaminase; AMPK, AMP-activated protein kinase; ANT, adenine nucleotide translocator; AP5A, diadenosine pentaphosphate; BSA, bovine serum albumin; CAT, carboxyatractyloside; CK, creatine kinase; CM, cardiomyocyte; CSC, cancer stem cells; Cyt-c, cytochrome c; DMEM, Dulbecco's Modified Eagle Medium; dN2a, differentiated N2a cells; DTT, dithiothreitol; FBS, fetal bovine serum; HBC, human breast cancer; HK, hexokinase; I_{AK}, adenylate kinase index; IMP, inosine monophosphate; Km, Michaelis-Menten constant; MIM, mitochondrial inner membrane; MOM, mitochondrial outer membrane; MtCK, mitochondrial creatine kinase; N2a, Neuro-2a; NB, neuroblastoma; NEM, N-ethylmaleimide; OXPHOS, oxidative phosphorylation; PBS, phosphate buffered saline; PEP, phosphoenolpyruvate; PK, pyruvate kinase; RA, all-trans-retinoic acid; RCI, respiratory control index; SNS, sympathetic nerve system; uN2a, undifferentiated N2a cells; VDAC, voltage dependent anion channel; Vm, rates of maximal respiration; Vo, rates of basal respiration.

developmental marker. However, also the opposite has been found; in lung and hepatoma cancers, AK is down-regulated as compared to normal tissue (Balinsky et al. 1984; Criss et al. 1970).

To date, a variety of different analytical methods have been applied for evaluating the functional state of the AK phosphotransfer system such as: spectrophotometric measurements (Dzeja et al. 1999; Tanabe et al. 1993), gel-electrophoresis (Criss et al. 1970), immuno-histochemical analysis and Western blotting (Burkart et al. 2011; Carrasco et al. 2001; Dzeja et al. 1999; Liu et al. 2009; Tanabe et al. 1993), two-dimensional SDS-PAGE along with subsequent MALDI-MS/MS or LC-MS/MS (Fukada et al. 2004), RT-PCR (Noma et al. 2001), ^{18}O isotopic tracer studies (Dzeja et al. 1999), as well as two-photon excitation fluorescence imaging and fluorescence correlation spectroscopy (Ruan et al. 2002). These analytical procedures are mostly invasive, thus require extraction of tissue proteins or mRNA and in some cases also very expensive equipment. Finally, there are some known global inhibitors of the AK reaction like Ap5A (Daniel et al. 2003; Hampton et al. 1976; Rosano et al. 1976), but isoform-specific inhibitors for AK1 or AK2 are lacking.

In this study, we have developed a simple and rapid method for semi-quantifying the activity of AK1 and AK2 separately in different biological samples. This method is based on measuring the rate of cellular/tissue respiration due to stimulation of the mitochondrial respiration by ADP released via AK-catalyzed reactions, stimulated by external ATP and AMP. For this objective, corresponding experiments were carried out on a large set of normal and tumor cells with known and unknown profile of AK1/AK2 expression. In the present work, we also demonstrate that the elaborated analytical approach can be successfully applied for evaluating these AK isoforms activities in postoperative tissues of breast cancer patients.

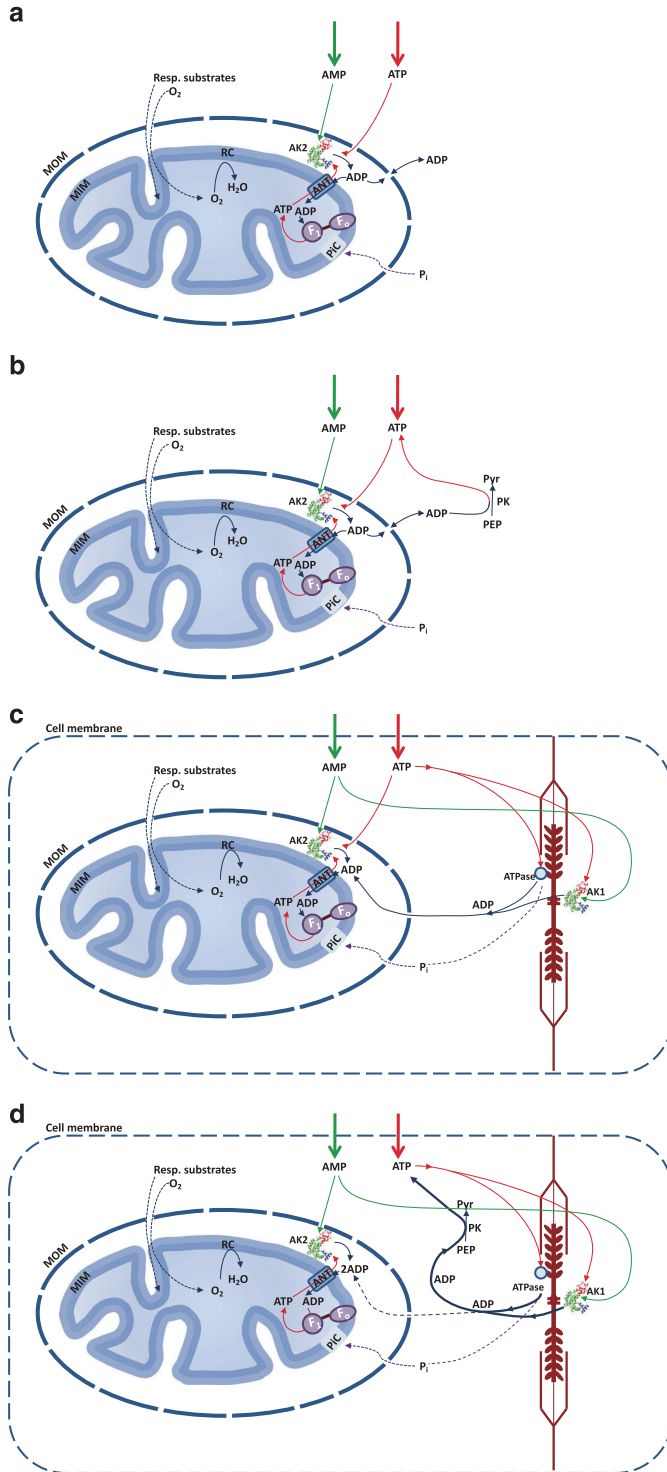
Results

Scheme 1 depicts our approach to quantify *in vitro* the presence of cytosolic AK1 and mitochondrial AK2 in mammalian cells and tissues. The basic principle is oxygraphic analysis of the connections between AK1/AK2 catalyzed reactions and mitochondrial OXPHOS, for this purpose permeabilized cells method are used since the plasma membrane is impermeable for adenine nucleotides. AMP can support ATP synthesis in mitochondria in the presence of endogenous ATP due to AK coupling with OXPHOS. According to Scheme 1, the ADP formed by the AK-catalyzed reaction (in the presence of exogenously-added ATP and AMP), either directly in the mitochondrial intermembrane space (AK2) (Scheme 1a), or in the cytosol (AK1) and accessing mitochondria via the VDAC pore (Scheme 1c), is finally using ADP/ATP exchange via the adenine nucleotide translocator (ANT) to stimulate

mitochondrial respiration. Since isoform-specific AK inhibitors do not exist, another approach is required to estimate non-invasively the contributions of AK1 and AK2 to total AK activity. Here, we use the phosphoenolpyruvate (PEP) – pyruvate kinase (PK) ADP trapping system in combination with respirometry (Saks et al. 2010; Timohhina et al. 2009). This system efficiently eliminates extra-mitochondrial ADP (Schemes 1b, d). It allows us to measure, in permeabilized cells, the total AK pool (AK1 + AK2) in absence of PEP-PK system (Scheme 1c) as well as specifically the mitochondrial AK2 coupled with OXPHOS in presence of PEP-PK system, which traps all cytosolic ADP accessible to AK1 (Scheme 1d).

The main isoform of adenylate kinase in a rat liver is AK2 (Supplement Fig. 1) (Noma 2005). Figure 1 shows oxygraph recording of isolated rat liver mitochondria. The mitochondrial respiration was activated by AMP and ATP via AK2 where AK2 produced 2 molecules ADP which directly transfer through adenine nucleotide translocator (ANT) into the mitochondria matrix (Scheme 1a). The respiratory control index (RCI) for the given mitochondrial preparations exceeded 8 (Table 1). Addition of exogenous Cyt-c did not increase the respiration rate, showing the intactness of the mitochondrial outer membrane (MOM) (Fig. 1a). Addition of carboxyatractyloside (CAT) decreased respiration rate back to the State II respiration level (V_0), indicating that the mitochondrial inner membrane (MIM) is also intact. Next, in the presence of the PK-PEP system (Fig. 1b) and under the same condition as Fig. 1a, (except using 2 mM ATP instead of 0.1 mM ATP) 80% of ADP formed in mitochondrial intermembrane space via AK2 were trapped by PK due to the high permeability of VDAC for adenine nucleotides (Scheme 1b). Thus, in presence of the PK-PEP system, the exogenous AMP activates only 20% of the maximal respiration, which is the part of AK2-generated ADP functionally coupled with OXPHOS. Addition of the AK inhibitor AP5A to the mitochondria almost entirely eliminated also these 20% of respiratory stimulation (Fig. 1b). This data is in correlation with Dr. F.N. Gellerich results (Gellerich 1992). Dr. F.N. Gellerich studied dynamic adenine nucleotide compartmentation in 1992, and found that ADP generated by AK2 in the mitochondrial intermembrane space can be channeled into mitochondrial matrix (Gellerich 1992).

Not only ADP but also AMP can control mitochondrial respiration due to AK functional coupling with OXPHOS. We hypothesized that the sensitivity of the proposed method could be applied at the cellular level to measure the ratio of AK1 and AK2, which is determined among others by the intracellular content of mitochondria and their OXPHOS capacity. For this purpose, a broad panel of normal and tumor cells with different OXPHOS rates was studied, including rat cardiomyocytes (CM) and human breast cancer (HBC) tissue samples. Heart muscle cells produce more than 90% of their



◀ **Scheme 1** The principles of this study are illustrated by four schemes of increasing complexity: Schemes A and B represent isolated liver mitochondrion as a reference system. Schemes C and D illustrate permeabilized cells chosen as experimental study model. Experiments were performed in two types of conditions: in the presence of ADP trapping system after or before activation cytosolic (AK1) and mitochondrial (AK2) adenylate kinase isoform. The ADP tapping system consist of phosphoenolpyruvate (PEP) and pyruvate kinase (PK), traps extramitochondrial ADP produced by AK1 and MgATPase reactions and subsequently regenerates extramitochondrial ATP. In mitochondrial AK2 forms micro-domain within the intermembrane space where AK2 produces 2 molecules ADP which is re-imported into the matrix via adenine nucleotide translocator (ANT) due to its functional coupling with AK2

ATP via mitochondrial respiration (Ventura-Clapier et al. 2011), whereas tumor cells are usually highly glycolytic and have low rates of mitochondrial respiration (Hanahan and Weinberg 2011). The following parameters were measured for every cell model: the rates of basal respiration (V_0) and maximal AMP- and ADP-activated respiration (V_{AMP} , V_{ADP}), as well as the respiratory control index (RCI) (Table 1). Among the studied cells, adult rat CM(s) were characterized by the highest V_{ADP} and RCI values. The RCI exceeded about 5–7 times those for human HBC tissue cells. Although, HL-1 cardiac sarcoma cells have relatively high rates of mitochondrial respiration, their V_{ADP} values were nearly 10 times lower as compared to normal CM(s). This result is consistent with several studies which showed reprogramming of mitochondrial morphology and function during carcinogenesis. It is important to emphasize that in cardiomyocytes V_{ADP} was at a similar level as AMP induced respiration (V_{AMP}), while HL-1 cells showed decreased V_{AMP} (Table 1). This indicates that there is decreased AK expression in HL-1 cells as compared to cardiomyocytes, but it is not clear, how exactly the AK profile changes in cardiac sarcoma cells. This question can be addressed by introducing the PEP-PK trapping system as outlined above.

Respiratory measurements were conducted with permeabilized cells, and AK1/AK2 distribution was first analyzed in rat heart CM(s) and in HL-1 tumor cells of the cardiac origin (Fig. 2). Functional coupling between ANT and mitochondrial AK2 is known to exist in human CM(s) (Seppet et al. 2005). In permeabilized CM and HL-1 cells, the addition of AMP and ATP activated AK1 and AK2 (Scheme 1c). This activation led to increased rates of cellular O_2 consumption (V_{AMP}) (Fig. 2) as a result of ADP produced and transported into the mitochondrial matrix via VDAC and/or ANT. Subsequent addition of PK to the assay systems (Scheme 1d) decreased the rates of O_2 consumption (V_{PK}) (Fig. 2), since the added PK removes efficiently extramitochondrially-generated ADP generated by AK1 and MgATPases (Scheme 1d), as well as intra-mitochondrially-generated ADP not coupled to respiration and escaping mitochondria. A PK activity of 10 U/ml was sufficient to trap all ADP available in the bulk phase of the cytoplasm. Residual respiration is associated with AK2 fully coupled with

OXPHOS. That functional coupling between AK2 and mitochondrial respiration is indeed responsible for this residual respiration was confirmed by AP5A which decreased respiration back to V_0 (Fig. 2). According to this protocol, AK indexes (I_{AK1} and I_{AK2}) were defined which semi-quantify distribution of AK1 and AK2 in cells (Fig. 3a, see also Material and Methods) and calculated for adult rat CM(s) and HL-1 tumor cells (Fig. 3a). These values were in a good agreement with the results of standard spectrophotometric activity assays in cell extracts (Table 2). This method provides information on the distribution of AK1 and coupled AK2 in cells. It is known that AK1 is the predominant AK isoform in cardiac muscle cells with only a minor level of mitochondrial AK2 (Tanabe et al. 1993), and this observation is in accordance with our oxygraphic studies (Table 2). The specificity of current oxygraphic method was confirmed by western blot and spectrophotometric methods (Fig. 4) which showed that in rat cardiomyocytes main AK isoform was AK1 as well as only AK1 was present in cytosol. HL-1 cardiac tumor cells have decreased V_{AMP} which is associated with downregulation of AK1 (Fig. 3a, Table 2). Here, carcinogenesis shifts the AK profile from AK1 to AK2.

The current study revealed few differences in the ratio of AK1 and AK2 in rat cardiomyocytes when comparing oxygraphic (Fig. 3a) and spectrophotometric AK activity assays (Table 2). Therefore to control specificity of N-ethylmaleimide (NEM) in inhibition of AK1 (Khoo and Russell 1972) rat liver where only AK2 expressed (Noma 2005) and rat skeletal muscle soleus where predominantly expressed AK 1 (Makarchikov et al. 2002) were used. Our study confirmed specificity of NEM to inhibit AK1 (Supplement Fig.1). Incubation with NEM decreased 99% of total AK activity in rat soleus homogenate, at the same time NEM did not influence on rat liver AK activity (Supplement Fig.1) In addition, commercial pure AK1 enzyme from rabbit muscle (Sigma-Aldrich) was used where NEM fully inhibited AK activity (data not shown).

The PK–PEP protocol, which enables the determination of cytosolic (mainly AK1) and coupled mitochondrial AK2 activity in the same sample, was also applied to examine the effect of neuroblastoma (NB) N2a cell differentiation induced by all-trans-retinoic acid (RA) on AK isoenzymes. Earlier, we had shown that the treatment of undifferentiated N2a cells with RA led to formation of a cell population morphologically similar to mature neurons of the sympathetic nerve system (SNS) and characterized by elevated acetylcholinesterase activity, a marker enzyme for the SNS cells (Klepinin et al. 2014). The elaborated oxygraphic method demonstrated that RA had no effect on the profile of AK1 and coupled AK2 activities in these NB cells (Fig. 3b). Western blot and spectrophotometric analysis (Fig. 4) confirmed that AK1 and AK2 expressed equally in N2a cells and that AK1 indeed localized to the cytosol. The spectrophotometric activity assays also

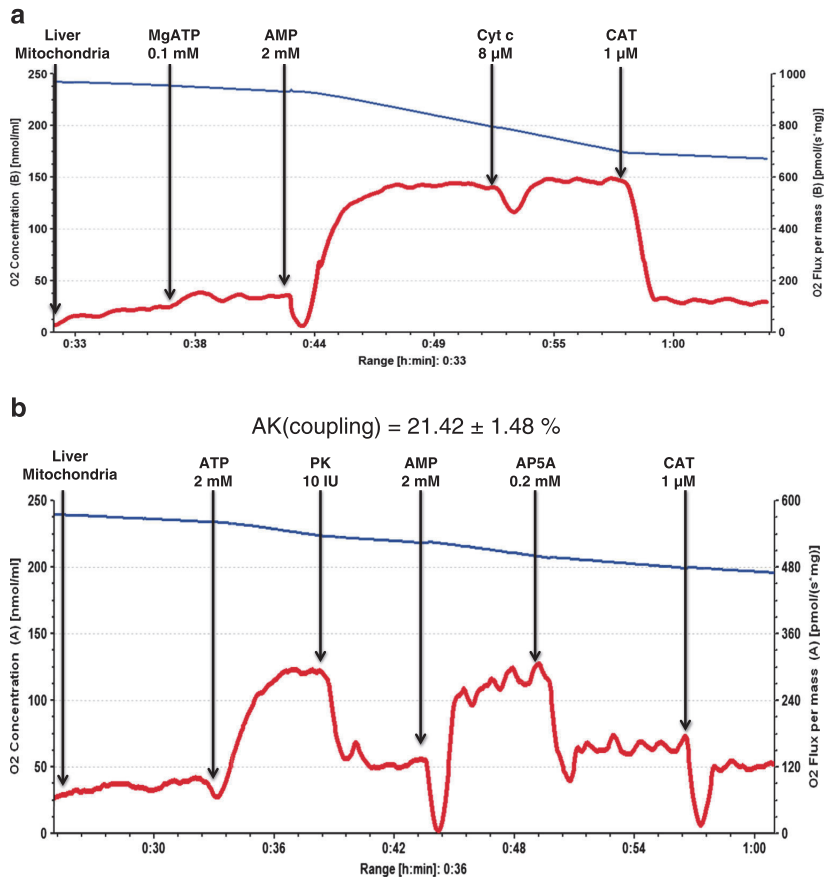


Fig. 1 Oxygraphic analysis of the functional coupling between the AK pathway and OXPHOS in isolated rat liver mitochondria: A – Recording of original traces of AMP-activated respiration; the addition of 2 mM AMP to mitochondria (in the presence of 0.1 mM ATP) resulted in a ~ 5 times increase in the rate O₂ consumption due to activation of mitochondrial AK2 which coupled with OXPHOS. Outer mitochondrial intactness was controlled by exogenously-added cytochrome c (Cyt-c). The AMP-activated respiration was inhibited by carboxyatractyloside (CAT; final concentration, 1 μM) to the initial level showing that the respiration is well controlled by adenine nucleotide translocator in the intact inner mitochondrial membrane. B – Testing the influence of a pyruvate kinase (PK)–phosphoenolpyruvate (PEP) ADP trapping

system on the coupling of AK-catalyzed processes with OXPHOS. The addition of PK to isolated mitochondria suppressed almost completely the ATP (2 mM) activated respiration due to elimination of ADP formed in ATPase reactions, further addition of AMP (final concentration, 2 mM) caused a powerful increase in the rate of O₂ consumption due to local release of ADP in AK2-catalyzed processes. Part ADP, which was produced via AK2 was trapped by PK. The presence of AK2 activity was confirmed by addition of diadenosine pentaphosphate (AP5A, an inhibitor of AK). This inhibitor, at a concentration of 0.2 mM, suppressed the AMP-stimulated respiration up to initial level indicating thereby that it was largely mediated by ADP produced in AK reactions

revealed a decrease in total AK activity during NB cell differentiation (Table 2).

We finally applied high-resolution respirometry for estimating the AK activity distribution in cancerous tissue biopsy material. Unfortunately, it was not possible to measure the rate V_{AMP} for adjacent normal tissue. This tissue consists of a mix of connective and adipose tissue and exhibited low rates of State II and State III respiration. Since our previous work on human HBC showed that MtCK plays a minor role in cellular energy transfer (Kaambre et al. 2012), we examined here the

coupling of AK with OXPHOS. Respirometry experiments suggested that the mitochondrial respiration rate in the presence of 2 mM AMP is close to maximal rate with 2 mM ADP (Table 1) which indicated that the AK system is a main energy transfer system in HBC. The spectrophotometrically determined activities demonstrated that both AK1 and AK2 increased 5- to 7-fold during breast carcinogenesis with AK1 remaining the predominant isoform (Table 2).

The main limiting factor for the described AK respirometric assay is the low mitochondrial respiration of an examined

Table 1 Rates of basal (V_o), ADP (V_{ADP})- and AMP (V_{AMP})-activated respiration, respiratory control index (RCI) and apparent K_m (AMP) values for human breast cancer tissue, isolated rat liver mitochondria and cardiomyocytes (CMs) as well as some tumor cells of different histological type

Cells and tissues	$V_o^{(a)}$ mean \pm SEM	$V_{ADP}^{(b)}$ mean \pm SEM	RCI ^(b) , ADP	$V_{AMP}^{(c)}$ mean \pm SEM	K_m (AMP) mean \pm SEM
Mitochondria	4.75 \pm 0.44	42.4 \pm 4.06	8.88 \pm 0.72	41.5 \pm 6.3	23.5 \pm 6.9
Rat CM(s)	7.5 \pm 1.6 ^(d)	84.5 \pm 13.9 ^(d)	11.2 \pm 4.2 ^(d)	88.1 \pm 2.7	369 \pm 88
HL-1 cells	1.91 \pm 0.8	9.12 \pm 2.3	4.51 \pm 0.63	2.9 \pm 0.2	67 \pm 9.3
uN2a cells	3.38 \pm 0.12	11.0 \pm 0.43	3.28 \pm 0.05	7.2 \pm 0.40	92 \pm 14
dN2a cells	4.07 \pm 0.46	12.05 \pm 1.06	3.13 \pm 0.16	6.8 \pm 0.5	207 \pm 24
Breast cancer	0.56 \pm 0.04 ^(e)	1.09 \pm 0.04 ^(f) (range, 0.10–2.02) ^(f)	1.95 \pm 0.21	0.72 \pm 0.07 ^(f) (range, 0.59–1.03)	-
Breast control tissue	0.02 \pm 0.01 ^(f)	-	-	-	-

^a Rates of O_2 consumption are expressed in nmol O_2 /min per mg protein

^b V_{ADP} and RCI values were measured in the presence of 2 mM ADP

^c These values were obtained in the presence of 2 mM AMP

^d From (Timohhina et al. 2009)

^e From (Kaambre et al. 2012)

^f Rates of respiration in nmol O_2 /min per mg dry weight of the tissue

biomaterial - cells or tissues with low (< 2) RCI values. In this respect, also ATP concentration should be adapted to the respiratory capacity of the cells to avoid interfering effects of ADP released by non-specific ATPase reactions. Cells with a decreased number of mitochondria and/or with low OXPHOS rates and RCI values in the range of 2–4 should be measured at low (0.1 mM) ATP concentrations, while for cells with higher RCI values the use of higher (2 mM) ATP concentrations is recommended.

In a previous study, Gellerich (Gellerich 1992) showed that PEP-PK could be used to examine the affinity of mitochondria for exogenously added AMP. However, the roles of AK2 in the regulation of OXPHOS and mitochondrial MOM permeability for AMP have remained unclear. Here we have determined mitochondrial AMP affinity in isolated rat liver mitochondria and permeabilized rat heart muscle fibers (Figs. 5a and b) using the PK-PK protocol. Isolated liver mitochondria had high affinity for AMP with a Michaelis-Menten constant (K_m) for AMP of $23.5 \pm 6.9 \mu\text{M}$ (Fig. 6a). This value is close to isolated AK2 enzymes ($\leq 10 \mu\text{M}$) (Dzeja and Terzic 2009). The same result was obtained in isolated heart mitochondria ($\sim 20 \mu\text{M}$) (Doliba et al. 2015). However, in permeabilized adult rat heart muscle fibers and tumor cells, K_m (AMP) values were significantly higher and seem to depend on their proliferation and differentiation status. Non-proliferating, highly-differentiated adult rat heart muscle have the highest K_m value ($369 \pm 88 \mu\text{M}$) (Fig. 6b) for exogenously-added AMP, whereas the K_m values found for rapidly-proliferating HL-1 cardiac sarcoma and NB cells were at least 4- times lower (Fig. 6b, c). It was also found that N2a cell differentiation induced by RA is

associated with suppression of their proliferative activity (Klepiniin et al. 2014) and accompanied by a 2-fold increase in the K_m (AMP) value (Fig. 6c).

In resting muscle, cellular AMP concentration is $\sim 10 \mu\text{M}$, while during muscle contraction AMP concentration increases up to $100 \mu\text{M}$ (Plaideau et al. 2014). Since our data for heart muscle and dN2a cells suggest an apparent K_m (AMP) that is several times higher than the physiological AMP concentration, we became interested in reactions that could compete for the AMP substrate, such as AMPD. Total AMPD activity was about 2.5-fold higher in HL-1 and uN2a cells as compared to CM, and decreased during N2a cell differentiation with RA about 2.4-fold (Table 3).

Discussion

In the present work, a simple new method is used for quantitative estimation of cellular compartmentation of AK activity in permeabilized mammalian cells or tissues. It distinguishes between mitochondrial AK2-dependent activity strongly coupled to mitochondrial respiration, and less coupled AK activity mainly dependent on cytosolic AK1 activity. It is based on ATP/AMP-stimulated AK-catalyzed reactions delivering ADP to OXPHOS, cytosolic ADP trapping by the PEP/PK system and measurements of O_2 consumption rates. The main advantage of this method is its capacity to estimate the relative ratio of AK1 and AK2 activities in one sample without extraction of cellular protein(s). However, the method is limited by poor mitochondrial respiration of an examined biomaterial, i.e. by a RCI below 2.

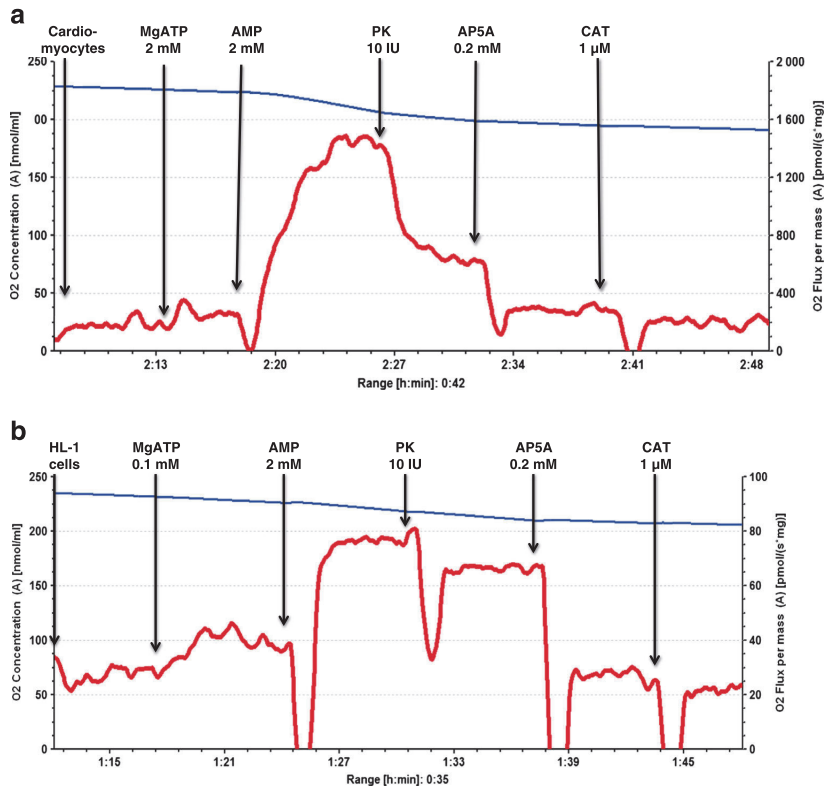


Fig. 2 Illustration of analytical protocols (original recording of rates of O₂ uptake, in red) applied to permeabilized rat cardiomyocytes (a) and HL-1 tumor cells (b) which permit to estimate, quantitatively, the presence of AK-1 and -2 isoforms in studied cell or tissue material. This can be accomplished through analysis of these isoenzymes functional coupling with the OXPHOS system. The addition of AMP (final concentration, 2 mM) to the model cells (in the presence of ATP (0.1 mM) and PEP at a final concentration of 5 mM) which increased mitochondrial respiration due to activation both AK1 and AK2.

Subsequent addition of pyruvate kinase (PK) decreases O₂ consumption since the added PK removes efficiently extramitochondrially-generated ADP from AK1 and MgATPases. Remain respiration is associated with AK2 coupling with OXPHOS. The functional coupling between AK2 and mitochondrial respiration was confirmed by diadenosine pentaphosphate (AP5A, a selective inhibitor of AK) which decreased respiration back to basal respiration. Finally, carboxyatractyloside (CAT) was added in order to control mitochondrial inner membrane intactness

In human HBC which has low mitochondrial respiration ($RCI < 2$) only total AK mediated respiration can be measurement by the respirometry method. In such cases, as we have shown earlier (Kaldma et al. 2014), the functional coupling between AK and OXPHOS can be estimated by the adenylate kinase index ($I_{AKtotal}$) without PK-PEP system. The $I_{AKtotal}$ value for HBC ($I_{AKtotal} = 0.37 \pm 0.06$) was 1.35 times lower than in human colorectal cancer ($I_{AKtotal} = 0.50 \pm 0.06$) but close to normal large intestine tissue ($I_{AKtotal} = 0.31 \pm 0.03$) (Kaldma et al. 2014). These respirometry data correlate well with total AK activity in HBC (Table 2), large intestine and colorectal tissue (Kaldma et al. 2014). This result indicates that the respirometry methods can be used to detect changes in AK activity in clinical postoperative tissues.

Although, the AK phosphotransfer network has been well studied in heart muscle (Dzeja and Terzic 2009), the expression of AK isoforms and their putative role in carcinogenesis is much less clear. In this work, we have demonstrated that the oxygraphic assay can be successfully applied for estimating the alterations in AK1 and AK2 activities in cardiac muscle cells, differentiating N2a cells and cancer cells in vitro and in situ (on biopsy material). Furthermore, in presence of the PK-PEP system, the method can determine permeability of MOM for exogenous AMP.

AK1 is predominantly expressed in cells and organs with a high energy consumption (such as CM(s) and mature neural cells) (Tanabe et al. 1993), while AK2 expression is rather pronounced in rapidly proliferating

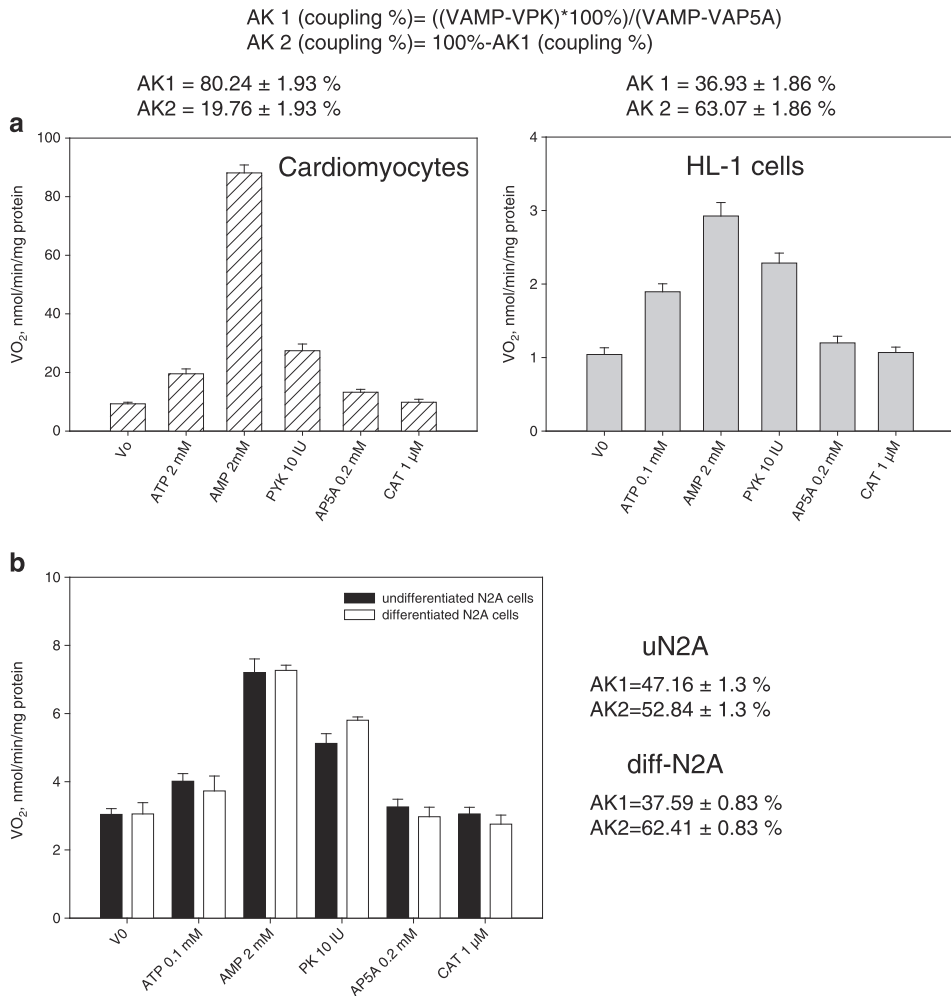


Fig. 3 Application of a pyruvate kinase (PK)–phosphoenolpyruvate (PEP) protocol for determination of the presence of cytosolic (AK1) and mitochondrial (AK2) isoforms in one sample: **(a)** rat cardiomyocytes and HL-1 cardiac sarcoma cells; **(b)** undifferentiated and retinoic acid differentiated N2a cells (uN2a and dN2a,

respectively). The presence of AK1 and AK2 in studied material can be quantified as the adenylate kinase index (I_{AK}) that reflects the strength of AK coupling with the OXPHOS system; the value of I_{AK} for AK1 and AK2 can be calculated as indicated in the corresponding section of “Materials and methods”. On these charts, bars are SEM, $n = 5$

cells (Abdul Khalek et al. 2010; Bjorkholm et al. 2003). Consistent with these data, we found high values of AK1 activity and minor levels of AK2 in fully-differentiated rat CM(s), but more important AK2 activity in HL-1 tumor cells from adult rat ventricular myocardium and poorly-differentiated rapidly proliferating neuroblastoma cells (N2a line). Mature neurons in contrast to N2a cells mature neurons, the prevailing isoenzyme is cytosolic AK1 (Noma 2005).

It is important to emphasize that in several tumors, including NB(s) and HL-1 cells, the up-regulation of AK2 is associated with a loss of mitochondrial creatine kinase (Eimre

et al. 2008; Kaambre et al. 2012; Kaldma et al. 2014; Klepinin et al. 2014; Patra et al. 2012). The current study shows that during breast cancer carcinogens the AK1/AK2 ratio did not change, while the AK1 and AK2 activities were higher than in normal tissue, with AK1 remaining the predominant isoform. Previously, it was shown that in breast cancer the up-regulation of AK2 was associated with an increase in cancer stem cells (CSC) (Lamb et al. 2015), NB also contains numerous CSC (Ross and Spengler 2007).

Although, AK1 associates with the mitotic spindle apparatus, probably to supply energy for cell proliferation (Dzeja et al. 2011), but AK1 knockout in NB cells did not affect

Table 2 The activity of adenylate kinase (AK) in human breast cancer tissue, adult rat cardiomyocytes (CMs), and some tumor cells of different histological type along with corresponding adenylate kinase indexes (I_{AK})

Cells and tissues	Total activity, mU/mg protein*	AK1, mU/mg protein	AK2, mU/mg protein	I_{AK1} , %	I_{AK2} , %
Rat CM(s)	2493 ± 113; n = 5	2394 ± 102 (96%**)	99 ± 18 (4%**)	80	20
HL-1 cells	311 ± 10; n = 5	174 ± 9 (56%)	137 ± 2 (44%)	37	63
uN2a cells	245 ± 12; n = 5	136 ± 9 (56%)	109 ± 8 (44%)	53	47
dN2a cells	172 ± 15; n = 5	81 ± 10 (47%)	91 ± 8 (53%)	39	61
Breast cancer	290 ± 89; n = 6	208 ± 64 (69%)	82 ± 15 (31%)	-	-
Non-tumor tissue	53 ± 5; n = 6	42 ± 4 (80%)	11 ± 2 (20%)	-	-

*all data presented in the Table 2 are mean values ± SEM from at least 5 independent experiments; ** % from the total AK activity; uN2a and dN2a are undifferentiated and retinoic acid differentiated Neuro-2A cells, respectively

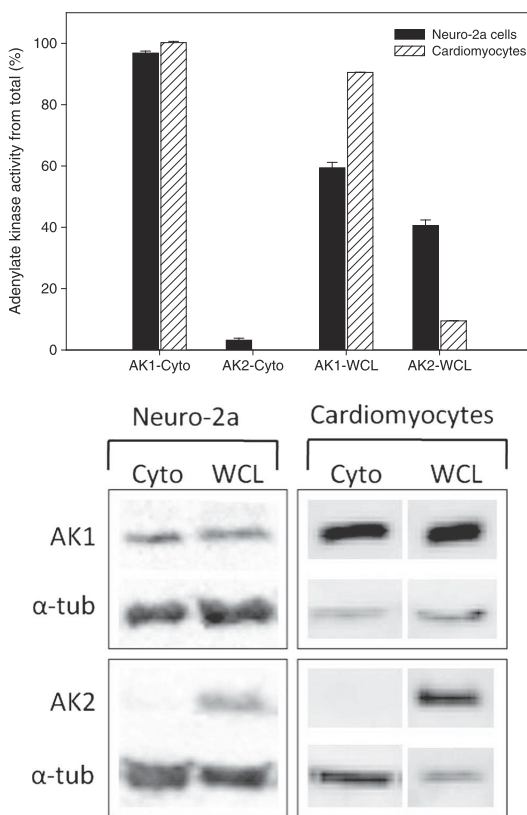


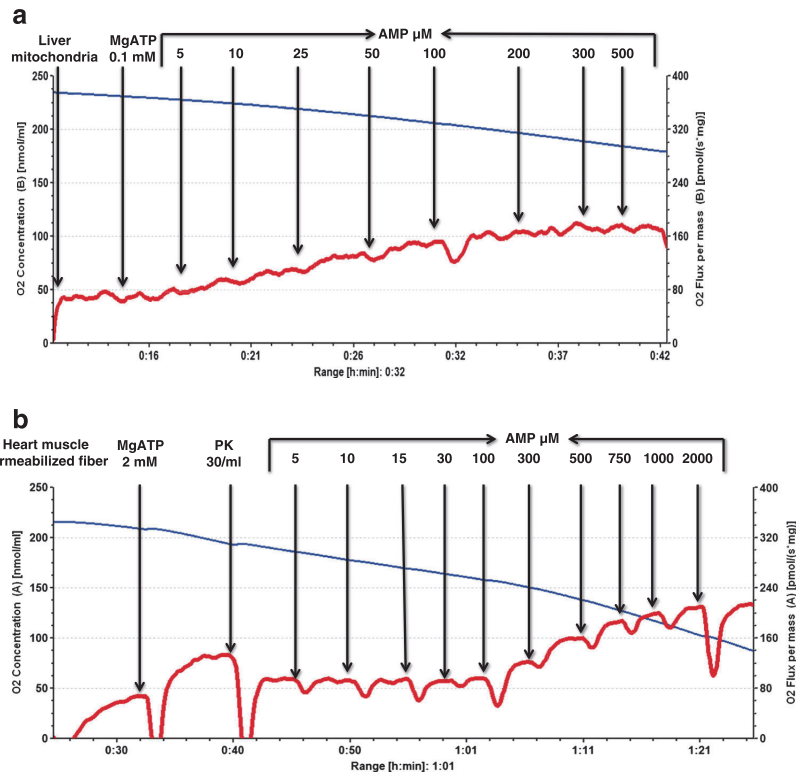
Fig. 4 Intracellular localization of adenylate kinase 1 (AK1) and adenylate kinase 2 (AK2) in Neuro-2a cell line and cardiomyocytes. The 10,000 × g supernatants of cytosolic fraction (Cyto) from digitonin permeabilized Neuro-2a and cardiomyocytes were prepared for adenylate kinase (AK) spectrophotometric assay (upper panel) and Western blot analysis (lower panel). Whole cell lysates (WCL) of Neuro-2a and cardiomyocytes were used as a control. Enzymes samples for AK1 and AK2 activity assay were incubated in the presence or absent of specific AK1 inhibitor N-ethylmaleimide for 1 h at 25°C. For Western blot analysis, α -tubulin was used as a loading control, bars are SEM, n = 3

cancer cells growth (de Bruin et al. 2004). Proteomics studies have also revealed the up-regulation of AK2 in human prostate and pancreatic cancer cells (Lam et al. 2010; Liu et al. 2010). It was shown that AK2 can promote cell proliferation under normal circumstances (Dzeja and Terzic 2009; Lagresle-Peyrou et al. 2009) and full AK2 deletion (AK2^{-/-}) in mice is embryonically lethal (Zhang et al. 2010). Although, this would suggest AK2 as a target for antitumor therapy, literature data on its association with tumor progression remain contradictory. Kim and colleagues have postulated that AK2 is rather a negative regulator of tumor growth (Kim et al. 2014). They showed that AK2 can interact with dual-specificity phosphatase 26 in the nucleus and this protein complex can dephosphorylate fas-associated protein with death domain leading to suppressed cell growth.

Adenine nucleotides and some respiratory substrates are transported into mitochondria via VDAC (Maldonado et al. 2013) which is also the binding partner for HK-1/2 (Pastorino and Hoek 2008). Hence, in tumor cells, the observed increased level of VDAC(s) (Simamura et al. 2008) can enhance the binding of HK-2 to mitochondria and, according to the model proposed by Majewski and coauthors (Majewski et al. 2004), this interaction would support VDAC in the open state. It was reported (Simamura et al. 2008) that tumor cells contain an increased amount of VDAC(s) per mitochondrion, and this circumstance could be responsible for the higher permeability of tumor mitochondria for ADP and AMP.

Further, it is well-known that the lipid composition of tumor mitochondria differs substantially from that in normal cells (Baggetto et al. 1992; Kiebish et al. 2008; Park and Wenner 1970). This could also affect adenine nucleotide permeability of MOM in malignant cells. Finally, the difference in the Km(AMP) values between poorly-differentiated tumor cells and highly-differentiated cells could be due to varying AMPD activity. This enzyme catalyzes the deamination of AMP to inosine monophosphate and plays an important role

Fig. 5 Measurements of the apparent K_m (AMP) value (a) for rat liver mitochondria and (b) for rat heart fiber; representative oxygraphic tracings. The right scale show the rate of oxygen uptake expressed in $\text{pmol O}_2 \text{ sec}^{-1}$ per mg protein. Samples were incubated in respiratory buffer (with 2 mM malate and 5 mM glutamate as respiratory substrates) in the presence of a PK-PEP system and 0.1 mM ATP (for rat heart fiber 2 mM ATP), the rates of O_2 consumption were recorded after a step-wise addition of AMP



in the purine nucleotide cycle (Morisaki et al. 1992). The highest expression of AMPD was found in muscle where main isoform was AMPD1. Other tissues have much lower activity of AMPD. AMPD2 is predominant in nonmuscle tissues, and AMPD3 is found in erythrocytes (Plaideau et al. 2012). In 2014 Catheline Plaideau showed pharmacological inhibition of AMPD or AMPD 1 deletion in muscle increased nucleotide level especially AMP (Plaideau et al. 2014). Our work suggested that in HL-1 cells AMPD activity (Table 3) was 6 times higher than previously reported for mouse heart muscle (Rybakowska et al. 2014). Similarly, in NB cells had 2.4 times higher AMPD activity than RA-treated N2a cells (Table 3). At the same time, we did not find correlation between AMPD activity and increased K_m values for AMP in heart muscle and RA-differentiated N2a cells (Tables 1, 3). There is presumably another AMP removal pathway which can regulate cellular AMP concentration. Altogether, further work is needed to understand the role of increased MOM permeability for ADP and AMP as well as AMP removal pathway different enzymes in the regulation of adenine nucleotides level in malignant cells.

In summary, we developed here a simple oxygraphic method for semi-quantifying the ratio between mostly AK1- and AK2-related activities in mammalian tissues and cultured cells. This method is rapid and enables to estimate the activities related to these two AK isoforms in one sample. We tested this method on two tumor cell lines, isolated cardiac muscle cells, and human breast cancer postoperative material. The method is sensitive enough to be performed on tumor biopsies. The data show that AK2 is expressed predominantly in poorly differentiated cells with high proliferative index, and that strong differences exist between highly-differentiated and tumor cells in the affinity of their mitochondrial respiration for exogenous AMP. Further studies will be required to identify the underlying molecular mechanisms and to evaluate their value for cancer diagnosis and therapy.

Materials and methods

Chemicals

Unless otherwise stated, all materials and reagents were purchased from Sigma-Aldrich Company (St. Louis USA).

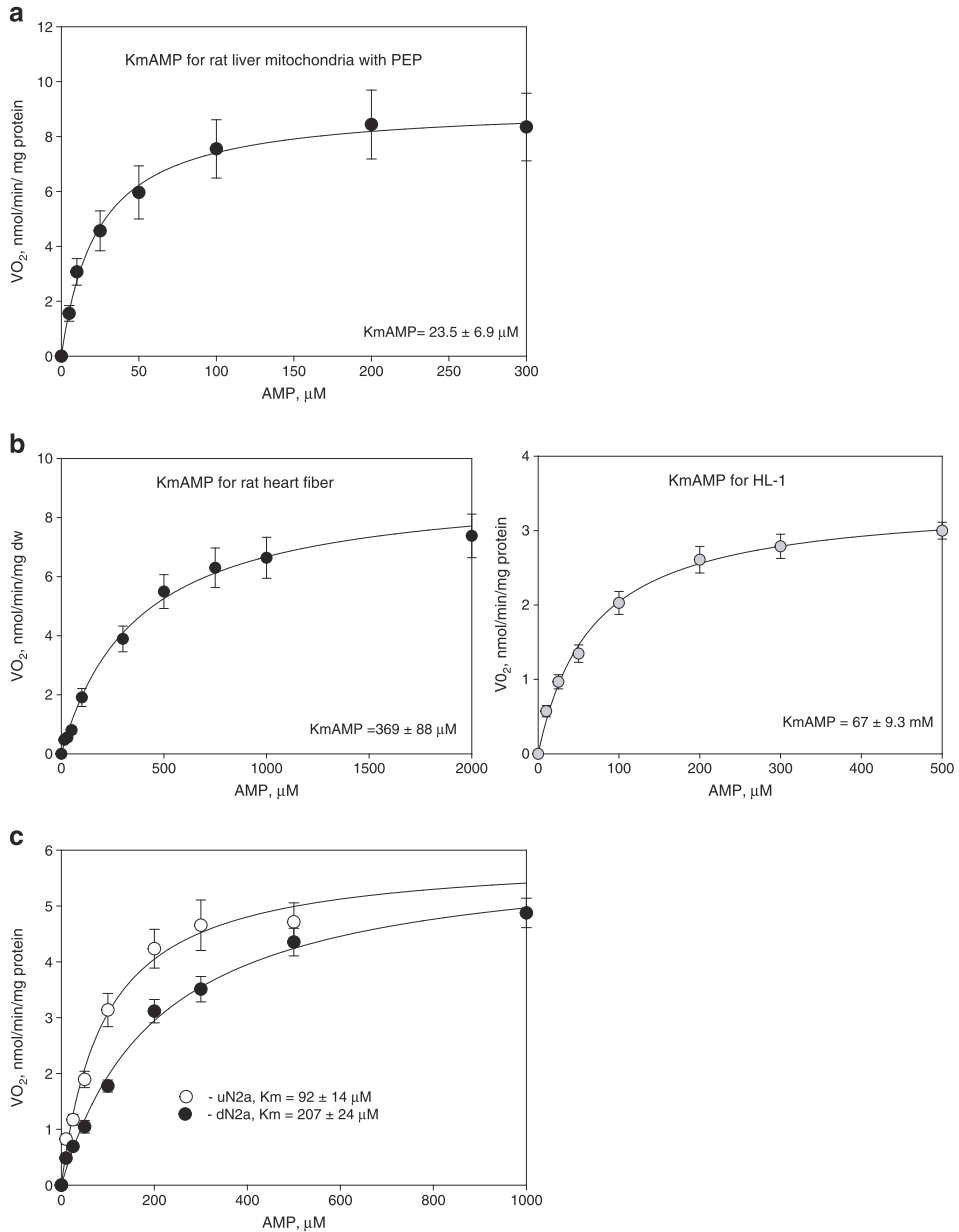


Fig. 6 Kinetic analysis of regulation of the AMP-activated respiration in isolated rat liver mitochondria (**a**), for skinned rat heart myocytes (**b**) and HL-1 cardiac tumor cells (**c**) as well as for undifferentiated or retinoic acid differentiated murine neuroblastoma cells; uN2a and dN2a, respectively

(**d**). The corresponding apparent Michaelis-Menten constant (K_m) values towards exogenously-added AMP were determined. These measurements were performed in the presence of a PEP-PK ADP-trapping system, bars are SEM, $n = 5$

Dulbecco's Modified Eagle Medium (DMEM) and phosphate buffered saline (PBS, Ca/Mg free) were obtained from Corning (USA) whereas heat-inactivated fetal bovine serum

(FBS), accutase, penicillin-streptomycin solution (100 \times), gentamicin and 0.05% Trypsin-EDTA were purchased from Gibco Life Technologies (Grand Island, NY).

Table 3 The activity of AMP deaminase (AMPD) in differentiated neuron and adult rat cardiomyocytes (CM) cells and appropriate cancer cells

Enzyme activities, mU(s)/mg protein	HL-1 cells mean ± SEM, <i>n</i> = 3	Rat CM(s) mean ± SEM, <i>n</i> = 3	uN2a cells mean ± SEM, <i>n</i> = 3	dN2a cells mean ± SEM, <i>n</i> = 3
AMPD	40.1 ± 2.6 *	16.4 ± 0.4	36.0 ± 1.7 **	15.1 ± 1.3

P* < 0.001 vs Rat CM(s), *P* < 0.001 vs dN2a cells; uN2a and dN2a are undifferentiated and retinoic acid differentiated Neuro-2A cells, respectively

Clinical material and patients

All women (with ages ranging from 50 to 71 years, *n* = 10) had local or locally advanced disease (T1–4 N0–2 M0, st. IA–IIIB). Invasive ductal carcinoma accounted for 87% and lobular carcinoma for 13% of these tumors. These patients had not received prior radiation or chemotherapy. Postoperational samples of human HBC and normal tissue (0.1–0.5 g) were acquired by the Oncology and Hematologic Clinic at the North Estonia Medical Centre (NEMC, Tallinn). They were obtained under general anesthesia and then within 1 h after surgery were delivered to the Laboratory of Bioenergetics for corresponding studies. During transportation, clinical material was stored on ice in solution consisting of 0.5 mM EGTA, 3 mM MgCl₂, 60 mM K-lactobionate, 3 mM KH₂PO₄, 20 mM taurine, 20 mM HEPES (pH 7.1), 110 mM sucrose, 0.5 mM dithiothreitol (DTT) and 5 mg/ml fatty acid free bovine serum albumin (BSA).

Cell cultures

Our *in vitro* studies were carried out on several different cell types, such as mouse neuroblastoma Neuro-2A (N2a) cells, both undifferentiated and subjected to retinoic acid-induced differentiation, HL-1 cardiac sarcoma cells as well as on isolated rat heart CM(s).

Stock culture of N2a cells was obtained from American Type Culture Collection, Cat. No CCL-131. These NB cells were grown as a loosely adhering monolayer in T75 plates (Greiner bio-one) in high glucose DMEM with L-glutamine supplemented with 10% heat inactivated fetal bovine serum (FBS) and antibiotics: penicillin (100 U/ml), streptomycin (100 µg/ml) and 50 µg/ml gentamicin (complete growth medium). N2a cells were grown and maintained at 37°C in a humidified incubator containing 5% CO₂ in air. The cells were sub-cultured at 3 day intervals and had received no more than 20 cell culture passages. Neural differentiation of N2a cells to cholinergic neurons was induced by their treatment with 10 µM all-trans-retinoic acid (RA) in complete growth medium, for details see in (Blanco et al. 2001; Klepinin et al. 2014).

The HL-1 cardiac sarcoma cell line was originally established by William Claycomb (Claycomb et al. 1998) and was kindly provided to us by Dr. Andrey V. Kuznetsov (Innsbruck Medical University, Austria). These tumor cells

were grown in fibronectin–gelatin (5 µg/ml/0.2%) coated T75 flasks containing Claycomb medium (Sigma-Aldrich), supplemented with 10% FBS, 100 U/ml penicillin, 100 µg/ml streptomycin, 50 µg/ml gentamicin, 2 mM L-glutamine, 0.1 mM norepinephrine, and 0.3 mM ascorbic acid. HL-1 cells were cultured at 37°C in humid air with 5% CO₂.

Isolation of rat cardiomyocytes and liver mitochondria

Adult (3-month-old) male Wistar rats weighing about 350 g were used in experiments. These animals were kept on a standard laboratory diet and given tap water *ad libitum*. The organs (heart or liver) were removed for sacrificed animals under deep anesthesia; 50 mg/kg of Bioketan® plus 0.6 mg/kg of Dexdomitor®, intraperitoneally.

CMs were obtained after perfusion of the isolated rat heart with collagenase-A (Roche) as described in our previous studies (Saks et al. 1991; Tepp et al. 2010). Isolated CMs contained approximately 90% of rod-like cells when observed under the light microscope. In order to examine the functional coupling of AK-catalyzed processes with OXPHOS in CM(s), the cells sarcolemma was permeabilized by saponin treatment. The permeabilization procedure was carried out directly in oxygraph chambers with 25 µg/ml saponin during 10 min before starting the measurements of respiration rates at 25°C with continuous magnetic stirring; it is important to note that the applied parameters of saponin treatment of CM(s) keep the intactness of their mitochondrial membranes (Guzun et al. 2009).

Rat liver mitochondria were isolated by mild protease digestion (trypsin, at a final concentration of 1 mg/ml for 10 min on melting ice) of the tissue homogenate, exactly as described previously (Saks et al. 1975; Timohhina et al. 2009). After differential centrifugation, the final mitochondrial pellet was suspended in isolation medium containing 1 mg/ml BSA to a mitochondrial protein concentration of 10–15 mg/ml, and this suspension was stored on melting ice until use.

Preparation of skinned tumor and rat heart fibers, cell permeabilization, and high-resolution respirometry

Skinned fibers from human HBC postoperative samples and adult rat heart tissue were prepared according to the method described earlier (Kaambre et al. 2012; Kuznetsov et al. 2008).

In order to study the ADP- or AMP-mediated mitochondrial respiration in tumor tissues, the plasma membranes in HBC fibers was completely permeabilized by saponin treatment (50 $\mu\text{g}/\text{ml}$; for 30 min at 4°C upon mild stirring) exactly as described in our prior work (Kaambre et al. 2012). This permeabilization procedure had no effect on the intactness of mitochondrial membranes in the obtained HBC tissue fibers (Kaambre et al. 2012). Prior to respiratory experiments, N2a cells were permeabilized by saponin (40 $\mu\text{g}/\text{ml}$) treatment for 5 min at 25°C directly in oxygraphic chambers, whereas the plasma membrane in HL-1 tumor cells was permeabilized in similar manner but in the presence of digitonin (25 $\mu\text{g}/\text{ml}$). All protocols used for cell permeabilization provided the maximal respiratory response for exogenously-added ADP, whereas the integrity of the mitochondrial membranes was preserved. Measurements of cellular O_2 consumption rates in the presence of exogenous ADP (2 mM) served as an indicator for mitochondrial respiratory chain function.

Rates of O_2 consumption by the permeabilized, N2a, HL-1 tumor cells (at a density of $\sim 0.5\text{--}1.0 \times 10^6$ cells/ml), CMs, HBC samples or liver mitochondria were measured under magnetic stirring (300 rpm) at 25°C in 2-ml glass chambers of a two-channel titration-injection respirometer (Oxygraph-2 K, OROBOROS Instruments, Austria) in medium-B supplemented with 5 mM glutamate, 2 mM malate and 10 mM succinate as respiratory substrates; solubility of oxygen was taken as 240 nmol/ml (Gnaiger 2001). All respiration rates of tissue samples and cells were normalized per mg dry weight or mg protein respectively.

Oxygraphic analysis for the presence AK1 and mitochondrially-bound AK-2 in normal and tumor cells

Total adenylate kinase coupling with OXPHOS was measured by respirometry in permeabilized human HBC fibers according to our previous study (Kaldma et al. 2014). The total AK coupling with OXPHOS is expressed by adenylate kinase index ($I_{AK \text{ total}}$): $[I_{AK \text{ total}} = (V_{AMP} - V_{AP5A}) / V_{AP5A}]$ where V_{AMP} is mitochondrial respiration rate in the presence of 2 mM AMP and V_{AP5A} remain respiration rate after inhibition total AK by 0.2 mM diadenosine pentaphosphate (AP5A). AK coupling with OXPHOS is measured in the presence of 0.1 mM ATP.

The presence of cytosolic (AK1) and mitochondrial AK2 (which catalyze the phosphotransfer reaction of “AMP + ATP \leftrightarrow 2ADP”) in permeabilized tumor and normal cells was assayed quantitatively by respirometry through their coupling with OXPHOS due to the formation of ADP in these enzymes catalyzed reactions. These measurements were performed in medium-B in the presence or absence of phosphoenolpyruvate (PEP, 5 mM) – pyruvate kinase (PK, 10 U/ml) ADP trapping system (Tepp et al. 2011; Timohhina et al. 2009).

The mitochondrial respiration assay is performed in medium-B. Respiration was activated by addition of 0.1 mM ATP or 2 mM ATP to initiate the endogenous ADP production by ATPases. Then AMP (up to a final concentration of 2 mM) was added to activate the coupled reaction of AK (AK1 and AK2) system with adenine nucleotide translocator (ANT). Next addition of PK removes ADP from cytosolic which is produced by AK1. Residual respiration which is associated with specific coupling of AK2 with OXPHOS is inhibited by 0.2 mM AP5A. Finally, CAT 1 μM is added to control mitochondrial inner membrane intactness.

The AK1 functional coupling with OXPHOS system, linked with this isoenzyme activity, was characterized by the corresponding AK index (I_{AK1}). The I_{AK1} was calculated according to the equation: $[I_{AK1} = ((V_{AMP} - V_{PK}) / (V_{AMP} - V_{AP5A}) \times 100\%]$, where V_{AMP} , V_{PK} and V_{AP5A} are rates of O_2 consumption that were measured after subsequent addition of 2 mM AMP, 10 U/ml PK and 0.2 mM AP5A, respectively.

The AK2 functional coupling with OXPHOS was calculated as $I_{AK2} = 100\% - I_{AK1}$. The use of PEP–PK ADP-trapping system allows us to distinguish the rate of cellular O_2 consumption associated with the presence of AK2 from cytosolic AK1 mediated respiration. Thus, in our assay system the inhibitory effect of PK on the AMP-mediated O_2 consumption correlate with intracellular AK1/AK2 ratio. In cells where mitochondrial AK2 is the predominant AK isoenzyme, the effect of PK addition on AMP-activated respiration will be negligible.

Determination of apparent Michaelis-Menten constant values for exogenously-added AMP as well as rates of maximal ADP- or AMP-activated respiration for normal and malignant cells

The maximal respiration with ADP (final concentration, 2 mM) was measured in the presence of respiratory substrate (5 mM glutamate, 2 mM malate and 10 mM succinate). The maximal AMP-activated respiration rates were assayed in the same medium after preliminary addition of 0.1 mM ATP (or 2 mM ATP for CMs) in the presence of 2 mM AMP.

To determine the Michaelis-Menten constants (K_m) for AMP the respiration rate of permeabilized fiber is measured in medium-B in the presence of PK–PEP ADP trapping system with exogenously-added ATP at a final concentration of 2 mM (0.1 mM ATP for isolated mitochondria). Due to the presence of PK–PEP (trapped ADP produced from AK1) addition of ATP with AMP activates only AK2. Using AK2 coupling with OXPHOS is able to determinate mitochondrial affinity for AMP via stepwise increased AMP concentration. Corresponding K_m (AMP) values were calculated by fitting experimental data to a non-linear regression.

Immunoblot analysis

Fresh cells were washed with PBS and pelleted by centrifugation at $150 \times g$ for 7 min. Cytosolic fractions were isolated by selective lysis of the plasma membrane with $35 \mu\text{g}$ of digitonin per 4×10^6 N2a cells (Single et al. 1998) or with $25 \mu\text{g}/\text{ml}$ of digitonin for rat cardiomyocytes (Dedkova and Blatter 2012) followed by centrifugation at $1000 \times g$ for 10 min. Supernatants containing cytosolic fraction of proteins were centrifuged at $10,000 \times g$ for 15 min to pellet any remaining cellular debris.

Whole cell extracts were isolated using Tris-Triton X lysis buffer (10 mM Tris pH 7.4, 100 mM NaCl, 1 mM EDTA, 1% Triton X-100, 10% glycerol, 0.1% SDS) supplemented with protease inhibitors (Cytoskeleton). Lysates were homogenized by Retsch Mixer Mill at 25 Hz for 2 min, incubated for 20 min on ice, and clarified by centrifugation at $21,000 \times g$ for 30 min at 4°C . The concentration of the isolated proteins was determined using BCA Protein Assay Reagent (Pierce, Rockford, IL). Protein samples ($20 \mu\text{g}$ per fraction) were separated by a 12% Tris-Glycine SDS-PAGE and electrophoretically transferred onto PVDF membrane (Millipore) by Trans-Blot Semi-Dry Transfer system (Bio-Rad). Membranes were then incubated with the primary antibodies against AK1 (sc365316), AK2 (sc374095) or α -tubulin (ab7291) and the appropriate secondary antibodies.

Enzymatic activities

AMPD activity was measured spectrophotometrically in whole cell or tissue extract by an enzyme-coupled spectrophotometric assay in the direction of IMP formation in the presence of 50 mM Hepes (pH 7.1), 100 mM KCl, 1 mM EDTA, 1 mM DTT, 5 mM α -ketoglutarate, 0.15 mM NADH, and 5 U of glutamate dehydrogenase containing 0.25 mg of extract protein and reaction was initiated by 10 mM AMP and following the decrease in absorbance at 340 nm at 25°C (Ashby and Frieden 1978) One unit of AMPD activity was defined as 1 μmole of AMP deaminated to IMP.

AK1 and AK2 activities were measured in whole cell or tissue extracts at 25°C by an enzyme-coupled spectrophotometric assay in the direction of ATP formation, essentially as described earlier by Dzeja et al. and Tanabe et al. (Dzeja et al. 1999; Tanabe et al. 1993). The reaction mixture contained 20 mM Hepes (pH 7.5), 0.1 M KCl, 4 mM Mg-acetate, 1 mM EDTA, 20 mM glucose, 2 mM NADP⁺, 4.5 units/ml hexokinase, and 2 units/ml glucose-6-phosphate dehydrogenase as the coupled enzymes. The reaction was initiated with 2 mM ADP, and the increase in absorbance at 340 nm was recorded using a Cary 100 Bio UV-visible spectrophotometer. One unit of AK activity was defined as 1 μmole of ATP produced per minute at 25°C . The extinction coefficient of

NADPH ($6.22 \times 10^3 \text{ M}^{-1} \text{ cm}^{-1}$) was used to convert its absorbance to molar concentration of the product formed.

AK1 is a thiol-containing enzyme that is inhibited by N-ethylmaleimide (NEM), while AK2 is not (Khoo and Russell 1972). For the NEM treatment, enzyme samples (in 20 mM MOPS-buffered solution with 0.2 M NaCl, pH 8.0) were incubated in the presence of 1 mM NEM for 1 h at 25°C before assay. AK2 activity was determined as the activity remaining after the NEM treatment of cell/tissue extracts. AK1 activity was measured as total AK activity minus activity remaining after the NEM treatment. For the NEM treatment, enzyme samples (in 20 mM MOPS-buffered solution with 0.2 M NaCl, pH 8.0) were incubated in the presence of 1 mM NEM for 1 h at 25°C before assay. Protein concentration of the used cell/tissue homogenates was determined by a Pierce BCA Protein Assay Kit according to the manufacturer recommendations using BSA as a standard.

Statistical analysis of data

All data points are presented as means \pm standard error (SEM) from at least five parallel experiments. Significance was calculated by Student's t-test; differences between two data groups were considered to be statistically significant when $P < 0.05$.

Acknowledgements This work was supported by institutional research funding IUT23-1 of the Estonian Ministry of Education and Research and the Estonian Science Foundation grant No.8987.

Compliance with ethical standards Aleksandr Klepinin, Lyudmila Ounpuu, Rita Guzun, Vladimir Chekulayev, Natalja Timohhina, Kersti Tepp, Igor Shevchuk, Uwe Schlattner, and Tuuli Kaambre declare that they have no conflict of interest.

All institutional and national guidelines for the care and use of laboratory animals were followed.

All procedures followed were in accordance with the ethical standards of the responsible committee on human experimentation (institutional and national) and with the Helsinki Declaration of 1975, as revised in 2000 (5). Informed consent was obtained from all patients for being included in the study.

References

- Abdul Khalek FJ, Gallicano GI, Mishra L (2010) Colon Cancer stem cells. *Gastrointestinal cancer research*. GCR, pp. S16–S23
- Amiri M, Conserva F, Panayiotou C, Karlsson A, Solaroli N (2013) The human adenylate kinase 9 is a nucleoside mono- and diphosphate kinase. *Int J Biochem Cell Biol* 45:925–931
- Ashby B, Frieden C (1978) Adenylate deaminase. Kinetic and binding studies on the rabbit muscle enzyme *J Biol Chem* 253:8728–8735
- Baggetto LG, Clottes E, Vial C (1992) Low mitochondrial proton leak due to high membrane cholesterol content and cytosolic creatine kinase as two features of the deviant bioenergetics of Ehrlich and AS30-D tumor cells. *Cancer Res* 52:4935–4941

- Balinsky D, Greengard O, Cayanis E, Head JF (1984) Enzyme activities and isozyme patterns in human lung tumors. *Cancer Res* 44:1058–1062
- Bjorkholm B, Falk P, Engstrand L, Nyren O (2003) *Helicobacter pylori*: resurrection of the cancer link. *J Intern Med* 253:102–119
- Blanco V, Lopez Camelo J, Carri NG (2001) Growth inhibition, morphological differentiation and stimulation of survival in neuronal cell type (neuro-2a) treated with trophic molecules. *Cell Biol Int* 25:909–917
- Burkart A, Shi X, Chouinard M, Corvera S (2011) Adenylate kinase 2 links mitochondrial energy metabolism to the induction of the unfolded protein response. *J Biol Chem* 286:4081–4089
- Carrasco AJ, Dzeja PP, Alekseev AE, Pucar D, Zingman LV, Abraham MR, Hodgson D, Bienengraeber M, Puceat M, Janssen E et al (2001) Adenylate kinase phosphotransfer communicates cellular energetic signals to ATP-sensitive potassium channels. *Proc Natl Acad Sci U S A* 98:7623–7628
- Chekulayev V, Mado K, Shevchuk I, Koit A, Kaldma A, Klepinin A, Timohhina N, Tepp K, Kandashvili M, Ounpuu L et al (2015) Metabolic remodeling in human colorectal cancer and surrounding tissues: alterations in regulation of mitochondrial respiration and metabolic fluxes. *Biochemistry and Biophysics Reports* 4:111–125
- Claycomb WC, Lanson NA Jr, Stallworth BS, Egeland DB, Delcarpio JB, Bahinski A, Izzo NJ Jr (1998) HL-1 cells: a cardiac muscle cell line that contracts and retains phenotypic characteristics of the adult cardiomyocyte. *Proc Natl Acad Sci U S A* 95:2979–2984
- Criss WE, Litwack G, Morris HP, Weinhouse S (1970) Adenosine triphosphate: adenosine monophosphate phosphotransferase isozymes in rat liver and hepatomas. *Cancer Res* 30:370–375
- Daniel JM, McCombie G, Wendt S, Zenobi R (2003) Mass spectrometric determination of association constants of adenylate kinase with two noncovalent inhibitors. *J Am Soc Mass Spectrom* 14:442–448
- Dasgupta B, Chhipa RR (2016) Evolving lessons on the complex role of AMPK in normal physiology and cancer. *Trends Pharmacol Sci* 37:192–206
- de Bruin W, Oerlemans F, Wieringa B (2004) Adenylate kinase I does not affect cellular growth characteristics under normal and metabolic stress conditions. *Exp Cell Res* 297:97–107
- Dedkova EN, Blatter LA (2012) Measuring mitochondrial function in intact cardiac myocytes. *J Mol Cell Cardiol* 52:48–61
- Doliba NM, Babsky AM, Doliba NM, Wehrli SL, Osbakken MD (2015) AMP promotes oxygen consumption and ATP synthesis in heart mitochondria through the adenylate kinase reaction: an NMR spectroscopy and polarography study. *Cell Biochem Funct* 33:67–72
- Dyck JR, Lopuschuk GD (2006) AMPK alterations in cardiac physiology and pathology: enemy or ally? *J Physiol* 574:95–112
- Dzeja PP, Terzic A (2003) Phosphotransfer networks and cellular energetics. *J Exp Biol* 206:2039–2047
- Dzeja P, Terzic A (2009) Adenylate kinase and AMP signaling networks: metabolic monitoring, signal communication and body energy sensing. *Int J Mol Sci* 10:1729–1772
- Dzeja PP, Vitkevicius KT, Redfield MM, Burnett JC, Terzic A (1999) Adenylate kinase-catalyzed phosphotransfer in the myocardium: increased contribution in heart failure. *Circ Res* 84:1137–1143
- Dzeja, P.P., Chung, S., and Terzic, A. (2007). Integration of Adenylate Kinase and Glycolytic and Glycogenolytic Circuits in Cellular Energetics. In *Molecular system bioenergetics: energy for life*, S. Prof. Valdur, ed. (Weinheim, Germany, Wiley-VCH Verlag GmbH & Co. KGaA), pp. 265–301.
- Dzeja PP, Chung S, Faustino RS, Behfar A, Terzic A (2011) Developmental enhancement of adenylate kinase-AMPK metabolic signaling axis supports stem cell cardiac differentiation. *PLoS One* 6:e19300
- Eimre M, Paju K, Pelloux S, Beraud N, Roosimaa M, Kadaja L, Gruno M, Peet N, Orlova E, Remmelkoo R et al (2008) Distinct organization of energy metabolism in HL-1 cardiac cell line and cardiomyocytes. *Biochim Biophys Acta* 1777:514–524
- Fukada K, Zhang F, Vien A, Cashman NR, Zhu H (2004) Mitochondrial proteomic analysis of a cell line model of familial amyotrophic lateral sclerosis. *Mol Cell Proteomics* 3:1211–1223
- Gellerich FN (1992) The role of adenylate kinase in dynamic compartmentation of adenine nucleotides in the mitochondrial intermembrane space. *FEBS Lett* 297:55–58
- Gnaiger E (2001) Oxygen solubility in experimental media. *OROBOROS Bioenerg News* 6:1–6
- Greengard O, Head JF, Goldberg SL (1980) Uridine kinase, adenylate kinase, and guanase in human lung tumors. *Cancer Res* 40:2295–2299
- Guzun R, Timohhina N, Tepp K, Monge C, Kaambre T, Sikk P, Kuznetsov AV, Pison C, Saks V (2009) Regulation of respiration controlled by mitochondrial creatine kinase in permeabilized cardiac cells in situ. Importance of system level properties. *Biochim Biophys Acta* 1787:1089–1105
- Guzun R, Gonzalez-Granillo M, Karu-Varikmaa M, Grichine A, Usson Y, Kaambre T, Guerrero-Roesch K, Kuznetsov A, Schlattner U, Saks V (2012) Regulation of respiration in muscle cells in vivo by VDAC through interaction with the cytoskeleton and MtCK within mitochondrial interactosome. *Biochim Biophys Acta* 1818:1545–1554
- Hall M, Mickey DD, Wenger AS, Silverman LM (1985) Adenylate kinase: an oncogene marker in an animal model for human prostatic cancer. *Clin Chem* 31:1689–1691
- Hampton A, Slotin LA, Kappler F, Sasaki T, Perini F (1976) Design of substrate-site-directed inhibitors of adenylate kinase and hexokinase. Effect of substrate substituents on affinity for the adenine nucleotide sites *Journal of medicinal chemistry* 19:1371–1377
- Hanahan D, Weinberg RA (2011) Hallmarks of cancer: the next generation. *Cell* 144:646–674
- Hardie DG, Alessi DR (2013) LKB1 and AMPK and the cancer-metabolism link - ten years after. *BMC Biol* 11:36
- Inouye S, Seo M, Yamada Y, Nakazawa A (1998) Increase of adenylate kinase isozyme I protein during neuronal differentiation in mouse embryonal carcinoma P19 cells and in rat brain primary cultured cells. *J Neurochem* 71:125–133
- Kaambre T, Chekulayev V, Shevchuk I, Karu-Varikmaa M, Timohhina N, Tepp K, Bogovskaja J, Kutner R, Valvere V, Saks V (2012) Metabolic control analysis of cellular respiration in situ in intraoperative samples of human breast cancer. *J Bioenerg Biomembr* 44:539–558
- Kaldma A, Klepinin A, Chekulayev V, Mado K, Shevchuk I, Timohhina N, Tepp K, Kandashvili M, Varikmaa M, Koit A et al (2014) An in situ study of bioenergetic properties of human colorectal cancer: the regulation of mitochondrial respiration and distribution of flux control among the components of ATP synthasome. *Int J Biochem Cell Biol* 55:171–186
- Khoo JC, Russell PJ (1972) Isoenzymes of adenylate kinase in human tissue. *Biochim Biophys Acta* 268:98–101
- Kiebish MA, Han X, Cheng H, Chuang JH, Seyfried TN (2008) Cardiolipin and electron transport chain abnormalities in mouse brain tumor mitochondria: lipidomic evidence supporting the Warburg theory of cancer. *J Lipid Res* 49:2545–2556
- Kim H, Lee HJ, Oh Y, Choi SG, Hong SH, Kim HJ, Lee SY, Choi JW, Su Hwang D, Kim KS et al (2014) The DUSP26 phosphatase activator adenylate kinase 2 regulates FADD phosphorylation and cell growth. *Nat Commun* 5:3351
- Klepinin A, Chekulayev V, Timohhina N, Shevchuk I, Tepp K, Kaldma A, Koit A, Saks V, Kaambre T (2014) Comparative analysis of some aspects of mitochondrial metabolism in differentiated and undifferentiated neuroblastoma cells. *J Bioenerg Biomembr* 46:17–31

- Kuznetsov AV, Veksler V, Gellerich FN, Saks V, Margreiter R, Kunz WS (2008) Analysis of mitochondrial function in situ in permeabilized muscle fibers, tissues and cells. *Nat Protoc* 3:965–976
- Lagresle-Peyrou C, Six EM, Picard C, Rieux-Laucat F, Michel V, Ditadi A, Demerens-de Chappedelaine C, Morillon E, Valensi F, Simon-Stoos KL et al (2009) Human adenylate kinase 2 deficiency causes a profound hematopoietic defect associated with sensorineural deafness. *Nat Genet* 41:106–111
- Lam YW, Yuan Y, Isaac J, Babu CV, Meller J, Ho SM (2010) Comprehensive identification and modified-site mapping of S-nitrosylated targets in prostate epithelial cells. *PLoS One* 5:e9075
- Lamb R, Bonuccelli G, Ozsvari B, Peiris-Pages M, Fiorillo M, Smith DL, Bevilacqua G, Mazzanti CM, McDonnell LA, Naccarato AG et al (2015) Mitochondrial mass, a new metabolic biomarker for stem-like cancer cells: understanding WNT/FGF-driven anabolic signaling. *Oncotarget* 6:30453–30471
- Lee HJ, Pyo JO, Oh Y, Kim HJ, Hong SH, Jeon YJ, Kim H, Cho DH, Woo HN, Song S et al (2007) AK2 activates a novel apoptotic pathway through formation of a complex with FADD and caspase-10. *Nat Cell Biol* 9:1303–1310
- Liu R, Strom AL, Zhai J, Gal J, Bao S, Gong W, Zhu H (2009) Enzymatically inactive adenylate kinase 4 interacts with mitochondrial ADP/ATP translocase. *Int J Biochem Cell Biol* 41:1371–1380
- Liu X, Zhang M, Go VL, Hu S (2010) Membrane proteomic analysis of pancreatic cancer cells. *J Biomed Sci* 17:74
- Majewski N, Nogueira V, Bhaskar P, Coy PE, Skeen JE, Gottlob K, Chandel NS, Thompson CB, Robey RB, Hay N (2004) Hexokinase-mitochondria interaction mediated by Akt is required to inhibit apoptosis in the presence or absence of Bax and Bak. *Mol Cell* 16:819–830
- Makarchikov AF, Wins P, Janssen E, Wieringa B, Grisar T, Bettendorff L (2002) Adenylate kinase 1 knockout mice have normal thiamine triphosphate levels. *Biochim Biophys Acta* 1592:117–121
- Maldonado EN, Sheldon KL, DeHart DN, Patnaik J, Manevich Y, Townsend DM, Bezrukov SM, Rostovtseva TK, Lemasters JJ (2013) Voltage-dependent anion channels modulate mitochondrial metabolism in cancer cells: regulation by free tubulin and erastin. *J Biol Chem* 288:11920–11929
- Martel C., Wang, Z., and Brenner, C. (2014). VDAC phosphorylation, a lipid sensor influencing the cell fate. *Mitochondrion* 19 Pt A, 69–77.
- Mather M, Rottenberg H (2001) Polycations induce the release of soluble intermembrane mitochondrial proteins. *Biochim Biophys Acta* 1503:357–368
- Mathupala SP, Ko YH, Pedersen PL (2006) Hexokinase II: cancer's double-edged sword acting as both facilitator and gatekeeper of malignancy when bound to mitochondria. *Oncogene* 25:4777–4786
- Morisaki T, Gross M, Morisaki H, Pongratz D, Zollner N, Holmes EW (1992) Molecular basis of AMP deaminase deficiency in skeletal muscle. *Proc Natl Acad Sci U S A* 89:6457–6461
- Nelson BD, Kabir F (1985) Adenylate kinase is a source of ATP for tumor mitochondrial hexokinase. *Biochim Biophys Acta* 841:195–200
- Noma T (2005) Dynamics of nucleotide metabolism as a supporter of life phenomena. *The journal of medical investigation* : JMI 52:127–136
- Noma T, Fujisawa K, Yamashiro Y, Shinohara M, Nakazawa A, Gondo T, Ishihara T, Yoshinobu K (2001) Structure and expression of human mitochondrial adenylate kinase targeted to the mitochondrial matrix. *Biochem J* 358:225–232
- Panayiotou C, Solaroli N, Karlsson A (2014) The many isoforms of human adenylate kinases. *Int J Biochem Cell Biol* 49:75–83
- Park CE, Wenner CE (1970) Mitochondrial lipids of Ehrlich letre ascites tumor cells. *Oncology* 24:241–260
- Park H, Kam TI, Kim Y, Choi H, Gwon Y, Kim C, Koh JY, Jung YK (2012) Neuropathogenic role of adenylate kinase-1 in Abeta-mediated tau phosphorylation via AMPK and GSK3beta. *Hum Mol Genet* 21:2725–2737
- Pastorino JG, Hoek JB (2008) Regulation of hexokinase binding to VDAC. *J Bioenerg Biomembr* 40:171–182
- Patra S, Ghosh A, Roy SS, Bera S, Das M, Talukdar D, Ray S, Wallimann T, Ray M (2012) A short review on creatine-creatine kinase system in relation to cancer and some experimental results on creatine as adjuvant in cancer therapy. *Amino Acids* 42:2319–2330
- Plaideau C, Liu J, Hartleib-Geschwindner J, Bastin-Coyette L, Bontemps F, Oscarsson J, Hue L, Rider MH (2012) Overexpression of AMP-metabolizing enzymes controls adenine nucleotide levels and AMPK activation in HEK293T cells. *FASEB J* 26:2685–2694
- Plaideau C, Lai YC, Kviklyte S, Zanou N, Lofgren L, Andersen H, Vertommen D, Gailly P, Hue L, Bohlooly YM et al (2014) Effects of pharmacological AMP deaminase inhibition and Ampd1 deletion on nucleotide levels and AMPK activation in contracting skeletal muscle. *Chem Biol* 21:1497–1510
- Rosano TG, Clayton KJ, Strandjord PE (1976) Evaluation of adenosine 5'-monophosphate and fluoride as adenylate kinase inhibitors in the creatine kinase assay. *Clin Chem* 22:1078–1083
- Ross RA, Spengler BA (2007) Human neuroblastoma stem cells. *Semin Cancer Biol* 17:241–247
- Ruan Q, Chen Y, Gratton E, Glaser M, Mantulin WW (2002) Cellular characterization of adenylate kinase and its isoform: two-photon excitation fluorescence imaging and fluorescence correlation spectroscopy. *Biophys J* 83:3177–3187
- Rybakowska I, Slominska EM, Romaszko P, Lipinski M, Zukowska P, Smolenski RT (2014) Activity of AMP-regulated protein kinase and AMP-deaminase in the heart of mice fed high-fat diet. *Nucleosides Nucleotides Nucleic Acids* 33:347–352
- Saks VA, Chernousova GB, Gukovsky DE, Smirnov VN, Chazov EI (1975) Studies of energy transport in heart cells. Mitochondrial isoenzyme of creatine phosphokinase: kinetic properties and regulatory action of Mg²⁺ ions. *Eur J Biochem* 57:273–290
- Saks VA, Belikova YO, Kuznetsov AV (1991) In vivo regulation of mitochondrial respiration in cardiomyocytes: specific restrictions for intracellular diffusion of ADP. *Biochim Biophys Acta* 1074:302–311
- Saks V, Guzun R, Timohhina N, Tepp K, Varikmaa M, Monge C, Beraud N, Kaambre T, Kuznetsov A, Kadaja L et al (2010) Structure-function relationships in feedback regulation of energy fluxes in vivo in health and disease: mitochondrial interactosome. *Biochim Biophys Acta* 1797:678–697
- Seppet E, Eimre M, Peet N, Paju K, Orlova E, Ress M, Kovask S, Piirsoo A, Saks VA, Gellerich FN et al (2005) Compartmentation of energy metabolism in atrial myocardium of patients undergoing cardiac surgery. *Mol Cell Biochem* 270:49–61
- Shackelford DB, Shaw RJ (2009) The LKB1-AMPK pathway: metabolism and growth control in tumour suppression. *Nat Rev Cancer* 9:563–575
- Simamura E, Shimada H, Hatta T, Hirai K (2008) Mitochondrial voltage-dependent anion channels (VDACs) as novel pharmacological targets for anti-cancer agents. *J Bioenerg Biomembr* 40:213–217
- Single B, Leist M, Nicotera P (1998) Simultaneous release of adenylate kinase and cytochrome c in cell death. *Cell Death Differ* 5:1001–1003
- Tanabe T, Yamada M, Noma T, Kajii T, Nakazawa A (1993) Tissue-specific and developmentally regulated expression of the genes encoding adenylate kinase isozymes. *J Biochem* 113:200–207
- Tanimura A, Horiguchi T, Miyoshi K, Hagita H, Noma T (2014) Differential expression of adenine nucleotide converting enzymes in mitochondrial intermembrane space: a potential role of adenylate kinase isozyme 2 in neutrophil differentiation. *PLoS One* 9:e89916
- Tepp K, Timohhina N, Chekulayev V, Shevchuk I, Kaambre T, Saks V (2010) Metabolic control analysis of integrated energy metabolism in permeabilized cardiomyocytes - experimental study. *Acta Biochim Pol* 57:421–430

- Tepp K, Shevchuk I, Chekulayev V, Timohhina N, Kuznetsov AV, Guzun R, Saks V, Kaambre T (2011) High efficiency of energy flux controls within mitochondrial interactosome in cardiac intracellular energetic units. *Biochim Biophys Acta* 1807:1549–1561
- Timohhina N, Guzun R, Tepp K, Monge C, Varikmaa M, Vija H, Sikk P, Kaambre T, Sackett D, Saks V (2009) Direct measurement of energy fluxes from mitochondria into cytoplasm in permeabilized cardiac cells in situ: some evidence for mitochondrial interactosome. *J Bioenerg Biomembr* 41:259–275
- Ventura-Clapier R, Garnier A, Veksler V, Joubert F (2011) Bioenergetics of the failing heart. *Biochim Biophys Acta* 1813:1360–1372
- Zhang S, Nemetlu E, Dzeja P (2010) Metabolomic profiling of adenylate kinase AK1^{-/-} and AK2^{+/-} transgenic mice: effect of physical stress. *Circulation* 122
- Zhang S, Nemetlu E, Terzic A, Dzeja P (2014) Adenylate kinase isoform network: a major hub in cell energetics and metabolic signaling. In: Aon MA, Saks V, Schlattner U (eds) *Systems biology of metabolic and signaling networks*. Springer, Berlin Heidelberg, pp. 145–162

Curriculum vitae

Personal data

Name: Ljudmila Klepinina
formerly Ljudmila Õunpuu
Date of birth: 10.02.1990
Place of birth: Tallinn, Estonia
Citizenship: Estonian

Contact data

Email: ljudmila.klepinina@gmail.com

Education

2014–2021 Tallinn University of Technology, PhD study, Chemistry and Biotechnology
2012–2014 Tallinn University of Technology, MSc, Gene technology
2009–2012 Tallinn University of Technology, BSc, Gene technology
1997–2009 Tallinn Läänemere Gymnasium (gold medal)

Language competence

Russian native language
Estonian fluent
English fluent
French basic

Professional employment

2018–.... National Institute of Chemical Physics and Biophysics, Junior Researcher (1,00)
2014–2016 National Institute of Chemical Physics and Biophysics, Junior Researcher (1,00)

Memberships

2017–... Estonian Biochemical Society
2017–... COST Action CA15203 Mitochondrial fitness mapping MITOEAGLE project
2017–... Mitochondrial Physiology Society

Honours & Awards

2019 Finalist and nominee of the three-minute lecture competition of the Estonian Academy of Sciences
2017 Conference award for the best poster presentation at MiP2017 (Hradec Kralove, Czech Republic)
2017 Travel award for participation in FEBS conference in Jerusalem

Special courses

2017 Mitochondrial Physiology, University of Copenhagen, Denmark
2014–2016 Engineering Pedagogy, Tallinn University of Technology, Estonia
2016, 2015 Laboratory Animal Science, Estonian University of Life Sciences, Tartu, Estonia

Conferences

- September, 2018 13th Mitochondrial Physiology Conference, Jurmala, Latvia. Poster presentation: "Metabolic plasticity of cancer stem-like cells"
- April, 2018 MITOEST conference, Tallinn. Poster presentation: "The role of dietary fibers in the energy metabolism of human colon cancer cells"
- August, 2018 20th European Bioenergetics Conference, Budapest, Hungary. Poster presentation: "The phosphotransfer system and metabolic plasticity of colon cancer cells"
- November, 2017 Mitochondrial Physiology conference, Hradec Kralove, Czech Republic. Poster presentation: "The role of dietary fibers in the energy metabolism of human colon cancer cells"
- September, 2017 42nd FEBS conference, Jerusalem, Israel. Poster presentation: "Human embryonal carcinoma cells display distinct bioenergetic profile compared to normal embryonic stem cells"
- April, 2015 Environmental and System Biology Conference, University of Joseph Fourier, Grenoble, France. Poster presentation: "Regulation of mitochondrial respiration in neuroblastoma cells"

Publications

Klepina L, Klepinin A, Truu L, Chekulayev V, Kuus K, Teino I, Pook M, Maimets T, Kaambre T. (2021). Colon cancer cell differentiation by sodium butyrate modulates metabolic plasticity of Caco-2 cells via alteration of phosphotransfer network. *PLOS ONE* 16(1): e0245348.

Puurand M, Tepp K, Klepinin A, Klepina L, Shevchuk I, Kaambre T. (2018). Intracellular Energy-Transfer Networks and High-Resolution Respirometry: A Convenient Approach for Studying Their Function. *International Journal of Molecular Sciences*, 19 (10).

Ounpuu L, Truu L, Shevchuk I, Chekulayev V, Klepinin A, Koit A, Tepp K, Puurand M, Rebane-Klemm E, Käämbre T. (2018). Comparative analysis of the bioenergetics of human adenocarcinoma Caco-2 cell line and postoperative tissue samples from colorectal cancer patients. *Biochemistry and cell biology = Biochimie et biologie cellulaire*.

Klepinin A, Ounpuu L, Mado K, Truu L, Chekulayev V, Puurand M, Shevchuk I, Tepp K, Planken A, Kaambre T. (2018). The complexity of mitochondrial outer membrane permeability and VDAC regulation by associated proteins. *Journal of Bioenergetics and Biomembranes*.

Ounpuu L, Klepinin A, Pook M, Teino I, Peet N, Paju K, Tepp K, Chekulayev V, Shevchuk I, Koks S, Maimets T, Kaambre T. (2017). 2102Ep embryonal carcinoma cells have compromised respiration and shifted bioenergetic profile distinct from H9 human embryonic stem cells. *Biochimica et Biophysica Acta - General Subjects*, 1861, 2146–2154.

Koit A, Shevchuk I, Ounpuu L, Klepinin A, Chekulayev V, Timohhina N, Tepp K, Puurand M, Truu L, Heck K, Valvere V, Guzun R, Kaambre T. (2017). Mitochondrial Respiration in Human Colorectal and Breast Cancer Clinical Material Is Regulated Differently. *Oxidative Medicine and Cellular Longevity*, 2017 (1372640), 1–16.

Klepinin A, Ounpuu L, Guzun R, Chekulayev V, Timohhina N, Tepp K, Shevchuk I, Schlattner U, Kaambre T. (2016). Simple oxygraphic analysis for the presence of adenylate kinase 1 and 2 in normal and tumor cells. *Journal of Bioenergetics and Biomembranes*, 48 (5), 531–548.

Chekulayev V, Mado K, Shevchuk I, Koit A, Kaldma A, Klepinin A, Timohhina N, Tepp K, Kandashvili M, Ounpuu L, Heck K, Truu L, Planken A, Valvere V, Kaambre T. (2015). Metabolic remodeling in human colorectal cancer and surrounding tissues: alterations in regulation of mitochondrial respiration and metabolic fluxes. *Biochemistry and Biophysics Reports*, 4, 111–125.

Elulookirjeldus

Isikuandmed

Nimi: Ljudmila Klepinina
neiupõlvenimi Öunpuu
Sünniaeg: 10.02.1990
Sünnikoht: Tallinn, Eesti
Kodakondsus: Eesti

Kontaktandmed

E-post: ljudmila.klepinina@gmail.com

Hariduskäik

2014–2019 Tallinna Tehnikaülikool, doktoriõpe, keemia ja biotehnoloogia
2012–2014 Tallinna Tehnikülikool, magistriõpe geenitehnoloogia erialal
2009–2012 Tallinna Tehnikülikool, bakalaureuseõpe geenitehnoloogia erialal
1997–2009 Tallinna Läänemere Gümnaasium (kuldmedal)

Keelteoskus

Vene keel emakeel
Eesti keel kõrgtase
Inglise keel kõrgtase
Prantsuse keel algtase

Teenistuskäik

2018–.... Keemilise ja bioloogilise füüsika instituut, nooremteadur (1,00)
2014–2016 Keemilise ja bioloogilise füüsika instituut, nooremteadur (1,00)

Teadusorganisatsiooniline ja -administratiivne tegevus

2017–... Eesti Biokeemia Seltsi liige
2017–... COST Action CA15203 Mitochondrial fitness mapping MITOEAGLE projekti liige
2017–... Mitochondrial Physiology Society liige

Teaduspreemiad ja tunnustused

2019 Eesti Teaduste Akadeemia „Teadus kolme minutiga“ loengute konkursi finalist ja laureaat
2017 Konverentsiauhind parima poster ettekande eest rahvusvahelisel konverentsil MiP2017 (Hradec Kralove, Tšehhimaa)
2017 FEBS stipendium osalemaks ettekandega FEBS konverentsil Jerusalemmas

Täiendusõpe

2017 Taani, Kopenhaageni ülikool, kursus: “Mitochondrial Physiology”
2014–2016 Eesti, TalTech Avatud ülikool. Täiendusõpe ja lisaeriala: “Insenerpedagoogika”
2016 Eesti, Tartu, Maaülikool, kursus: “Laboratory Animal Science II”
2015 Eesti, Tartu, Maaülikool, kursus: “Laboratory Animal Science I”

Konverentsiettekanded

- September, 2018 13th Mitochondrial Physiology konverents, Jurmala, Läti. Poster-ettekane: "Metabolic plasticity of cancer stem-like cells"
- Aprill, 2018 MITOEST konverents, Tallinn. Poster-ettekane: "The role of dietary fibers in the energy metabolism of human colon cancer cells"
- August, 2018 20th European Bioenergetics konverents, Budapest, Ungari. Poster presentation: "The phosphotransfer system and metabolic plasticity of colon cancer cells"
- November, 2017 Mitochondrial Physiology konverents, Hradec Kralove, Tšehhima. Poster-ettekane: "The role of dietary fibers in the energy metabolism of human colon cancer cells"
- September, 2017 42nd FEBS konverents, Jeruusalemm, Iisrael. Poster-ettekane: "Human embryonal carcinoma cells display distinct bioenergetic profile compared to normal embryonic stem cells"
- Aprill, 2015 Environmental and System Biology konverents, Joseph Fourier ülikool, Grenoble, Prantsusmaa. Poster-ettekane: "Regulation of mitochondrial respiration in neuroblastoma cells"

Publikatsioonid

Klepinina L, Klepinin A, Truu L, Chekulayev V, Kuus K, Teino I, Pook M, Maimets T, Kaambre T. (2021). Colon cancer cell differentiation by sodium butyrate modulates metabolic plasticity of Caco-2 cells via alteration of phosphotransfer network. *PLOS ONE* 16(1): e0245348.

Puurand M, Tepp K, Klepinin A, Klepinina L, Shevchuk I, Kaambre T. (2018). Intracellular Energy-Transfer Networks and High-Resolution Respirometry: A Convenient Approach for Studying Their Function. *International Journal of Molecular Sciences*, 19 (10).

Ounpuu L, Truu L, Shevchuk I, Chekulayev V, Klepinin A, Koit A, Tepp K, Puurand M, Rebane-Klemm E, Käämbre T. (2018). Comparative analysis of the bioenergetics of human adenocarcinoma Caco-2 cell line and postoperative tissue samples from colorectal cancer patients. *Biochemistry and cell biology = Biochimie et biologie cellulaire*.

Klepinin A, Ounpuu L, Mado K, Truu L, Chekulayev V, Puurand M, Shevchuk I, Tepp K, Planken A, Kaambre T. (2018). The complexity of mitochondrial outer membrane permeability and VDAC regulation by associated proteins. *Journal of Bioenergetics and Biomembranes*.

Ounpuu L, Klepinin A, Pook M, Teino I, Peet N, Paju K, Tepp K, Chekulayev V, Shevchuk I, Koks S, Maimets T, Kaambre T. (2017). 2102Ep embryonal carcinoma cells have compromised respiration and shifted bioenergetic profile distinct from H9 human embryonic stem cells. *Biochimica et Biophysica Acta - General Subjects*, 1861, 2146–2154.

Koit A, Shevchuk I, Ounpuu L, Klepinin A, Chekulayev V, Timohhina N, Tepp K, Puurand M, Truu L, Heck K, Valvere V, Guzun R, Kaambre T. (2017). Mitochondrial Respiration in Human Colorectal and Breast Cancer Clinical Material Is Regulated Differently. *Oxidative Medicine and Cellular Longevity*, 2017 (1372640), 1–16.

Klepinin A, Ounpuu L, Guzun R, Chekulayev V, Timohhina N, Tepp K, Shevchuk I, Schlattner U, Kaambre T. (2016). Simple oxygraphic analysis for the presence of adenylate kinase 1 and 2 in normal and tumor cells. *Journal of Bioenergetics and Biomembranes*, 48 (5), 531–548.

Chekulayev V, Mado K, Shevchuk I, Koit A, Kaldma A, Klepinin A, Timohhina N, Tepp K, Kandashvili M, Ounpuu L, Heck K, Truu L, Planken A, Valvere V, Kaambre T. (2015). Metabolic remodeling in human colorectal cancer and surrounding tissues: alterations in regulation of mitochondrial respiration and metabolic fluxes. *Biochemistry and Biophysics Reports*, 4, 111–125.

ISSN 2585-6901 (PDF)
ISBN 978-9949-83-698-7 (PDF)